IMMERSION AND INVARIANCE CONTROL DESIGN FOR UNMANNED AERIAL VEHICLE

BY

ARIEF BARKAH KOESDWIADY

A Thesis Presented to the
DEANSHIP OF GRADUATE STUDIES

KING FAHD UNIVERSITY OF PETROLEUM & MINERALS

DHAHRAN, SAUDI ARABIA

In Partial Fulfillment of the
Requirements for the Degree of

MASTER OF SCIENCE

In

SYSTEMS ENGINEERING

May 2013

IMMERSION AND INVARIANCE CONTROL DESIGN FOR UNMANNED AERIAL VEHICLE

by

ARIEF BARKAH KOESDWIADY

A Thesis Presented to the
DEANSHIP OF GRADUATE STUDIES

In Partial Fulfillment of the Requirements
for the degree

MASTER OF SCIENCE

IN

SYSTEMS ENGINEERING

KING FAHD UNIVERSITY
OF PETROLEUM & MINERALS

Dhahran, Saudi Arabia

MAY 2013

KING FAHD UNIVERSITY OF PETROLEUM & MINERALS
DHAHRAN 31261, SAUDI ARABIA

DEANSHIP OF GRADUATE STUDIES

This thesis, written by **ARIEF BARKAH KOESDWIADY** under the direction of his thesis advisor and approved by his thesis committee, has been presented to and accepted by the Dean of Graduate Studies, in partial fulfillment of the requirements for the degree of **MASTER OF SCIENCE IN SYSTEMS ENGINEERING**.

Thesis Committee

Dr. Sami El Ferik (Advisor)

May 26, 13
Dr. Fouad Al Sunni (Member)

Dr. Mousfata Elshafei (Member)

Dr. Samir Al Amer (Member)

Dr. Fakhreddine Karray (Member)

May 26, 13
Dr. Fouad Al Sunni
Department Chairman

Dr. Salam A. Zummo
Dean of Graduate Studies

27/5/13
Date

Dedicated to my beloved parents, brothers, wife, and son

ACKNOWLEDGEMENTS

This thesis is the result of my Masters degree from September 2010 through May 2013. It has taken place at the Department of Systems Engineering at King Fahd University of Petroleum and Minerals under the counselling of my supervisor Dr. Sami El Ferik. First, I would like to thank my supervisor and mentor Dr. Sami El Ferik. His exceptional motivational skills and ability to continuously guide me in the right directions have been much needed assets in my struggle towards finishing the Master Degree. I would like to thank also Dr. Fouad Al-Sunni, Dr. Mustafa El Shafei, Dr. Samir Al Amer, and Dr. Fakhreddine Karray for being my thesis committee members.

TABLE OF CONTENTS

LIST OF TABLES

LIST OF FIGURES

LIST OF ABBREVIATIONS

ADP adaptive dynamic programming

CoG Centre of Gravity

DOF degree-of-freedom

EFFSZM Explicit Force, Finitely Sharp, Zero Mass

I&I immersion and invariance

NN neural network

PD proportional-derivative

PID proportional-integral-derivative

SMO sliding mode observer

UAV unmanned aerial vehicle

w.r.t with respect to

THESIS ABSTRACT

NAME:	Arief Barkah Koesdwiady
TITLE OF STUDY:	Immersion and Invariance Control Design for Unmanned Aerial Vehicle
MAJOR FIELD:	Systems Engineering
DATE OF DEGREE:	May 2013

This thesis presents the application of recent techniques in stabilizing controller, observer and adaptive controller for quadrotor unmanned aerial vehicle (UAV). The objective is to achieve asymptotic tracking performance in the position and attitude angles of the quadrotor. In the stabilizing controller, the immersion and invariance (I&I) technique is presented and the performance of the controller is compared to the backstepping technique. I&I reduced-order observer is utilized for translational velocity estimation and the classical Luenberger observer is developed as comparison. For adaptive control, I&I-based adaptive control technique is applied to the quadrotor with $\mathcal{L}_1$ adaptive control as the benchmark. For system with an internal delay, the I&I and $\mathcal{L}_1$ adaptive control are compared. The mathematical derivations of each design are validated by simulation.

CHAPTER 1

INTRODUCTION

Since the last decade, study in autonomous UAV control system has shown significant growth. The UAV structure that is selected in this thesis is a rigid body with constant mass and has four symmetrical rotors. This structure is also known as quadrotor. The quadrotor dynamics are highly nonlinear, hence a nonlinear control method has to be applied in order to achieve stable autonomous system. In this research, the development of nonlinear stabilizing controller, observer, and adaptive control for autonomous quadrotor UAV are investigated. The objective of the controller is to minimize the error between the desired predefined trajectory and the actual trajectory of the UAV.

1.1 Motivation

UAV is an aerial vehicle operated without human on board. It is operated either remotely or autonomously. The idea of UAV extends the scope of mission performed by the aerial vehicle without any risk to human life. UAV usually is

preferred in high risk missions such as military (espionage or invasion), fire fighting, early detection of natural disasters, and many more. Not limited to only high-risk missions, UAVs are also attractive for commercial or civil applications such as geo-mapping, transportation of medical supplies to remote area, etc. By utilizing the UAV, in addition to eliminating the risk of human life, it increases the efficiency of time and money. The developments in miniaturization of the UAV together with advances in mechatronics and microelectronics offer a wide potential for commercialization of small and inexpensive UAV. The quadrotor emerges as a promising vehicle in the midst of many small UAVs present because of its size, simplicity, and maneuverability.

The quadrotor is categorized as rotor-craft as opposed to fixed-wing aircraft. It is propelled and lifted by the thrust generated by the rotors. Generally, the quadrotor uses symmetrical blades (see Figure(1.1)). By changing its rotation rate it achieves different motions. The quadrotor does not require the mechanism to vary the rotor blades as they rotate, therefore the design is simpler compared to the conventional helicopter. The four rotors use smaller rotor diameter compared to the helicopter, resulting in less kinetic energy during flight which may reduce the damage caused by the collision with other objects. With all these advantages, many researchers are trying to develop the unmanned quadrotor for many applications. Specifically for the control engineer, fully autonomous quadrotor is an interesting subject to be investigated. The absence of human operator requires sophisticated and reliable control system for indoor and outdoor applications. Many

Figure 1.1: Quadrotor (Image taken from www.cmuquadrotor.com)

obstacles can be seen when one tries to develop a control system for outdoor applications, such as wind and dust disturbances. Therefore, the problem of designing the control system for autonomous quadrotor that can give good performance for a wide application became a major issue.

In order to design a control system for the quadrotor, one needs to have equations that reflect the motion of the vehicle, either by modelling or using system identification techniques. The dynamics of the quadrotor is usually described by a set of differential equations derived using Euler-Lagrangian framework. It is generally known that Euler Lagrange systems can be highly nonlinear for some parameters that are influenced by the rotation matrix. This condition presents a challenge in designing a control system, since the classical methods for linear system are not adequate and may produce results that are far from satisfactory.

Another challenging property of the dynamics of the quadrotor is the underactuation. Quadrotor has six degree-of-freedom (DOF) and four actuations. A

system with total number of actuations less than the DOF is called underactuated system. In underactuated system, control design problem becomes more complex. The common method for solving the underactuated problem in the quadrotor is by separating the control loop into two loops, the inner loop for attitude angles control, and the outer loop for position control. In Zuo's work [1], the underactuated problem of the quadrotor is solved by determining the desired attitude angles for the inner loop from the stable closed-outer-loop dynamics. By this method, the attitude angles of the quadrotor are compatible with the position.

Several designs of nonlinear control for Euler Lagrange system, particularly for the quadrotor have been proposed, such as sliding mode, feedback linearisation, and backstepping. Each of these proposed controllers has weakness, for instance in sliding mode control, the control law is discontinuous and fast switching (chattering) is possible. For backstepping technique, it is not always easy to find a suitable Lyapunov function and it is sensitive to parameter variation. In feedback linearization, once the parameter of the system changes, there is a high probability that the linearization becomes incorrect and creates unstable closed loop system. Based on these issues, a nonlinear control for the quadrotor that overcomes all the disadvantages coming from the above mentioned methods is developed.

In this thesis, the design of nonlinear control based on I&I technique for the quadrotor UAV is proposed. The development of this technique was first presented in [2]. The method is developed based on system immersion and manifold invariance. The main idea of I&I method is to stabilize the system by immersing

the object's dynamics into a target system with pre-specified desired behaviour. The main features of I&I that motivate our interest are three folds

- It does not require, in principle, the knowledge of Lyapunov function.
- Easier to solve, because it reduces the problem into subproblem.
- It provides framework for nonlinear observer design and adaptive control problem.

1.2 Problem Formulation and Contribution

In the development of the nonlinear trajectory tracking control for autonomous quadrotor, several tasks are completed.

1. The design of stabilizing trajectory tracking controller based on I&I for underactuated quadrotor.
2. Robustness analysis for I&I stabilizing controller.
3. The design of backstepping controller for I&I controller benchmark.
4. The design of global observer based on I&I for outer-loop of underactuated quadrotor.
5. The design of classical Luenberger observer for I&I observer benchmark.
6. The design of adaptive control based on I&I for underactuated quadrotor.
7. Analysis for I&I adaptive controller.

8. The design of $\mathcal{L}_1$ adaptive control for I&I adaptive control benchmark.

9. Another benchmark between I&I adaptive control and $\mathcal{L}_1$ adaptive control on drilling system with delay.

1.3 Thesis Organization

The thesis is organized as the following.

Chapter 1 contains introduction, motivation, problem formulation and objectives, and thesis organization.

Chapter 2 contains summary of the previous work on stabilizing controller, observer, and adaptive control for the quadrotor UAV. It also contains the summary of previous work on I&I based stabilizing controller, observer, and adaptive control. In addition to the benchmarking, previous research on $\mathcal{L}_1$ adaptive control is summarized.

Chapter 3 contains fundamental materials needed to understand the topic of the thesis. It explains the preliminary background in stability, vector and functional analysis and notations that are used throughout the thesis.

Chapter 4 explains the kinematics, dynamics, properties and assumptions in the quadrotor modelling.

Chapter 5 proposes the design of UAV stabilizing controller for the purpose of trajectory tracking of the quadrotor. Backstepping controller is designed for

comparison.

Chapter 6 presents the development of I&I based observer for inertial velocities estimation in the outer loop. Classical Luenberger observer is proposed as the benchmark study.

Chapter 7 contains the design of I&I adaptive control for unknown and uncertain parameters in the system. For comparison, $\mathcal{L}_1$ adaptive control is designed.

Chapter 8 proposes another benchmarking study for I&I and $\mathcal{L}_1$ adaptive control. The controllers are examined in the directional drilling system which contains internal delay.

Chapter 9 concludes all the work in the thesis with suggestions for possible extension for future work.

CHAPTER 2

LITERATURE REVIEW

2.1 Introduction

This chapter summarizes several research activities in the quadrotor UAV control area and research involving I&I methodology. The first part of this literature review contains the nonlinear stabilization of the quadrotor. The second part presents the development of observer in the quadrotor UAV system, and recent development in adaptive control of quadrotor is presented in the third part. Review on I&I technique as the main methodology is presented in the fourth part and $\mathcal{L}_1$ adaptive control as the benchmarking study is reviewed in the last part.

2.2 Nonlinear Stabilization of Quadrotor

In the literature, many studies addressed the quadrotor path-tracking control design. Several control strategies considering different techniques have been proposed with various performance. Feedback linearization-based controller to track

a predefined trajectory has been investigated in [3]. [4] proposes proportional-integral-derivative (PID)-based multi-channel control scheme and dynamic inversion for a simplified dynamic model of quadrotor. In [5], a controller that compensates the gyroscopic torques and Coriolis has been proposed and in [6] backstepping method has been developed for stabilization of a quadrotor by tracking the different positions and keeping the yaw angle constant while regulating the pitch and roll angles. Sliding mode controller has been studied in [7] and [8] where in the latter the controller is a combination of sliding mode and backstepping controllers. In [9] trajectory tracking utilizing sliding mode control to overcome the system uncertainties and external disturbances has been considered and a fuzzy controller is employed to reduce the chattering and improve the performance of the system. [10] proposed a control configuration composed of an inner loop and an outer-loop, the study considered feedback linearization to develop the inner-loop controller for attitude tracking. In [1], backstepping technique with command-filtered compensation has been considered.

2.3 Observer Design of Quadrotor

In this section, several developments of observer for the quadrotor are presented. Generally, the unknown states are estimated by the observer by utilizing information gathered from input and output. In some cases, the unknown inertial velocities and exogenous disturbances such as wind gust and additive parameter uncertainties have to be estimated. The design of backstepping control and

feedback linearization working together with a sliding mode observer (SMO) for a quadrotor UAV has been investigated in [11] and [12]. The SMO observes the inertial translational velocities and estimates wind gust disturbance and uncertainty. The objective of the controller is to minimize the tracking error in the flight trajectory and yaw angle, and stabilize the pitch and roll angles in the presence of exogenous disturbances. The stabilizing backstepping controller design is based on Lyapunov stability theorem.

In [13], nonlinear tracking control for underactuated quadrotor UAV in discrete time is combined with an observer. It is shown that the separation principle between controller and observer is satisfied. In[14], the time-varying reduced-order Luenberger like observer is employed for quadrotor speed estimation. Asymptotic stability of the estimation error is proved using Lyapunov approach and Barbalat lemma. Another approach has been developed in [15], online neural network (NN) is employed to study the complete dynamics of the quadrotor UAV. The NN observer was also utilized for translational and angular velocities estimation. Output feedback control is designed using information from position and attitude angles.

Several different research approaches have been presented in the recent years, but generally they have similar goals as those mentioned before. Using I&I method [16], an asymptotic observer that estimates translational velocities of the quadrotor using the information gathered from the inertial position is proposed.

2.4 Adaptive Control Design of Quadrotor

Adaptive scheme is suitable when one is dealing with a system having unknown parameters or a system in the presence of parameter uncertainties. For the quadrotor, parameter uncertainty is highly possible in the coefficient of translational drag, rotational drag coefficients, propeller's inertia and quadrotor's inertia. If the controller is not robust enough to absorb the uncertainty of the parameters, the stability of the system can not be guaranteed. In this work, the I&I adaptive scheme is applied so that the quadrotor adapts with the uncertainty in rotational drag coefficient, propeller's inertia, and quadrotor's inertia.

In [17], backstepping based adaptive scheme is utilized for an underactuated quadrotor system with model parameter uncertainty. Based on Lyapunov stability analysis, the proposed controller yields asymptotic tracking for inertial position and yaw angle. In [18], adaptive dynamic programming (ADP) is applied in quadrotor platform flying in a random environment and imposed to exogenous disturbances and parameter uncertainties. In this scheme, the controller changes its control action based on stimuli received in response to its actions by the critic (cost function, reward).

Fuzzy-adaptive or neural-adaptive control developed in [19] offers the adaptation scheme for arbitrary nonlinearities that is efficient. E-modification is a common method used to create robust adaptive control with respect to disturbances but it is found to be unsuitable when applied to the quadrotor in simulation. Alternate adaptive parameters in the adaptation scheme is proposed and it suc-

cessfully stabilizes the quadrotor in the simulation. Another work that utilized adaptive scheme as the solution for stabilization was presented in [20].

Many studies in the design of adaptive control for quadrotor UAV are available in the literature. In this work, adaptive control based on I&I methodology developed in [16] and [2] is proposed for trajectory tracking of quadrotor UAV.

2.5 Invariance and Immersion

Recently, I&I for stabilization of nonlinear systems has been proposed by [2] and has been summarized in [21]. Since then, several studies investigated the applicability of the approach to different cases (see for example [22], [23], [24]). In [22], the development of I&I control for underactuated cart-pendulum system is presented and in [23] I&I control for an antagonistic joint with nonlinear mechanical stiffness is considered. Stabilization of a synchronous generator with a controllable series capacitor via I&I has been studied in [25]. As stated previously, many control techniques with relative success have been investigated to control the quadrotor. The six-DOF rotor-craft airframe dynamics allow for both translational as well as rotational motions. More importantly, it is a multi-input-multi-output system with unknown linearities, underactuation, and a strong coupling between the pitch, yaw and roll dynamics [26].

One of the popular methods for quadrotor is Backstepping control. The Lyapunov-based design is not simple when compared to I&I. In addition, the Lyapunov stability condition is easily unsatisfied once there is a parameter change

in the system. Moreover, most of the studies ignored the drag forces and never addressed the nonlinear actuator dynamics.

The main contribution of this thesis is the application of I&I control approach to design a controller and a observer for the quadrotor taking into consideration the drag forces and the gyroscopic effect. Application of I&I based adaptive control of four-rotor mini helicopter is presented in [27], in order to simplify the complex multivariable parameter adaptation a parameterization with smaller number uncertain coefficient is developed. In this work, a complete uncertain or unknown parameters in inertia, propeller inertia, drag coefficient, and disturbance are estimated.

TheI&I control is applied to the inner loop attitude control, which produces a closed loop stable linear system. A simple proportional-derivative (PD) control is used in the outer loop to control the position and velocity. The approach adopted is based on determining the correct attitude of the quadrotor with respect to desired position as in [10], [1] and [28]. In addition, the control design has been developed with an I&I observer.

2.6 $\mathcal{L}_1$ Adaptive Control

$\mathcal{L}_1$ adaptive control was first introduced in [29], [30], followed by series of articles, and then summarized in [31]. The main attractive feature of $\mathcal{L}_1$ adaptive control is the decoupling between robustness and fast adaptation [32]. In [33], application of $\mathcal{L}_1$ adaptive control for safety-critical systems has been developed. A novel $\mathcal{L}_1$

adaptive control based on NN for autonomous aerial refueling autopilot has been investigated in [34]. Nonlinear $\mathcal{L}_1$ adaptive control for NASA AirSTAR flight test vehicle has been presented in [35].

Research in autonomous vehicle employing $\mathcal{L}_1$ adaptive control has been presented in [36], [37], and [38]. In [36], the design of $\mathcal{L}_1$ adaptive control and flight testing for indoor autonomous vehicles is presented. $\mathcal{L}_1$ adaptive control has been employed for the UAV for aero-biological sampling. In [38], the design of $\mathcal{L}_1$ adaptive control for pitch and depth of underwater vehicle is proposed and tested. In [39], $\mathcal{L}_1$ adaptive control is designed for quadrotor but only for longitudinal movement. While in this work all 6-degree of freedom (DOF) dynamics of quadrotor is considered.

The application of $\mathcal{L}_1$ adaptive control for a system which contains internal delay has been investigated in [40], with Explicit Force, Finitely Sharp, Zero Mass (EFFSZM) directional drilling system as the object.

2.7 Conclusions

In this chapter, several research in the area of quadrotor control, observer, and adaptive control have been reviewed. Research employing the I&I methodology and $\mathcal{L}_1$ adaptive control concept has been summarized.

CHAPTER 3

PRELIMINARIES

3.1 Introduction

This chapter presents the mathematical and system analysis background necessary for all theoretical developments and simulation in this thesis. In section 3.2, the notation that is used throughout the thesis is presented. Section 3.3 covers the fundamentals in vector and matrix norm. Lyapunov stability theory is presented in section 3.4, and invariant manifold and system immersion are covered in section 3.5. Nonlinear system parametrization and projection operator are covered in section 3.6 and 3.7, respectively.

3.2 Notations

Throughout the thesis, the variables in bold typing denote vector or matrix variables, see for example Table (3.1). The "$^\top$" denotes the vector/matrix transposition. The "$\|.\|$" denotes the norm operator, and "$\mathcal{L}$" denotes the Lebesgue

Vector/Matrix	$\mathbf{x}$	$\mathbf{y}$	$\mathbf{Q}$	$\boldsymbol{\varphi}$	$\boldsymbol{\Lambda}$
Scalar	x	y	Q	φ	Λ

Table 3.1: Vector/Matrix Notation

space.

3.3 Vector and Matrix Norm

Definition 3.1. The norm $\|.\|$ of a vector or a matrix, e.g $\mathbf{x}$, $\mathbf{y}$, is a real-valued function defined in the vector or matrix space, satisfying the following properties

1. $\|\mathbf{x}\| > 0$ if $\mathbf{x} \neq 0$, and $\|\mathbf{x}\| = 0 \Leftrightarrow \mathbf{x} = 0$.

2. $\|\mathbf{x} + \mathbf{y}\| \leq \|\mathbf{x}\| + \|\mathbf{y}\|$.

3. $\|\lambda\mathbf{x}\| = |\lambda|\|\mathbf{x}\|, \quad \lambda \in \mathbb{R}$.

It is clear that in Definition 3.1 the norm is not uniquely defined. The next definition introduces the most commonly used norms

Definition 3.2. For $1 \leq p < \infty$, the p-norm of a vector $\mathbf{x} \in \mathbb{R}^m$ is defined as

$$\|\mathbf{x}\|_p \triangleq \left(\sum_{i=1}^{m} |x_i|^p \right)^{1/p} \tag{3.1}$$

hence

$$\|\mathbf{x}\|_1 \triangleq \sum_{i=1}^{m} |x_i| \tag{3.2}$$

$$\|\mathbf{x}\|_2 \triangleq \sqrt{\mathbf{x}^\top \mathbf{x}} \tag{3.3}$$

The ∞-norm of a vector $\mathbf{x} \in \mathbb{R}^m$ is defined as

$$\|\mathbf{x}\|_\infty \triangleq \max_{1 \le i \le m} |x_i| \tag{3.4}$$

Throughout the thesis, if the type of the norm is not stated, the 2-norm is used.

Definition 3.3. The $\mathcal{L}_p$-norm of piecewise-continuous integrable functions $\mathbf{f} : [0, +\infty] \to \mathbb{R}^n$ with bounded $\mathcal{L}_p$-norm is defined as

$$\|\mathbf{f}\|_{\mathcal{L}_p} \triangleq \left(\int_0^\infty (\|\mathbf{f}(\tau)\|_p)^p d\tau \right)^{1/p} < \infty, \quad 1 \le p < \infty \tag{3.5}$$

The $\mathcal{L}_\infty$-norm of piecewise-continuous integrable functions $\mathbf{f} : [0, +\infty] \to \mathbb{R}^n$ with bounded $\mathcal{L}_\infty$-norm is defined as

$$\|\mathbf{f}\|_{\mathcal{L}_\infty} \triangleq \max_{1 \le i \le n} \left\{ \sup_{\tau \ge 0} |\mathbf{f}_i(\tau)| \right\} < \infty \tag{3.6}$$

3.4 Lyapunov Stability Theory

This section recalls several fundamental results of Lyapunov stability theory. Consider the nonlinear autonomous system given by the following

$$\dot{\mathbf{x}} = \mathbf{f}(\mathbf{x}), \quad \mathbf{x}(0) = \mathbf{x}_0 \tag{3.7}$$

where $\mathbf{x} \in \mathbb{R}^n$ is the state, and $\mathbf{f}(\mathbf{x}) : \mathbb{R}^n \to \mathbb{R}^n$ is a locally Lipshictz nonlinearity. Before we proceed with the stability theory, consider the following definitions that

is useful in selecting the Lyapunov function.

Definition 3.4 (Symmetric Matrix). The matrix $\mathbf{M} \in \mathbb{R}^{n \times n}$ is symmetric if $\mathbf{M} = \mathbf{M}^\top$

Definition 3.5. The following criteria are defined for the matrix $\mathbf{M} \in \mathbb{R}^{n \times n}$.

1. $\mathbf{M}$ is positive definite if

$$\mathbf{x}^\top \mathbf{M} \mathbf{x} > 0, \quad \forall\, \mathbf{x} \in \mathbb{R}^n - \{0\}, \qquad \mathbf{x}^\top \mathbf{M} \mathbf{x} = 0, \ \text{ for } \mathbf{x} = 0 \tag{3.8}$$

2. $\mathbf{M}$ is positive semi-definite if

$$\mathbf{x}^\top \mathbf{M} \mathbf{x} \geq 0, \quad \forall\, \mathbf{x} \in \mathbb{R}^n \tag{3.9}$$

3. $\mathbf{M}$ is negative definite if

$$\mathbf{x}^\top \mathbf{M} \mathbf{x} < 0, \quad \forall\, \mathbf{x} \in \mathbb{R}^n - \{0\}, \qquad \mathbf{x}^\top \mathbf{M} \mathbf{x} = 0, \ \text{ for } \mathbf{x} = 0 \tag{3.10}$$

4. $\mathbf{M}$ is negative semi-definite if

$$\mathbf{x}^\top \mathbf{M} \mathbf{x} \leq 0, \quad \forall\, \mathbf{x} \in \mathbb{R}^n \tag{3.11}$$

Assume that the nonlinear system (3.7) has an equilibrium at the origin, i.e $\mathbf{x} = 0$. The following stability theorem is presented.

Theorem 3.1 (Lyapunov Stability Theorem) *Let $V : \mathcal{D} \to \mathbf{R}$ be a positive definite continuously differentiable function called Lyapunov function/candidate. If*

1. $V(0) = 0$
2. $V(\mathbf{x}) > 0, \ \ \forall\, x \in \mathcal{D} - \{0\}$
3. $\dot{V}(\mathbf{x}) \leq 0, \ \ \forall\, x \in \mathcal{D} - \{0\}$

then the origin is Lyapunov stable. In addition, if

$$\dot{V}(\mathbf{x}) < 0, \ \ \forall\, x \in \mathcal{D} - \{0\} \tag{3.12}$$

then the origin is asymptotically stable. Moreover, if

$$V(\mathbf{x}) \to \infty \quad as \quad \|\mathbf{x}\| \to \infty \tag{3.13}$$

then the origin is globally asymptotically stable.

Definition 3.6 (Hurwitz Matrix). The matrix $\mathbf{A}$ is Hurwitz if it is a stable matrix, i.e each eigenvalue has a negative real part.

Lemma 3.1 (Lyapunov Equation) *Given the arbitrary symmetric and positive definite matrix $\mathbf{Q} = \mathbf{Q}^\top > 0$, if the matrix $\mathbf{A}$ is Hurwitz, there exists a unique symmetric and positive definite matrix $\mathbf{P} = \mathbf{P}^\top > 0$ satisfying the following Lya-*

punov equation

$$\mathbf{A}^\top \mathbf{P} + \mathbf{P}\mathbf{A} = -\mathbf{Q} \tag{3.14}$$

Proof: Proof can be seen in standard nonlinear control book. ∎

3.5 Invariant Manifolds and System Immersion

For the fundamentals of I&I methodology, the definition of invariant manifold [41] and system immersion [42] are presented here.

Consider an unforced system given by the following

$$\dot{\mathbf{x}} = \mathbf{f}(\mathbf{x}) \tag{3.15}$$

$$\mathbf{y} = \mathbf{h}(\mathbf{x}) \tag{3.16}$$

where $\mathbf{x} \in \mathbb{R}^n$ and $\mathbf{y} \in \mathbb{R}^m$

Consider now the following target system

$$\dot{\boldsymbol{\xi}} = \boldsymbol{\alpha}(\boldsymbol{\xi}) \tag{3.17}$$

$$\boldsymbol{\zeta} = \boldsymbol{\beta}(\boldsymbol{\xi}) \tag{3.18}$$

where $\boldsymbol{\xi} \in \mathbb{R}^p$ $(p < n)$ and $\boldsymbol{\zeta} \in \mathbb{R}^m$

Definition 3.7. For smooth $\mathbf{z}(\mathbf{x})$, the manifold $\mathcal{M} = \{\mathbf{x} \in \mathbb{R}^n \mid \mathbf{z}(\mathbf{x}) = 0\}$ is

called invariant manifold for (3.15) if

$$\mathbf{z}(\mathbf{x}(0)) = 0 \Rightarrow \mathbf{z}(\mathbf{x}(t)) = 0 \quad \forall t \geq 0 \tag{3.19}$$

Definition 3.8. The system (3.17)-(3.18) is called to be immersed into system (3.15)-(3.18), if there exists a smooth mapping $\boldsymbol{\pi} : \mathbb{R}^p \to \mathbb{R}^n$ that satisfies a restricted initial conditions $\mathbf{x}(0) = \boldsymbol{\pi}(\boldsymbol{\xi}(0))$, and $\boldsymbol{\beta}(\xi_1) \neq \boldsymbol{\beta}(\xi_2) \Rightarrow \mathbf{h}(\boldsymbol{\pi}(\xi_1)) \neq \mathbf{h}(\boldsymbol{\pi}(\xi_2))$ such that

$$\mathbf{f}(\boldsymbol{\pi}(\xi)) = \frac{\partial \boldsymbol{\pi}}{\partial \boldsymbol{\xi}} \boldsymbol{\alpha}(\boldsymbol{\xi}), \quad \forall \boldsymbol{\xi} \in \mathbb{R}^p \tag{3.20}$$

3.6 Nonlinear Systems Parametrization

This section presents a lemma needed when dealing with $\mathcal{L}_1$ adaptive control for nonlinear system. For the nonlinear map $f(t, \mathbf{x}(t)) : [0, \infty] \times \mathbb{R}^n \to \mathbb{R}$, suppose the following assumptions hold

Assumption 3.1 (Uniform boundedness of $f(t, \mathbf{x}(t))$). $\exists\ B > 0$ such that

$$|f(t, \mathbf{x}(t))| \leq B, \ \ \forall t \geq 0 \tag{3.21}$$

Assumption 3.2 (Semiglobal uniform boundedness of partial derivatives). for $\delta > 0$, $\exists\ d_{f_x}(\delta) > 0$ and $d_{f_t}(\delta) > 0$ independent of time, such that for arbitrary

$\|\mathbf{x}\|_\infty \leq \delta$, the following holds

$$\left\| \frac{\partial f(t,\mathbf{x})}{\partial \mathbf{x}} \right\|_1 \leq \ d_{f_x}(\delta), \quad \left| \frac{\partial f(t,\mathbf{x})}{\partial t} \right| \leq \ d_{f_t}(\delta) \tag{3.22}$$

Based on these assumptions, two time-varying parameters are obtained from the nonlinear function $f(t,\mathbf{x}(t))$ using $\|\mathbf{x}\|_\infty$ as a regressor. The next lemma proves this statement.

Lemma 3.2 (see [43]) *Let $\mathbf{x}(t)$ be a continuous and (piecewise)-differentiable function of t for $t \geq 0$. If $\|\mathbf{x}_\tau\|_{\mathcal{L}_\infty} \leq \rho$ and $\|\dot{\mathbf{x}}_\tau\|_{\mathcal{L}_\infty} \leq d_x$ for $\tau \geq 0$, where ρ and d_x are some positive constants, then $\exists$ continuous $\theta(t)$ and σ with (piecewise)-continuous derivative, such that $\forall t \in \ [0,\tau]$*

$$f(t,\mathbf{x}(t)) = \theta(t)\|\mathbf{x}\|_\infty + \sigma(t) \tag{3.23}$$

where

$$\begin{aligned} &|\theta(t)| < \theta_\rho, \quad |\dot{\theta}(t)| < d_\theta, \\ &|\sigma(t)| < \sigma_b, \quad |\dot{\sigma}(t)| < d_\sigma \end{aligned} \tag{3.24}$$

with $\theta_\rho \triangleq d_{f_x}$, $\sigma_b \triangleq B + \epsilon$, in which $\epsilon > 0$ is an arbitrary constant, and d_θ, d_σ are computable bounds.

Proof: For proof see [31]. ∎

3.7 Projection Operator

In adaptive control, parameter drift usually exists in the adaptation scheme. Here, one tool which prevents parameter drifting is presented. This tool is called projection operator.

Definition 3.9 (see [44]). Consider the following smooth convex function

$$f(\boldsymbol{\theta}) \triangleq \frac{(\epsilon_\theta + 1)\boldsymbol{\theta}^\top \boldsymbol{\theta} - \theta_{\max}^2}{\epsilon_\theta \theta_{\max}^2}, \quad f : \mathbb{R}^n \to \mathbb{R} \tag{3.25}$$

where $\theta_{\max}$ is the norm bound of vector $\boldsymbol{\theta}$, ϵ_θ is the projection tolerance, and the smooth boundary for the convex compact set is given by

$$\Omega_c \triangleq \{\boldsymbol{\theta} \in \mathbb{R}^n | f(\boldsymbol{\theta}) \leq c\}, \quad 0 \leq c \leq 1 \tag{3.26}$$

The projection operator is given by

$$\text{Proj}(\boldsymbol{\theta}, y) \triangleq \begin{cases} \mathbf{y} & \text{if} \quad f(\boldsymbol{\theta}) < 0 \\ \mathbf{y} & \text{if} \quad f(\boldsymbol{\theta}) \geq 0 \quad \text{and} \quad \nabla f^\top \mathbf{y} \leq 0 \\ \mathbf{y} - \frac{\nabla f}{\|\nabla f\|} \left\langle \frac{\nabla f}{\|\nabla \| f}, \mathbf{y} \right\rangle & \text{if} \quad f(\boldsymbol{\theta}) \geq 0 \quad \text{and} \quad \nabla f^\top \mathbf{y} < 0 \end{cases} \tag{3.27}$$

Property 3.1 (see [44]). For vectors $\mathbf{y} \in \mathbb{R}^n$, $\boldsymbol{\theta}^* \in \boldsymbol{\Omega}_0 \subset \boldsymbol{\Omega}_1 \subset \mathbb{R}^n$, and $\boldsymbol{\theta} \in \boldsymbol{\Omega}_1$, the following property holds

$$(\boldsymbol{\theta} - \boldsymbol{\theta}^*)^\top (\text{Proj}(\boldsymbol{\theta}, \mathbf{y}) - \mathbf{y}) \leq 0 \tag{3.28}$$

3.8 Conclusions

In this chapter, several basic definitions and preliminaries used in the thesis were covered. Next chapter will cover the modelling of the quadrotor UAV.

CHAPTER 4

MODELLING OF THE QUADROTOR UAV

4.1 Introduction

This chapter presents the modelling of the quadrotor UAV. In section 4.2, the introduction on basic concepts of quadrotor is presented. Section 4.3 introduces the derivation of the nonlinear equations of motion of the quadrotor. In this section the physical parameters used in the dynamics are also presented.

4.2 The Basic Concepts of a Quadrotor

A quadrotor is a six-DOF rigid body aerial vehicle, therefore the six different motions of quadrotor are defined. The first three motions of quadrotor are related to the translational motion, and the remaining are the rotational motions. In translational motions, the quadrotor is able to move forward/backward, lateral and vertical. In rotational motion the quadrotor has roll, pitch and yaw motion.

The quadrotor has four propellers, hence the combinations of them have to be

selected to represent the basic movement. The four possible basic movements of the quadrotor are defined in the following

1. Throttle $\triangleq u$ (Newton). By increasing or decreasing all the propeller speeds by the same amount, the throttle (u) is generated, it generates a vertical force with respect to (w.r.t) the body frame.

2. Roll $\triangleq \tau_p$ (Newton.meter). This command is produced by increasing (decreasing) the right propeller and decreasing (increasing) the left propeller at the same time. It provides the torque τ_p w.r.t the x-axis in the body frame. This torque creates roll motion in the quadrotor.

3. Pitch $\triangleq \tau_q$ (Newton.meter). This command is provided in similar way as the roll motion, it is produced by increasing (decreasing) the front propeller and decreasing (increasing) the rear propeller at the same time. This way, the torque τ_q w.r.t the y-axis in the body frame is generated. This torque creates pitch motion in the quadrotor.

4. Yaw $\triangleq \tau_r$ (Newton.meter). The fact that the front-rear and right-left propellers are rotated in different directions, when the speed of the front-rear propellers is increased (decrease) and the speed of the right-left propellers is decreased (increase), the yaw motion is achieved. It generates a torque τ_r w.r.t to the z-axis in the body frame.

The analysis of the motion in 6-DOF requires the use of two coordinate frames -the body-fixed frame and the inertial (earth) frame. As such, the position and

orientation are expressed with respect to the inertial frame and both linear and angular velocities are described w.r.t the body frame. These two coordinate frames are illustrated in Figure (4.1)

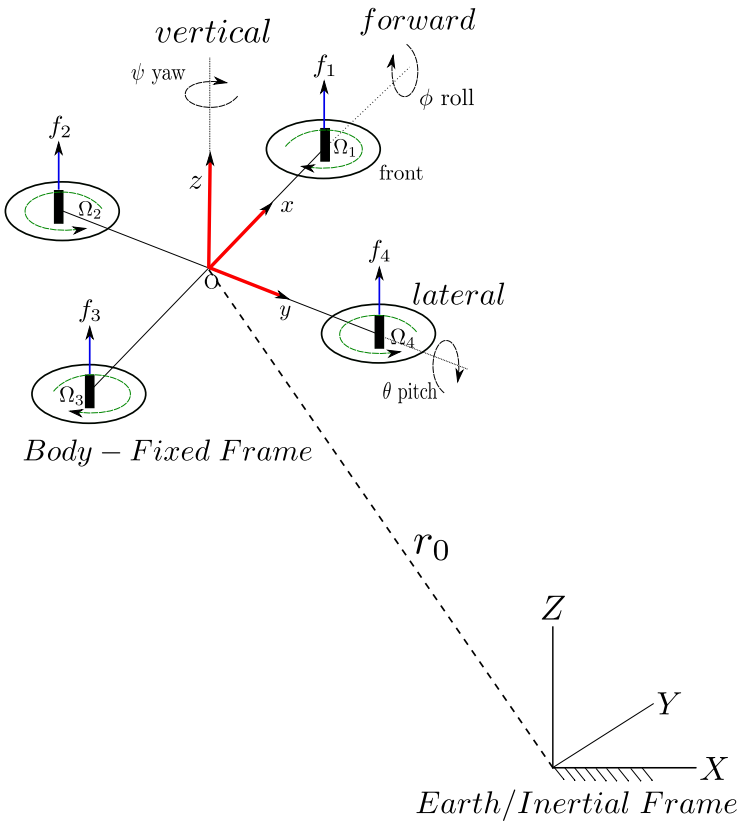

Figure 4.1: Body-Fixed and Earth Reference Frame

The general motion of a quadrotor in 6 DOF can be described by the following vectors

$$\boldsymbol{\eta} = [\boldsymbol{\eta}_1,\ \boldsymbol{\eta}_2]^\top \quad \boldsymbol{\eta}_1 = [x,\ y,\ z]^\top \quad \boldsymbol{\eta}_2 = [\phi,\ \theta,\ \psi]^\top$$
$$\boldsymbol{\nu} = [\boldsymbol{\nu}_1,\ \boldsymbol{\nu}_2]^\top \quad \boldsymbol{\nu}_1 = [u,\ v,\ w]^\top \quad \boldsymbol{\nu}_2 = [p,\ q,\ r]^\top \tag{4.1}$$

where $\boldsymbol{\eta}$ is composed of the position vector, $\boldsymbol{\eta}_1$ representing forward (x), lateral (y),

and vertical (z) motion respectively, and the orientation vector, $\boldsymbol{\eta}_2$ representing roll (ϕ), pitch (θ), and yaw (ψ) motion respectively. The velocity vector $\boldsymbol{\nu}$ is composed of the linear velocity vector , $\boldsymbol{\nu}_1$, and angular velocity vector, $\boldsymbol{\nu}_2$. The dynamic coupling between the inertial frame and the body frame is given by a velocity transformation

$$\dot{\boldsymbol{\eta}}_i = \mathbf{J}_i(\boldsymbol{\eta}_2)\boldsymbol{\nu}_i, \qquad \boldsymbol{\nu}_i = \mathbf{J}_i^{-1}(\boldsymbol{\eta}_2)\dot{\boldsymbol{\eta}}_i \tag{4.2}$$

where $\mathbf{J}_i(\boldsymbol{\eta}_2), \;\; i = 1, 2$ is the transformation matrix that is function of the Euler angles. The transformation matrix relating the translational velocity in the body frame to the translational velocity in the inertial frame is given by

$$\mathbf{J}_1(\boldsymbol{\eta}_2) = \begin{bmatrix} \cos\psi\cos\theta & -\sin\psi\cos\phi + \cos\psi\sin\theta\sin\phi & \sin\psi\sin\phi + \cos\psi\cos\phi\sin\theta \\ \sin\psi\cos\theta & \cos\psi\cos\phi + \sin\phi\sin\theta\sin\psi & -\cos\psi\sin\phi + \sin\psi\cos\phi\sin\theta \\ -\sin\theta & \cos\theta\sin\phi & \cos\phi\cos\theta \end{bmatrix} \tag{4.3}$$

and has the following property

$$\mathbf{J}_1^{-1}(\boldsymbol{\eta}_2) = \mathbf{J}_1^{\top}(\boldsymbol{\eta}_2) \tag{4.4}$$

The body fixed angular velocity vector $\boldsymbol{\nu}_2$ and the Euler rate vector $\dot{\boldsymbol{\eta}}_2$ are related through a transformation matrix $\mathbf{J}_2(\boldsymbol{\eta}_2)$ given by

$$\mathbf{J}_2(\boldsymbol{\eta}_2) = \begin{bmatrix} 1 & \sin\phi\tan\theta & \cos\phi\tan\theta \\ 0 & \cos\phi & -\sin\phi \\ 0 & \dfrac{\cos\phi}{\cos\theta} & \dfrac{\cos\phi}{\cos\theta} \end{bmatrix} \tag{4.5}$$

4.3 Equations of Motion

In the development of the equations of motion of the quadrotor UAV, the following assumptions are observed

Assumption 4.1.

1. The structure of the quadrotor is rigid.
2. The structure of the quadrotor is symmetrical.
3. The Centre of Gravity (CoG) is coincident with the body fixed frame
4. The propellers are rigid.
5. The body principal axes of inertia and the axes of the body frame are assumed to be coincident. So, the inertia matrix $\mathbf{I}_{\mathrm{M}}$ is diagonal.
6. The drag terms are assumed to obey Stoke's Law, hence the translational (rotational) drag is proportional to the translational (angular) velocity.

Lagrangian for the generalized coordinate with T_{trans} (kinetic energy for the translational motion), T_{rot} (kinetic energy of the orientation), and U(potential

energy), is given by the following

$$L(\mathbf{q}, \dot{\mathbf{q}}) = T_{\text{trans}} + T_{\text{rot}} - U = \frac{1}{2} m \dot{\boldsymbol{\eta}}_1^\top \dot{\boldsymbol{\eta}}_1 + \frac{1}{2} \dot{\boldsymbol{\eta}}_2^\top \mathbf{I}_{\boldsymbol{\eta}} \dot{\boldsymbol{\eta}}_2 - mgz \tag{4.6}$$

where $\mathbf{I}_\eta$ is given by the following

$$\mathbf{I}_{\boldsymbol{\eta}} = (\mathbf{J}_2^{-1})^\top \mathbf{I}_{\text{M}} \mathbf{J}_2^{-1}, \quad \mathbf{I}_{\text{M}} = \begin{bmatrix} I_{xx} & 0 & 0 \\ 0 & I_{yy} & 0 \\ 0 & 0 & I_{zz} \end{bmatrix} \tag{4.7}$$

The Euler-Lagrangian equation w.r.t the translational motion is given by

$$\frac{d}{dt} \frac{\partial L}{\partial \dot{\boldsymbol{\eta}}_1} - \frac{\partial L}{\partial \boldsymbol{\eta}_1} = \mathbf{F} \tag{4.8}$$

where F is the force responsible for the translational motion. The Euler-Lagrangian equation w.r.t the rotational motion is given by

$$\frac{d}{dt} \frac{\partial L}{\partial \dot{\boldsymbol{\eta}}_2} - \frac{\partial L}{\partial \boldsymbol{\eta}_2} = \boldsymbol{\tau} \tag{4.9}$$

where τ is the torque responsible for the rotational motion. The drag terms are represented by notations k_r for the rotational drag, and k_t for the translational drag. Using equation (4.8) and involving drag term k_t, the translational dynamics

of the quadrotor is conveniently expressed as

$$\ddot{\boldsymbol{\eta}}_1 = -g\mathbf{z}_e + \mathbf{J}_1(\boldsymbol{\eta}_2)\frac{u}{m}\mathbf{z}_e - \frac{k_t}{m}\dot{\boldsymbol{\eta}}_1 \tag{4.10}$$

where $\mathbf{z}_e = [0,\ 0,\ 1]^\top$. The main thrust force u generated by the four propellers is given by

$$u = f_1 + f_2 + f_3 + f_4 \tag{4.11}$$

where f_i's are the upward lifting forces generated by each rotor and are given by $f_i = k_i\Omega_i^2$, where $k_i (i = 1, \ldots, 4)$, are positive constant and Ω_i's are the angular speeds of the motors respectively. As seen in equation (4.10), the three translational motion of the quadrotor can be controlled only by one input u, this structure is called an underactuated system. Mathematically, the following definition of underactuated mechanical systems is suitable for this case, it is adapted from [45][46].

Definition 4.1 (Underactuated System). Consider an affine mechanical system described by

$$\ddot{\mathbf{q}} = \mathbf{f}(\mathbf{q}, \dot{\mathbf{q}}) + \mathbf{G}(\mathbf{q})\mathbf{u} \tag{4.12}$$

where $\mathbf{q}$ is a vector of generalized coordinates, $\mathbf{f}$ is the vector of the dynamics of the system, $\mathbf{G}$ is the input matrix, and $\mathbf{u}$ is the vector of control inputs. System

4.12 is called an underactuated system if

$$\text{rank}(\mathbf{G}) < \dim(\mathbf{q}) \tag{4.13}$$

From this definition, the inputs can not instantaneously set the acceleration in all directions of the configuration space. Using definition 4.1, if equation (4.10) is rewritten in the form of (4.12), the rank of input matrix is found to be less than the number of the states, hence it is underactuated.

Utilizing equation (4.9) and involving drag term k_r, the rotational motion of the quadrotor on the body frame is given by

$$\dot{\boldsymbol{\nu}}_2 = \mathbf{I}_{\mathrm{M}}^{-1}(-(\boldsymbol{\nu}_2 \times \mathbf{I}_{\mathrm{M}}\boldsymbol{\nu}_2) - I_R(\boldsymbol{\nu}_2 \times \mathbf{z}_e)\Omega - k_r\boldsymbol{\nu}_2 + \boldsymbol{\tau}) \tag{4.14}$$

where $\mathbf{I}_{\mathrm{M}} = \text{diag}(I_x, I_y, I_z)$ is the total inertia of the quadrotor, I_R is the propeller inertia, $\times$ represents the vector cross product, k_r is the rotational drag coefficient which is proportional to the angular velocity, $\boldsymbol{\tau} = [\tau_p,\ \tau_q,\ \tau_r]^\top$ is the torque acting on the body responsible for rotational movements, and $\Omega = \Omega_1 - \Omega_2 + \Omega_3 - \Omega_4$.

The relationship between the forces generated by the propellers and the force and torques acting around the body is given by the equation (4.15), where l is the distance from the motor to the center of mass, and d is ratio between drag and thrust coefficient of the blade,

$$\begin{bmatrix} \boldsymbol{\tau} \\ u \end{bmatrix} = \begin{bmatrix} \tau_p \\ \tau_q \\ \tau_r \\ u \end{bmatrix} = \begin{bmatrix} 0 & l & 0 & -l \\ l & 0 & -l & 0 \\ d & -d & d & -d \\ 1 & 1 & 1 & 1 \end{bmatrix} \begin{bmatrix} f_1 \\ f_2 \\ f_3 \\ f_4 \end{bmatrix} \tag{4.15}$$

The quadrotor model used in this thesis has parameters as mentioned in Table (4.1), these parameters are obtained from the previous work presented in [47].

Mass	m	0.52 kg
Gravity Acceleration	g	9.8 m/s^2
Translational Drag Coefficient	k_t	0.95
Rotational Drag Coefficient	k_r	0.105
Ratio Between Drag and Thrust Coefficient of the Blade	d	$7.5e^{-7}$ $kg.m^2$
Inertia Coefficient on x-axis	I_{xx}	0.0069 $kg.m^2$
Inertia Coefficient on y-axis	I_{yy}	0.0069 $kg.m^2$
Inertia Coefficient on z-axis	I_{zz}	0.0129 $kg.m^2$
Arm Length	l	0.205 m
Propeller Inertia	I_R	$3.36e^{-5}$ $kg.m^2$

Table 4.1: Quadrotor's physical parameters

4.4 Conclusions

This chapter covers the basic concepts and modelling of the quadrotor. This model will be used in the development of the controller in the next chapters.

CHAPTER 5

I&I STABILIZING CONTROLLER

5.1 Introduction

The I&I method for stabilization of nonlinear systems was first introduced by Astolfi in 2003 [2]. The idea of I&I method is based on the system immersion and manifold invariance concepts. The approach of I&I is applicable for stabilization of nonlinear system, design of nonlinear observer and adaptive control. In this chapter, the I&I stabilization problem is introduced and the backstepping control is used for the benchmarking.

5.1.1 I&I Stabilization

For the I&I stabilization, the objective of the controller is to stabilize the system by immersing the plant dynamics into a target dynamic with a desired behaviour. The major result of I&I stabilization method is summarized in the following theorem.

Theorem 5.1 (See [2]) *Consider the system*

$$\dot{\mathbf{x}} = \mathbf{f}(\mathbf{x}) + \mathbf{g}(\mathbf{x})\mathbf{u} \tag{5.1}$$

with state $\mathbf{x} \in \mathbb{R}^n$ *and control* $\mathbf{u} \in \mathbb{R}^m$*, with an equilibrium point* $\mathbf{x}_* \in \mathbb{R}^n$ *to be stabilized. Let* $p < n$ *and assume we can find mappings*

$$\begin{aligned} &\boldsymbol{\alpha} : \mathbb{R}^p \to \mathbb{R}^p, \quad \boldsymbol{\pi} : \mathbb{R}^p \to \mathbb{R}^n, \quad \mathbf{c} : \mathbb{R}^p \to \mathbb{R}^m, \\ &\boldsymbol{\phi} : \mathbb{R}^n \to ; \mathbb{R}^{n-p}, \quad \boldsymbol{\psi} : \mathbb{R}^n \to \mathbb{R}^{n \times (n-p)} \end{aligned} \tag{5.2}$$

such that the following hold.

H1*. (Target system) The system*

$$\dot{\boldsymbol{\xi}} = \boldsymbol{\alpha}(\boldsymbol{\xi}) \tag{5.3}$$

with state $\boldsymbol{\xi} \in \mathbb{R}^p$*, has an asymptotically stable equilibrium at* $\boldsymbol{\xi}_* \in \mathbb{R}^p$ *and* $\mathbf{x}_* = \boldsymbol{\pi}(\boldsymbol{\xi}_*)$*.*

H2*. (Immersion condition). For all* $\boldsymbol{\xi} \in \mathbb{R}^p$

$$\mathbf{f}(\boldsymbol{\pi}(\boldsymbol{\xi})) + \mathbf{g}(\boldsymbol{\pi}(\boldsymbol{\xi}))\mathbf{c}(\boldsymbol{\pi}(\boldsymbol{\xi})) = \frac{\partial \boldsymbol{\pi}}{\partial \boldsymbol{\xi}} \boldsymbol{\alpha}(\boldsymbol{\xi}) \tag{5.4}$$

H3. *(Implicit manifold).The set identity*

$$\{\mathbf{x} \in \mathbb{R}^n | \boldsymbol{\phi}(\mathbf{x}) = 0\} = \{\mathbf{x} \in \mathbb{R}^n | \mathbf{x} = \boldsymbol{\pi}(\boldsymbol{\xi}) \ \textit{for some} \ \boldsymbol{\xi} \in \mathbb{R}^p\} \tag{5.5}$$

holds.

H4. *(Manifold attractivity and trajectory boundedness). All trajectories of the system*

$$\dot{\mathbf{z}} = \frac{\partial \boldsymbol{\phi}}{\partial \mathbf{x}} \left(\mathbf{f}(\mathbf{x}) + \mathbf{g}(\mathbf{x})\boldsymbol{\psi}(\mathbf{x}, \mathbf{z})\right) \tag{5.6}$$

$$\dot{\mathbf{x}} = \mathbf{f}(\mathbf{x}) + \mathbf{g}(\mathbf{x})\boldsymbol{\psi}(\mathbf{x}, \mathbf{z}) \tag{5.7}$$

are bounded and satisfy

$$\lim_{t \to \infty} \mathbf{z}(t) = 0 \tag{5.8}$$

Then $\mathbf{x}_*$ *is an asymptotically equilibrium of the closed loop system*

$$\dot{\mathbf{x}} = \mathbf{f}(\mathbf{x}) + \mathbf{g}(\mathbf{x})\boldsymbol{\psi}(\mathbf{x}, \boldsymbol{\phi}(\mathbf{x}))$$

Proof: For the proof readers can refer to [2]. ∎

5.2 Quadrotor Trajectory Tracking Control

As mentioned earlier, the quadrotor is categorized as an underactuated system. In order to solve the underactuated problem, a two-loop controller is introduced. In the outer loop, translational dynamics are controlled and the desired attitude (ϕ, θ, ψ) is extracted and fed to the inner loop. PD tracking control is utilized as the outer loop controller since the dynamics are linear in terms of parameters and a predefined flight trajectory in the inertial frame is used as the reference for the tracking control.

To track the desired attitude produced by the the outer loop, the I&I technique is implemented in the inner loop. The results of the inner loop tracking control are used by the outer loop to govern the movements of the quadrotor in the inertial coordinates. The complete structure of the controller can be seen in Figure (5.1). Under I&I control, the equivalent closed loop system is linear.

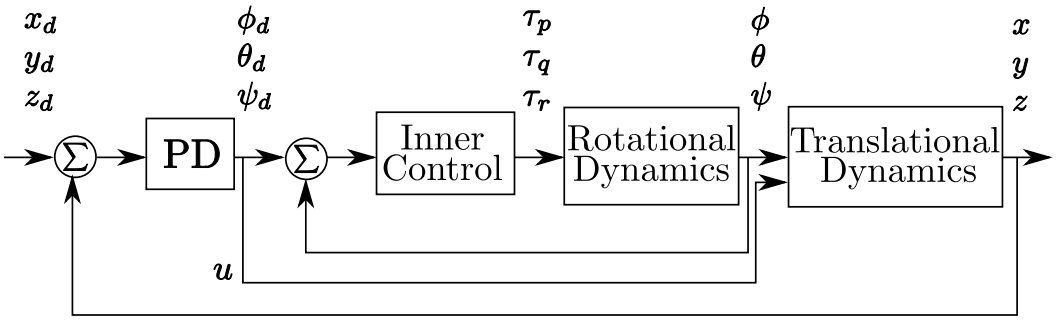

Figure 5.1: Control Structure of Quadrotor

5.2.1 Attitude Control Design: Invariance and Immersion

The objective of the inner loop is to achieve zero error between desired attitude provided by the outer loop and actual attitude measured by the sensors. The dynamics of the quadrotor in the inner loop are the angular velocities on the body frame, therefore, the rotation matrix $\mathbf{J}_2(\boldsymbol{\eta}_2)$ needs to be applied to transform the attitude in the inertial frame to the angular velocity in the body frame. One should note that the system is fully actuated w.r.t attitude dynamics.

From equation (4.14), the state space representation of the rotational dynamics can be expressed as

$$\dot{\boldsymbol{\nu}}_2 = \begin{bmatrix} \dot{p} \\ \dot{q} \\ \dot{r} \end{bmatrix} = \mathbf{F}(\boldsymbol{\nu}_2) + \mathbf{G}\boldsymbol{\tau} \tag{5.9}$$

The angular body velocity vector $\boldsymbol{\nu}_2 = [p, q, r]^\top$ cannot be integrated directly to obtain actual angular coordinates. This is due to the fact that $\left(\int_0^t \boldsymbol{\nu}_2(\mathrm{s})\mathrm{ds}\right)$ does not have any physical interpretation. For this reason, we introduce virtual state $\left(\mathbf{x}_1 = \int_0^t \boldsymbol{\nu}_2(\mathrm{s})\mathrm{ds}\right)$ for I&I control design purpose, such that the complete state equation for the rotational dynamics becomes

$$\begin{aligned} \dot{\mathbf{x}}_1 &= \boldsymbol{\nu}_2 = \mathbf{x}_2 \\ \dot{\mathbf{x}}_2 &= \dot{\boldsymbol{\nu}}_2 = \mathbf{F}(\boldsymbol{\nu}_2) + \mathbf{G}\boldsymbol{\tau} = \mathbf{F}(\mathbf{x}_2) + \mathbf{G}\boldsymbol{\tau} \end{aligned} \tag{5.10}$$

Using equation (5.10), for a smooth reference signal, the following body angular velocity error vectors are defined

$$\mathbf{e}_1 = \mathbf{x}_1 - \mathbf{x}_{1d}, \quad \dot{\mathbf{e}}_1 = \dot{\mathbf{x}}_1 - \dot{\mathbf{x}}_{1d} = \mathbf{x}_2 - \dot{\mathbf{x}}_{1d} = \mathbf{e}_2, \quad \dot{\mathbf{e}}_2 = \dot{\mathbf{x}}_2 - \ddot{\mathbf{x}}_{1d} \tag{5.11}$$

From equation (5.11), the error dynamics of the quadrotor body angular velocity are

$$\begin{aligned} \dot{\mathbf{e}}_1 &= \mathbf{e}_2 \\ \dot{\mathbf{e}}_2 &= \mathbf{F}(\mathbf{x}_2) + \mathbf{G}\boldsymbol{\tau} - \ddot{\mathbf{x}}_{1d} \end{aligned} \tag{5.12}$$

In order to apply the I&I controller, **H1**-**H4** conditions of theorem (5.1) need to be verified.

(H1) (Target system). The key idea is to immerse a one-dimensional system into a two-dimensional one. Thus, we define the global asymptotic stable target dynamic vector as

$$\dot{\boldsymbol{\xi}} = -\mu\boldsymbol{\xi} \tag{5.13}$$

with $\mu > 0$, and $\boldsymbol{\xi} \in \mathbb{R}$.

(H2) (Immersion condition). By fixing $\boldsymbol{\pi}_1(\boldsymbol{\xi}) = \boldsymbol{\xi}$, equation (5.4) becomes

$$\boldsymbol{\pi}_2(\boldsymbol{\xi}) = -\mu\boldsymbol{\xi} \tag{5.14}$$

(H3) (Implicit manifold). The manifold $\mathbf{e} = \boldsymbol{\pi}(\boldsymbol{\xi})$ can be implicitly described by $\mathcal{M} = \{\, \mathbf{e} \in \mathbb{R}^2 \mid \boldsymbol{\phi}(\mathbf{e}) = 0\}$, with

$$\boldsymbol{\phi}(\mathbf{e}) = \mathbf{e}_2 - \boldsymbol{\pi}_2(\boldsymbol{\xi}) = \mathbf{e}_2 + \mu \mathbf{e}_1 \tag{5.15}$$

(H4) (Manifold attractivity and trajectory boundedness). The off-the-manifold coordinates are $\mathbf{z} = \boldsymbol{\phi}(\mathbf{e})$ and straightforward calculations show that

$$\begin{aligned} \dot{\mathbf{z}} = \frac{\partial \boldsymbol{\phi}(\mathbf{e})}{\partial t} &= \begin{bmatrix} \dfrac{\partial \boldsymbol{\phi}(\mathbf{e})}{\partial \mathbf{e}_1} & \dfrac{\partial \boldsymbol{\phi}(\mathbf{e})}{\partial \mathbf{e}_2} \end{bmatrix} \begin{bmatrix} \dot{\mathbf{e}}_1 \\ \\ \dot{\mathbf{e}}_2 \end{bmatrix} \\ &= \mu \mathbf{e}_2 + \mathbf{F}(\mathbf{x}_2) + \mathbf{G}\boldsymbol{\psi}(\mathbf{e}, \mathbf{z}) - \ddot{\mathbf{x}}_{1d} \end{aligned} \tag{5.16}$$

where $\boldsymbol{\psi}(\mathbf{e}, \mathbf{z})$ is the actual controller that is applied. The desired off-the-manifold dynamics can be assigned arbitrarily, for instance fix it to $\dot{\mathbf{z}} = -\gamma \mathbf{z}$, with $\gamma > 0$. This yields

$$-\gamma \mathbf{z} = \mu \mathbf{e}_2 + \mathbf{F}(\mathbf{x}_2) + \mathbf{G}\boldsymbol{\psi}(\mathbf{e}, \mathbf{z}) - \ddot{\mathbf{x}}_{1d} \tag{5.17}$$

The controller design is completed by choosing

$$\boldsymbol{\psi}(\mathbf{e}, \mathbf{z}) = (\mathbf{G}^\top \mathbf{G})^{-1} \mathbf{G}^\top (-\gamma \mathbf{z} - \mathbf{F}(\mathbf{x}_2) - \mu \mathbf{e}_2 + \ddot{\mathbf{x}}_{1d}) \tag{5.18}$$

This yields the following closed loop dynamics

$$\begin{aligned}
\dot{\mathbf{z}} &= -\gamma \mathbf{z} \\
\dot{\mathbf{e}}_1 &= \mathbf{e}_2 \\
\dot{\mathbf{e}}_2 &= \mathbf{F}(\mathbf{x}_2) + \mathbf{G}\boldsymbol{\psi}(\mathbf{e}, \mathbf{z}) - \ddot{\mathbf{x}}_{1d}
\end{aligned} \tag{5.19}$$

5.2.2 Attitude Control Design: Backstepping

This section presents the derivation of the backstepping controller for benchmarking purpose. Inspired by Zuo's work [1] and taking into account the rotational drag terms, the attitude control of the quadrotor based on the backstepping technique is designed. The detail of the backstepping technique can be found in [48]. Defining the dynamic error as

$$\begin{aligned}
\mathbf{Z}_1 &= \boldsymbol{\eta}_2 - \boldsymbol{\eta}_{2d} \\
\mathbf{Z}_2 &= \boldsymbol{\nu}_2 - \boldsymbol{\nu}_{2d}
\end{aligned} \tag{5.20}$$

Select the Lyapunov candidate as

$$V_1(\mathbf{Z}_1) = \frac{1}{2}\mathbf{Z}_1^\top \mathbf{Z}_1 \tag{5.21}$$

Deriving the selected Lyapunov candidate along the trajectory of (5.20) gives

$$\dot{V}_1(\mathbf{Z}_1) = \mathbf{Z}_1^\top \dot{\mathbf{Z}}_1 = \mathbf{Z}_1^\top (\mathbf{J}_2(\boldsymbol{\eta}_2)\boldsymbol{\nu}_2 - \dot{\boldsymbol{\eta}}_{2d}) \tag{5.22}$$

If $\mathbf{J}_2(\boldsymbol{\eta}_2)$ is invertible, $\boldsymbol{\nu}_2$ can be seen as a virtual control signal $\boldsymbol{\nu}_{2v}$ and can be selected to satisfy $\dot{V}_1(\mathbf{Z}_1) < 0$ with

$$\boldsymbol{\nu}_{2v} = \mathbf{J}_2(\boldsymbol{\eta}_2)^{-1}(\dot{\boldsymbol{\eta}}_{2d} - \boldsymbol{\Gamma}_1 \mathbf{Z}_1) \tag{5.23}$$

where $\boldsymbol{\nu}_{2v}$ is the desired angular velocity and $\boldsymbol{\Gamma}_1$ is a positive definite matrix. To have a good numerical result, computation of the derivative of $\boldsymbol{\nu}_{2v}$ has to be avoided, hence the first-order command filter is introduced to track the desired angular velocity $\boldsymbol{\nu}_{2v}$

$$\dot{\boldsymbol{\nu}}_{2d} = -\mathbf{T}(\boldsymbol{\nu}_{2d} - \boldsymbol{\nu}_{2v}) \tag{5.24}$$

The time constant matrix $\mathbf{T} = \mathrm{diag}(t_1, t_2, t_3) > 0$ should be as large as possible to achieve fast tracking. To compensate the error in the tracking, a new vector $\boldsymbol{\varepsilon}$ is introduced and its dynamics is given by

$$\dot{\boldsymbol{\varepsilon}} = -\boldsymbol{\Gamma}_1 \boldsymbol{\varepsilon} + \mathbf{J}_2(\boldsymbol{\eta}_2)(\boldsymbol{\nu}_{2d} - \boldsymbol{\nu}_{2v}) \tag{5.25}$$

The Euler angles tracking errors are then redefined as

$$\bar{\mathbf{Z}}_1 = \mathbf{Z}_1 - \boldsymbol{\varepsilon} = \boldsymbol{\eta}_2 - \boldsymbol{\eta}_{2d} - \boldsymbol{\varepsilon} \tag{5.26}$$

Let candidate compound Lyapunov function

$$V_2(\bar{\mathbf{Z}}_1, \mathbf{Z}_2) = \frac{1}{2}\bar{\mathbf{Z}}_1^\top \bar{\mathbf{Z}}_1 + \frac{1}{2}\mathbf{Z}_2^\top \mathbf{Z}_2 \tag{5.27}$$

Taking the time derivative of $V_2(\bar{\mathbf{Z}}_1, \mathbf{Z}_2)$ along the trajectory of (5.20) and (4.14) yields

$$\begin{aligned}
\dot{V}_2(\bar{\mathbf{Z}}_1, \mathbf{Z}_2) &= \bar{\mathbf{Z}}_1^\top \dot{\bar{\mathbf{Z}}}_1 + \frac{1}{2}\mathbf{Z}_2^\top \dot{\mathbf{Z}}_2 \\
&= \bar{\mathbf{Z}}_1^\top [\mathbf{J}_2(\boldsymbol{\eta}_2)\boldsymbol{\nu}_2 - \dot{\boldsymbol{\eta}}_{2d} + \boldsymbol{\Gamma}_1 \boldsymbol{\varepsilon} - \mathbf{J}_2(\boldsymbol{\eta}_2)(\boldsymbol{\nu}_{2d} - \boldsymbol{\nu}_{2v})] + \mathbf{Z}_2^\top [\mathbf{I}_{\mathrm{M}}^{-1}(-(\boldsymbol{\nu}_2 + \mathbf{I}_{\mathrm{M}}\boldsymbol{\nu}_2) \\
&\quad - I_R(\boldsymbol{\nu}_2 \times \mathbf{z}_e)\Omega - k_r \boldsymbol{\nu}_2 + \boldsymbol{\tau} - \dot{\boldsymbol{\nu}}_{2d}] \\
&= -\bar{\mathbf{Z}}_1^\top \boldsymbol{\Gamma}_1 \bar{\mathbf{Z}}_1 + \mathbf{Z}_2^\top [\mathbf{I}_{\mathrm{M}}^{-1}(-(\boldsymbol{\nu}_2 + \mathbf{I}_{\mathrm{M}}\boldsymbol{\nu}_2) - I_R(\boldsymbol{\nu}_2 \times \mathbf{z}_e)\Omega - k_r \boldsymbol{\nu}_2 + \boldsymbol{\tau} - \dot{\boldsymbol{\nu}}_{2d} \\
&\quad + \mathbf{J}_2^\top(\boldsymbol{\eta}_2)\bar{\mathbf{Z}}_1]
\end{aligned} \tag{5.28}$$

If the control input $\boldsymbol{\tau}$ is selected to be

$$\begin{aligned}
\boldsymbol{\tau} =& (\boldsymbol{\nu}_2 \times \mathbf{I}_{\mathrm{M}}\boldsymbol{\nu}_2) + I_R(\boldsymbol{\nu}_2 \times \mathbf{z}_e)\Omega + k_r \boldsymbol{\nu}_2 - \mathbf{I}_{\mathrm{M}}\mathbf{T}\boldsymbol{\nu}_{2d} + \mathbf{I}_{\mathrm{M}}\mathbf{T}\mathbf{J}_2^{-1}(\boldsymbol{\eta}_2)\dot{\boldsymbol{\eta}}_{2d} \\
&- \mathbf{I}_{\mathrm{M}}\mathbf{T}\mathbf{J}_2^{-1}(\boldsymbol{\eta}_2)\boldsymbol{\Gamma}_1(\boldsymbol{\eta}_2 - \boldsymbol{\eta}_{2d}) - \mathbf{I}_{\mathrm{M}}\mathbf{J}^\top(\boldsymbol{\eta}_2)(\boldsymbol{\eta}_2 - \boldsymbol{\eta}_{2d} - \boldsymbol{\varepsilon}) - \mathbf{I}_{\mathrm{M}}\boldsymbol{\Gamma}_2(\boldsymbol{\nu}_2 - \boldsymbol{\nu}_{2d})
\end{aligned} \tag{5.29}$$

For $\mathbf{\Gamma}_2 > 0$, the $\dot{V}_2(\bar{\mathbf{Z}}_1, \mathbf{Z}_2)$ satisfies

$$\dot{V}_2(\bar{\mathbf{Z}}_1, \mathbf{Z}_2) = -\bar{\mathbf{Z}}_1^\top \mathbf{\Gamma}_1 \bar{\mathbf{Z}}_1 - \mathbf{Z}_2^\top \mathbf{\Gamma}_2 \mathbf{Z}_2 < 0 \tag{5.30}$$

From equation 5.30, the tracking errors $\bar{\mathbf{Z}}_1$ and $\mathbf{Z}_2$ converge to zero asymptotically. In the control input equation, the derivative action needs to be avoided. Linear tracking differentiator is introduced to obtain the derivative signal $\dot{\boldsymbol{\eta}}_{2d}$

$$\begin{aligned} \dot{\mathbf{X}}_1 =& \mathbf{X}_2 \\ \dot{\mathbf{X}}_2 =& -2\mathbf{\Lambda}\mathbf{X}_2 - \mathbf{\Lambda}^2(\mathbf{X}_1 - \boldsymbol{\eta}_{2d}) \end{aligned} \tag{5.31}$$

The linear tracking differentiator works like an overdamped second order filter with modes equal to $\mathbf{\Lambda} = \text{diag}(\lambda_1, \lambda_2, \lambda_3) > 0$, with λ_i large enough to guarantee fast tracking. Then, $\dot{\boldsymbol{\eta}}_{2d}$ can be replaced with $\mathbf{X}_2$

$$\begin{aligned} \boldsymbol{\tau} =& (\boldsymbol{\nu}_2 \times \mathbf{I}_\text{M}\boldsymbol{\nu}_2) + I_R(\boldsymbol{\nu}_2 \times \mathbf{z}_e)\Omega + k_r\boldsymbol{\nu}_2 - \mathbf{I}_\text{M}\mathbf{T}\boldsymbol{\nu}_{2d} + \mathbf{I}_\text{M}\mathbf{T}\mathbf{J}_2^{-1}(\boldsymbol{\eta}_2)\mathbf{X}_2 \\ & - \mathbf{I}_\text{M}\mathbf{T}\mathbf{J}_2^{-1}(\boldsymbol{\eta}_2)\mathbf{\Gamma}_1(\boldsymbol{\eta}_2 - \boldsymbol{\eta}_{2d}) - \mathbf{I}_\text{M}\mathbf{J}^\top(\boldsymbol{\eta}_2)(\boldsymbol{\eta}_2 - \boldsymbol{\eta}_{2d} - \boldsymbol{\varepsilon}) - \mathbf{I}_\text{M}\mathbf{\Gamma}_2(\boldsymbol{\nu}_2 - \boldsymbol{\nu}_{2d}) \end{aligned} \tag{5.32}$$

5.2.3 Position Control Design

In the outer loop, PD control for position tracking is utilized and the desired attitude for the inner loop is extracted. The scheme of control and extraction of desired attitude is inspired by [1], with translational drag taken into consideration.

The position error vector is defined as

$$\boldsymbol{\eta}_{1e} = \boldsymbol{\eta}_{1d} - \boldsymbol{\eta}_1 \tag{5.33}$$

where the vector $\boldsymbol{\eta}_{1d}$ is the desired position of the center mass of the quadrotor. The second order position error equation for the smooth reference signal is given by

$$\ddot{\boldsymbol{\eta}}_{1e} + \mathbf{K}_D \dot{\boldsymbol{\eta}}_{1e} + \mathbf{K}_P \boldsymbol{\eta}_{1e} = \mathbf{0} \tag{5.34}$$

Based on Routh-Hurwitz criterion, if $\mathbf{K}_D$ and $\mathbf{K}_P$ are selected to be positive definite matrices, then the position error $\boldsymbol{\eta}_{1e}$ converges to zero exponentially. Substituting (5.33) in (5.34) to obtain

$$\ddot{\boldsymbol{\eta}}_1 = \ddot{\boldsymbol{\eta}}_{1d} + \mathbf{K}_D(\dot{\boldsymbol{\eta}}_{1d} - \dot{\boldsymbol{\eta}}_1) + \mathbf{K}_P(\boldsymbol{\eta}_{1d} - \boldsymbol{\eta}_1) \tag{5.35}$$

Using equation (5.35) as the virtual input, and redefining it as $\mathbf{U} = \ddot{\boldsymbol{\eta}}_1 = [U_1\ U_2\ U_3]^\top$. Substituting $\mathbf{U}$ in equation (4.10) yields

$$\mathbf{U} = -g\mathbf{z}_e + \mathbf{J}_1(\boldsymbol{\eta}_2)\frac{u}{m}\mathbf{z}_e - \frac{k_t}{m}\dot{\boldsymbol{\eta}}_1 \tag{5.36}$$

Combining the gravity acceleration term and the translational drag term in

the left hand side, and using property (4.4), the equation transforms to

$$\mathbf{J}_1^\top(\boldsymbol{\eta}_2)(\mathbf{U} + g\mathbf{z}_e + \frac{k_t}{m}\dot{\boldsymbol{\eta}}_1) = \frac{u}{m}\mathbf{z}_e \tag{5.37}$$

Define the new variables

$$\begin{bmatrix} U_{11} \\ U_{22} \\ U_{33} \end{bmatrix} = (\mathbf{U} + g\mathbf{z}_e + \frac{k_t}{m}\dot{\boldsymbol{\eta}}_1) \tag{5.38}$$

Equation (5.37) becomes

$$\begin{bmatrix} C\theta C\psi & C\theta S\psi & S\theta \\ S\theta C\psi S\phi - S\psi C\phi & S\theta S\psi S\phi + C\psi C\phi & C\theta S\phi \\ S\theta C\psi C\phi + S_\psi S\phi & S\theta S\psi C\phi - C\psi S\phi & C\theta C\phi \end{bmatrix} \begin{bmatrix} U_{11} \\ U_{22} \\ U_{33} \end{bmatrix} = \frac{u}{m}\mathbf{z}_e \tag{5.39}$$

where $C(.)$ and $S(.)$ denote cos(.) and sin(.), respectively. This leads to

$$\begin{aligned} &U_{11}(C\theta C\psi) + U_{22}(C\theta S\psi) - U_{33}(S\theta) = 0 \\ &U_{11}(S\theta C\psi S\phi - S\psi C\phi) + U_{22}(S\theta S\psi S\phi + C\psi C\phi) + U_{33}(C\theta C\phi) = 0 \\ &U_{11}(C\theta C\psi C\phi + S\psi C\phi) + U_{22}(C\theta S\psi C\phi - C\psi S\phi) + U_{33}(C\theta C\phi) = \frac{u}{m} \end{aligned} \tag{5.40}$$

Assuming $\theta \neq 0$, and dividing both sides of the first equation (5.40) with $\cos\theta$,

then the desired pitch angle needed by the inner loop can be computed as

$$\theta_d = \tan^{-1}\left(\frac{U_{11}\cos\psi_d + U_{22}\sin\psi_d}{U_{33}}\right) \tag{5.41}$$

After some manipulation, the desired roll angle equation is also determined as

$$\phi_d = \sin^{-1}\left(\frac{U_{11}\sin\psi_d - U_{22}\cos\psi_d}{\sqrt{U_{11}^2 + U_{22}^2 + U_{33}^2}}\right) \tag{5.42}$$

where ψ_d is the desired yaw angle that can be selected to be zero for the quadrotor case. The control input for translational motion can be computed from (5.40), and given by the following equation

$$\begin{aligned} u = m(&U_{11}(\sin\theta\cos\psi\cos\phi + \sin\psi\sin\phi) + U_{22}(\sin\theta\sin\psi\cos\phi - \cos\psi\sin\phi) \\ &+ U_{33}(\cos\theta\cos\phi)) \end{aligned} \tag{5.43}$$

Throughout the thesis, the outer loop control of the quadrotor uses the algorithm presented in this section.

5.3 Stability Analysis

This section presents the stability and robustness analysis for I&I stabilizing controller. From the first equation in (5.19), it is clear that the $\mathbf{z}$ subsystem has a globally asymptotically stable equilibrium at zero, in order to complete the proof, the boundedness of all the trajectories of the system (5.19) needs to be shown.

Consider $\boldsymbol{\beta} = \mathbf{e}_2 + \mu\mathbf{e}_1$, one has

$$\begin{aligned} \dot{\mathbf{z}} &= -\gamma\mathbf{z} \\ \dot{\mathbf{e}}_1 &= \boldsymbol{\beta} - \mu\mathbf{e}_1 \\ \dot{\boldsymbol{\beta}} &= -\gamma\mathbf{z} \end{aligned} \tag{5.44}$$

Note that $\mathbf{z}(t)$ and $\boldsymbol{\beta}(t)$ are bounded for all t. Boundedness of $\mathbf{e}_1(t)$ can be proved by observing that $\mathbf{e}_1$ is bounded as $\boldsymbol{\beta}(t)$ is always bounded. To prove boundedness of $\mathbf{x}_1$ and $\mathbf{x}_2$, we can observe from the fact that $\mathbf{x}_{1d}$ and $\dot{\mathbf{x}}_{1d}$ are always bounded based on our design, and $\mathbf{e}_1(t)$ and $\mathbf{e}_2(t)$ are bounded, then from equation (5.11) $\mathbf{x}_1$ and $\mathbf{x}_2$ are bounded.

5.3.1 Robustness Analysis

The derived I&I control is based on assumption of system's nominal parameters and operating condition. However, modelling errors, parameter uncertainties, and disturbances may occur in real situations which may affect stability of the system. Let $\bar{I}_R = I_R + \Delta I_R$, ΔI_R = uncertainty on the propeller inertia, $\bar{k}_r = k_r + \Delta k_r$, Δk_r = uncertainty on the rotational drag coefficient. The rotational dynamics with modelling errors or uncertainties and exogenous is given by

$$\dot{\boldsymbol{\nu}}_2 = \mathbf{I}_{\mathrm{M}}^{-1}(-(\boldsymbol{\nu}_2 \times \mathbf{I}\boldsymbol{\nu}_2) - \bar{I}_R(\boldsymbol{\nu}_2 \times \mathbf{z}_e)\Omega - \bar{k}_r\boldsymbol{\nu}_2 + \boldsymbol{\tau}) + \mathbf{d}(t) \tag{5.45}$$

Assumption 5.1.

1. $\mathbf{d}(t)$ is an exogenous bounded random input, that is $\mathbf{d}(t) \leq \zeta$, where ζ is a positive real value.

2. The desired state vector over the tracking path is bounded.

Theorem 5.2 *Under assumption 1) and 2) and I&I control, all state trajectories related to the error dynamics are uniformely ultimately bounded if*

$$\sqrt{(\boldsymbol{\alpha}\mathbf{e}_2)^\top(\boldsymbol{\alpha}\mathbf{e}_2)} \leq \delta_1\|\mathbf{e}\|_2, \quad \delta_1 > 0 \tag{5.46}$$

where $\mathbf{e}_2 = \boldsymbol{\nu}_2 - \boldsymbol{\nu}_{2d}$

Proof: Substituting into equation (5.45), one will have

$$\begin{aligned}
\dot{\boldsymbol{\nu}}_2 =& \mathbf{I}_{\mathrm{M}}^{-1}(-(\boldsymbol{\nu}_2 \times \mathbf{I}\boldsymbol{\nu}_2) - (I_R + \Delta I_R)(\boldsymbol{\nu}_2 \times \mathbf{z}_e)\Omega - (k_r + \Delta k_r)\boldsymbol{\nu}_2 + \boldsymbol{\tau}) + \mathbf{d}(t) \\
=& \mathbf{I}_{\mathrm{M}}^{-1}(-(\boldsymbol{\nu}_2 \times \mathbf{I}\boldsymbol{\nu}_2) - I_R(\boldsymbol{\nu}_2 \times \mathbf{z}_e)\Omega - k_r\boldsymbol{\nu}_2 + \boldsymbol{\tau}) + \Delta\mathbf{I}_{RR}\boldsymbol{\nu}_2 + \Delta\mathbf{K}_{RR}\boldsymbol{\nu}_2 + \mathbf{d}(t) \\
=& \mathbf{I}_{\mathrm{M}}^{-1}(-(\boldsymbol{\nu}_2 \times \mathbf{I}\boldsymbol{\nu}_2) - I_R(\boldsymbol{\nu}_2 \times \mathbf{z}_e)\Omega - k_r\boldsymbol{\nu}_2 + \boldsymbol{\tau}) + \boldsymbol{\alpha}\boldsymbol{\nu}_2 + \mathbf{d}(t)
\end{aligned}$$

where

$$\Delta\mathbf{I}_{RR} \triangleq \begin{bmatrix} 0 & -\frac{\Delta I_R}{I_{xx}} & 0 \\ -\frac{\Delta I_R}{I_{yy}} & 0 & 0 \\ 0 & 0 & 0 \end{bmatrix}, \quad \Delta\mathbf{K}_{RR} \triangleq -\Delta k_r\mathbf{I}_{\mathrm{M}}^{-1} \tag{5.47}$$

and

$$\boldsymbol{\alpha} \triangleq \Delta \mathbf{I}_{RR} + \Delta \mathbf{K}_{RR} \tag{5.48}$$

Introducing (5.47) and (5.48)to the state space error equation form, one will have

$$\begin{aligned} \dot{\mathbf{e}}_1 =& \mathbf{e}_2 \\ \dot{\mathbf{e}}_2 =& \mathbf{F}(\boldsymbol{\nu}_2) + \mathbf{G}\boldsymbol{\tau} - \ddot{\mathbf{x}}_{1d} + \boldsymbol{\alpha}\boldsymbol{\nu}_2 + \mathbf{d}(t) \end{aligned} \tag{5.49}$$

Using controller given by (5.18), the closed loop dynamic becomes

$$\begin{aligned} \dot{\mathbf{e}}_1 &= \mathbf{e}_2 \\ \dot{\mathbf{e}}_2 &= -\gamma \mathbf{e}_1 - (\gamma + \mu)\mathbf{e}_2 + \boldsymbol{\alpha}\boldsymbol{\nu}_2 = -\gamma_1 \mathbf{e}_1 - \gamma_2 \mathbf{e}_2 + \boldsymbol{\alpha}\boldsymbol{\nu}_2 + \mathbf{d}(t) \end{aligned} \tag{5.50}$$

where $\gamma_1 = \gamma$, and $\gamma_2 = \gamma + \mu$. The system without perturbation term $\boldsymbol{\alpha}\boldsymbol{\nu}_2$ is globally exponentially stable provided $\gamma_1, \gamma_2 > 0$. Since $\mathbf{e}_2 = \boldsymbol{\nu}_2 - \boldsymbol{\nu}_{2d} \rightarrow \boldsymbol{\nu}_2 = \mathbf{e}_2 + \boldsymbol{\nu}_{2d}$. One can rewrite equation (5.50) as

$$\begin{bmatrix} \dot{\mathbf{e}}_1 \\ \dot{\mathbf{e}}_2 \end{bmatrix} = \underbrace{\begin{bmatrix} \mathbf{0} & \mathbf{I} \\ -\gamma_1 \mathbf{I} & -\gamma_2 \mathbf{I} \end{bmatrix}}_{\mathbf{E}} \begin{bmatrix} \mathbf{e}_1 \\ \mathbf{e}_2 \end{bmatrix} + \underbrace{\begin{bmatrix} \mathbf{0} \\ \boldsymbol{\alpha}\mathbf{e}_2 \end{bmatrix}}_{\mathbf{H}(e)} + \underbrace{\begin{bmatrix} \mathbf{0} \\ \boldsymbol{\nu}_{2d} + \mathbf{d}(t) \end{bmatrix}}_{\boldsymbol{\beta}} \tag{5.51}$$

As we can see the term $\mathbf{H}(e)$ vanishes at the origin while the term $\boldsymbol{\beta}$ does not vanish. The value of $\boldsymbol{\alpha}$ in $\mathbf{H}(e)$ is unknown, but it can be upper-bounded such

that

$$\|\mathbf{H}(e)\|_2 = \sqrt{(\boldsymbol{\alpha}\mathbf{e}_2)^\top(\boldsymbol{\alpha}\mathbf{e}_2)} \leq \delta_1\|\mathbf{e}\|_2, \quad \delta_1 > 0 \tag{5.52}$$

Since $\boldsymbol{\nu}_{2d}$ is bounded constant generated by the designer, and $\mathbf{d}(t)$ is assumed to be a uniformly bounded disturbance. Therefore, they can be upper-bounded by

$$\|\boldsymbol{\nu}_{2d} + \mathbf{d}(t)\|_\infty \leq \delta_2, \quad \delta_2 > 0, \quad \forall t \geq 0 \tag{5.53}$$

In order to analyze the stability of the system, Lyapunov Converse theorem is utilized[48]. Since the system without the uncertainty and disturbance is an exponentially stable system, one will have Lyapunov function $V(\mathbf{e})$ satisfying these three following conditions

$$\begin{aligned} \lambda_{\min}(\mathbf{P})\|\mathbf{e}\|_2^2 \leq V(\mathbf{e}) \leq \lambda_{\max}(\mathbf{P})\|\mathbf{e}\|_2^2 \\ \frac{\partial V}{\partial \mathbf{e}}\mathbf{E}\mathbf{e} = -\mathbf{e}^\top\mathbf{Q}\mathbf{e} \leq -\lambda_{\min}(\mathbf{Q})\|\mathbf{e}\|_2^2 \\ \left\|\frac{\partial V}{\partial \mathbf{e}}\right\|_2 = \|2\mathbf{e}^\top\mathbf{P}\|_2 \leq 2\|\mathbf{P}\|_2\|\mathbf{e}\|_2 = 2\lambda_{\max}(\mathbf{P})\|\mathbf{e}\|_2 \end{aligned} \tag{5.54}$$

where $V(\mathbf{e}) = \mathbf{e}^\top\mathbf{P}\mathbf{e}$. Since $\mathbf{E}$ is Hurwitz, for unique $\mathbf{P} = \mathbf{P}^\top > 0$, and $\mathbf{Q} = \mathbf{Q}^\top > 0$ the following Lyapunov equation is satisfied

$$\mathbf{P}\mathbf{E} + \mathbf{E}^\top\mathbf{P} = -\mathbf{Q}, \quad \mathbf{P} = \begin{bmatrix} \mathbf{P}_1 & \mathbf{P}_2 \\ \mathbf{P}_2 & \mathbf{P}_3 \end{bmatrix} \tag{5.55}$$

Taking the derivative of $V(\mathbf{e})$ along the trajectory of the system with uncertainty and disturbance (5.51), one obtains

$$\begin{aligned}
\dot{V}(\mathbf{e}) = & -\mathbf{e}^\top \mathbf{Q}\mathbf{e} + 2\mathbf{e}^\top \mathbf{P}\mathbf{H}(\mathbf{e}) + 2\mathbf{e}^\top \mathbf{P}\boldsymbol{\beta} \\
= & -\mathbf{e}^\top \mathbf{Q}\mathbf{e} + 2[\mathbf{e}_1^\top \mathbf{P}_2 + \mathbf{e}_2^\top \mathbf{P}_3]\boldsymbol{\alpha}\mathbf{e}_2 + 2[\mathbf{e}_1^\top \mathbf{P}_2 + \mathbf{e}_2^\top \mathbf{P}_3](\boldsymbol{\nu}_{2d} + \mathbf{d}(t)) \\
\leq & -\lambda_{\min}(\mathbf{Q})\|\mathbf{e}\|_2^2 + 2\lambda_{\max}(\mathbf{P})\delta_1\|\mathbf{e}\|_2^2 + 2\lambda_{\max}(\mathbf{P})\delta_2\|\mathbf{e}\|_2 \\
\leq & -\lambda_{\mathrm{M}}\|\mathbf{e}\|_2^2 + 2\lambda_{\max}(\mathbf{P})\delta_2\|\mathbf{e}\|_2
\end{aligned} \tag{5.56}$$

where $\lambda_{\mathrm{M}} = \lambda_{min}(\mathbf{Q}) - 2\lambda_{max}(\mathbf{P})\delta_1$. Suppose we have $0 < \theta < 1$,

$$\begin{aligned}
\dot{V}(\mathbf{e}) \leq & -\lambda_{\mathrm{M}}\|\mathbf{e}\|_2^2 + \theta\lambda_{\mathrm{M}}\|\mathbf{e}\|_2^2 - \theta\lambda_{\mathrm{M}}\|\mathbf{e}\|_2^2 + 2\lambda_{\max}(\mathbf{P})\delta_2\|\mathbf{e}\|_2 \\
= & -(1-\theta)\lambda_{\mathrm{M}}\|\mathbf{e}\|_2^2 - \theta\lambda_{\mathrm{M}}\|\mathbf{e}\|_2^2 + 2\lambda_{\max}(\mathbf{P})\delta_2\|\mathbf{e}\|_2 \\
\leq & -(1-\theta)\lambda_{\mathrm{M}}\|\mathbf{e}\|_2^2, \quad \forall\|\mathbf{e}\|_2 \geq \frac{2\lambda_{\mathrm{Max}}(\mathbf{P})\delta_2}{\theta\lambda_{\mathrm{M}}} = \kappa
\end{aligned} \tag{5.57}$$

If $\lambda_{\mathrm{M}} > 0$, then $\delta_1 < \frac{\lambda_{\min}(\mathbf{Q})}{2\lambda_{\max}(\mathbf{P})}$, therefore the stability of the perturbed system is preserved. Based on ultimate boundedness theorem[48], the trajectories of the system with uncertainty and disturbance are uniformly ultimately bounded by

$$b = \alpha_1^{-1}(\alpha_2(\kappa)) = \frac{\lambda_{\max}(\mathbf{P})^{3/2}\delta_2}{\theta\lambda_{\mathrm{M}}}\sqrt{\frac{2}{\lambda_{\min}(\mathbf{Q})}} \tag{5.58}$$

where $\alpha_1(r) = \lambda_{\min}(\mathbf{Q})r^2$, and $\alpha_2(r) = \lambda_{\max}(\mathbf{P})r^2$. It can be seen that the bounds for the uncertainty and disturbance are dependent on the selection of $\mathbf{Q}$, and the matrix $\mathbf{E}$ that generate $\mathbf{P}$ through the Lyapunov equation. In conclusion, the

selection of the I&I control parameters γ and μ will determine the robustness of the system. ∎

5.4 Simulation

In order to validate the theoretical developments of the controller, several simulations are conducted. In this simulation, all the states are considered accessible, and I&I technique is compared to the backstepping technique. Uncertainty and perturbation are injected to examine the performance for both the controllers.

5.4.1 Nominal Parameters

In the first simulation, 3D-space trajectory tracking control is considered with the desired position as a helix-shaped path. Using nominal values for the parameters, the performance of I&I and backstepping controller is examined. The results of the position and attitude angles tracking for both the controllers can be seen in Figures (5.2) to (5.7)

In Figure (5.2) and (5.3), it can bee seen that under nominal conditions both the controllers are able to perform trajectory tracking accurately. It can also be seen that the attitude of the quadrotor is compatible with the translational motion and compatible attitude angles lead to accurate tracking in the translational motion. Other plots of the trajectory tracking performance can be seen in Figure (5.6) and (5.7).

The control inputs generated by the I&I controller have less chattering than

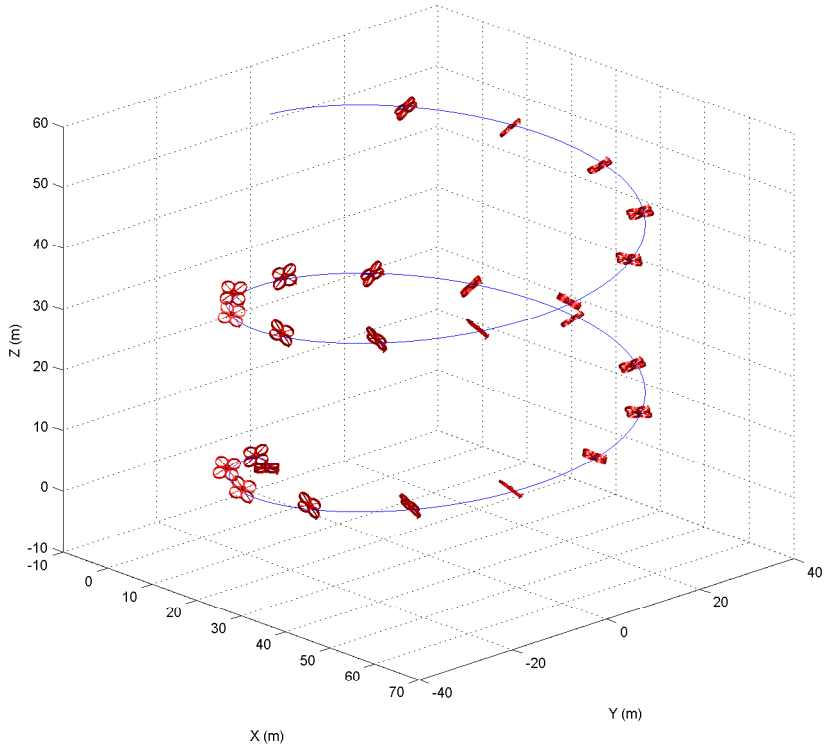

Figure 5.2: I&I 3D space trajectory tracking

the backstepping technique. This is due to the tuning parameters $\mathbf{T}$, $\mathbf{\Gamma}_1$, $\mathbf{\Gamma}_2$, and $\mathbf{\Lambda}$ for the backstepping control that are selected to ensure fast tracking. Low pass filter is employed in the backstepping attitude stabilization control design, so that the desired angular velocity and commanded attitude derivative dynamics are compensated.

The positive constant values μ and γ that are selected for the I&I controller are based on the need for fast rate of convergence of the system. The trajectories of the system need to go to the invariant manifold sufficiently fast (selection of

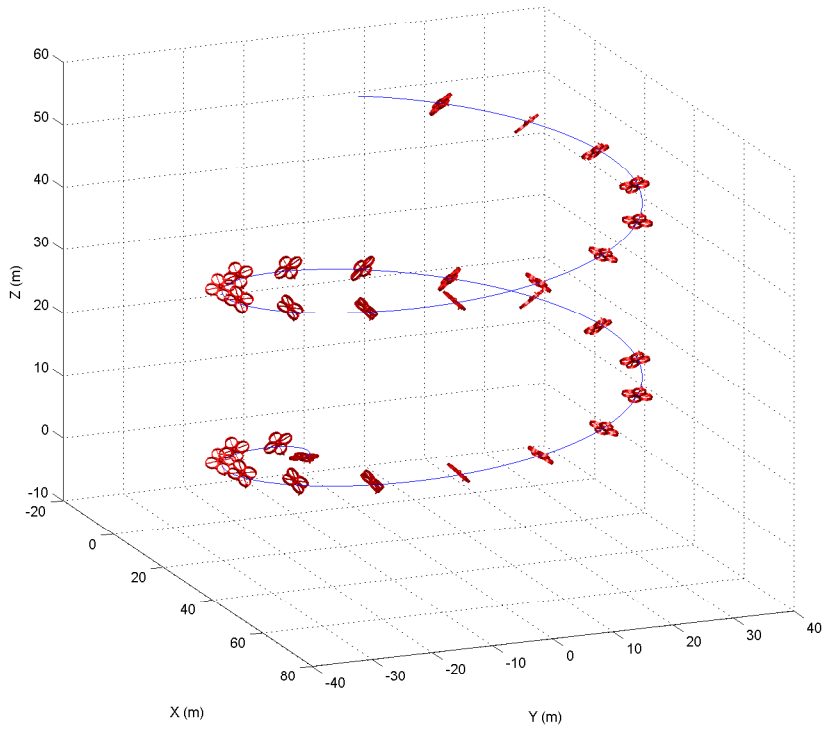

Figure 5.3: Backstepping 3D space trajectory tracking

γ) and once in the manifold the trajectories have to go to the stable equilibrium sufficiently fast (selection of μ). By this selection, the inner loop is guaranteed to be faster than the outer loop and the overall stability of the system is ensured.

For the outer loop PD control, $\mathbf{K}_P$ and $\mathbf{K}_D$ are tuned such that the tracking performance of the position control is fast, but not faster than the inner loop. The outer loop control parameters are selected to be the same for both I&I and backstepping control, so that the performance of both the inner controllers can be compared equally.

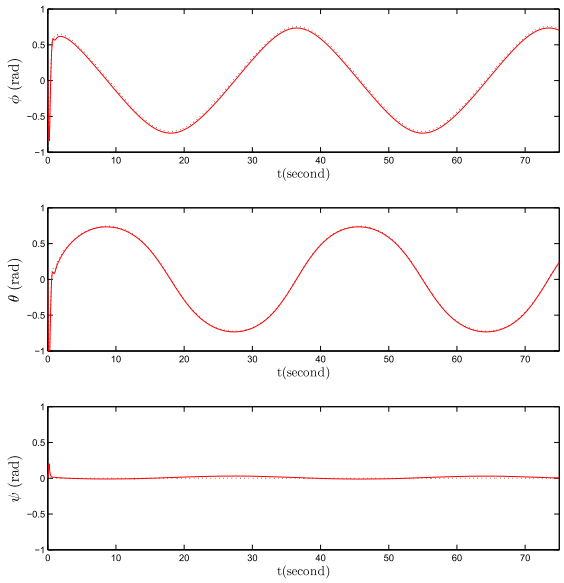

Figure 5.4: I&I Euler angles tracking

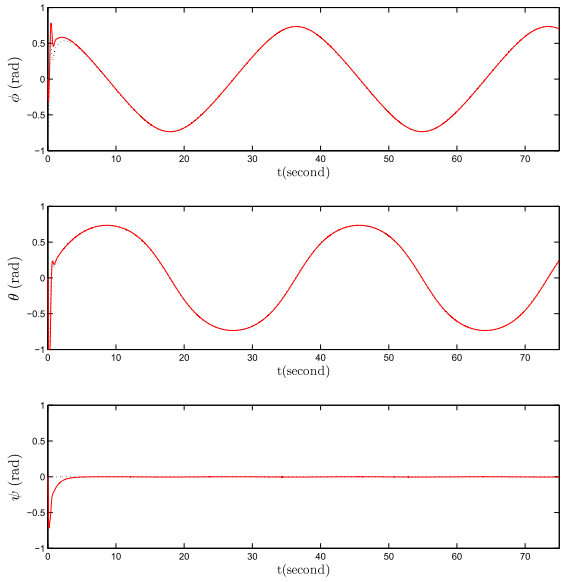

Figure 5.5: Backstepping Euler angles tracking

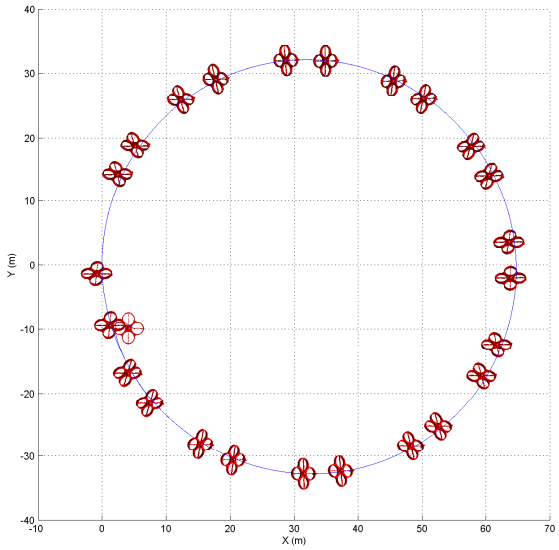

Figure 5.6: I&I x-y tracking

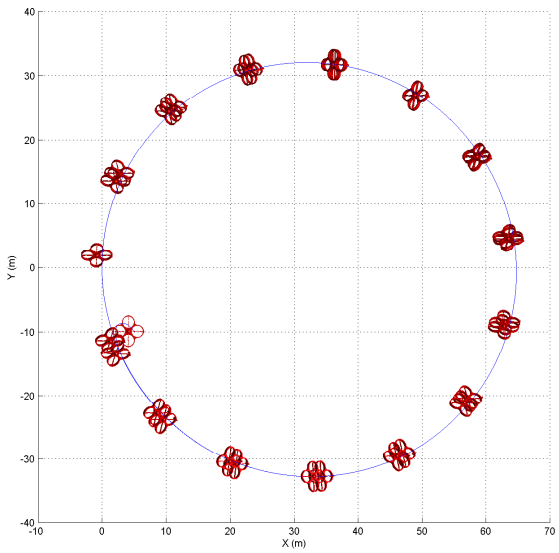

Figure 5.7: Backstepping x-y tracking

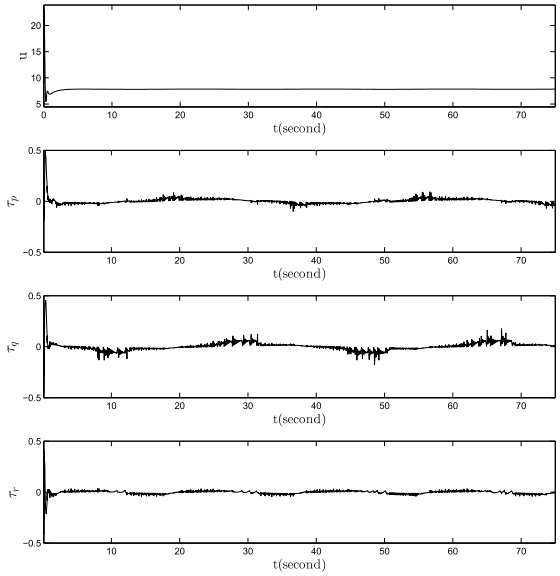

Figure 5.8: I&I control input

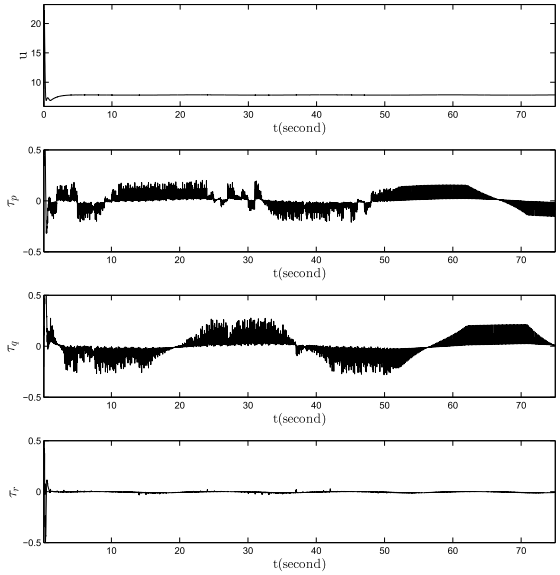

Figure 5.9: Backstepping control input

5.4.2 Uncertain Parameters

To compare the robustness of the inner loop controllers, uncertainty and a uniformly bounded disturbance are injected into the system. The uncertainty of the rotational drag coefficient k_r and propeller inertia I_R is selected to be time-varying with the form $A\ \sin(\omega t + \phi)$. Certain values for amplitude and frequency are chosen such that the robustness of the system is tested to the extreme point.

In the first scenario, variation of the uncertainty is injected with a value close to the unstable point of the backstepping controller. It can be seen that I&I provides better performance compared to the backstepping technique, Figure (5.10) and (5.11).

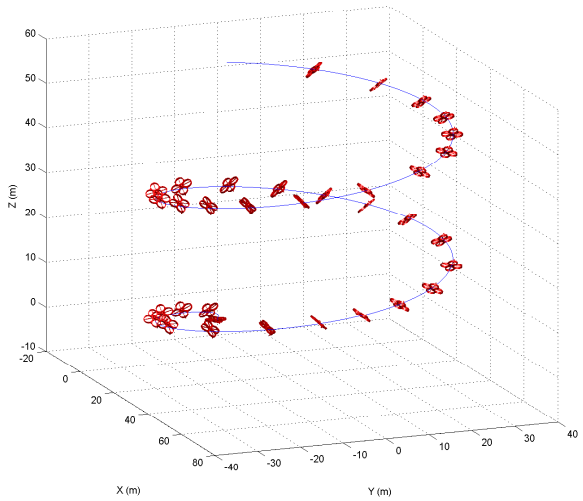

Figure 5.10: I&I 3D space trajectory tracking parameter changing before unstable point

In the second scenario, the uncertainty is introduced beyond the stable point

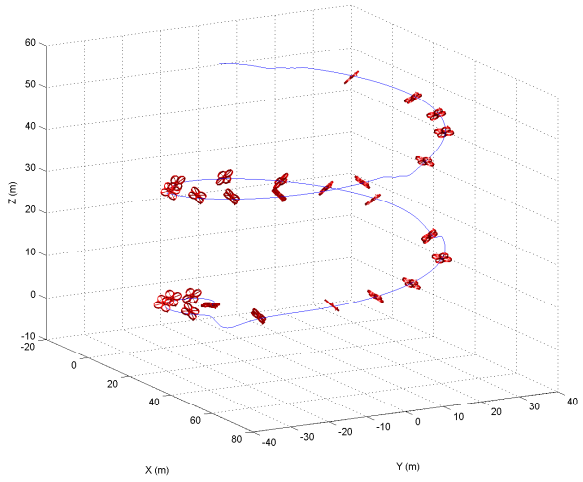

Figure 5.11: Backstepping 3D space trajectory tracking parameter changing before unstable point

of the backstepping controller. The results of the simulations can be seen in Figure (5.18) and (5.19). I&I controller produces stable and acceptable performance, while the backstepping technique is not able to maintain the stability of the system. In the backstepping technique, the Lyapunov condition for stability is easily violated once there are uncertainties or disturbances in the system.

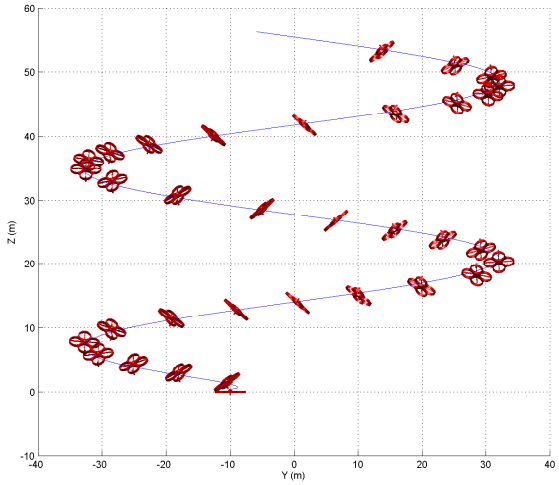

Figure 5.12: I&I y-z tracking under uncertainties

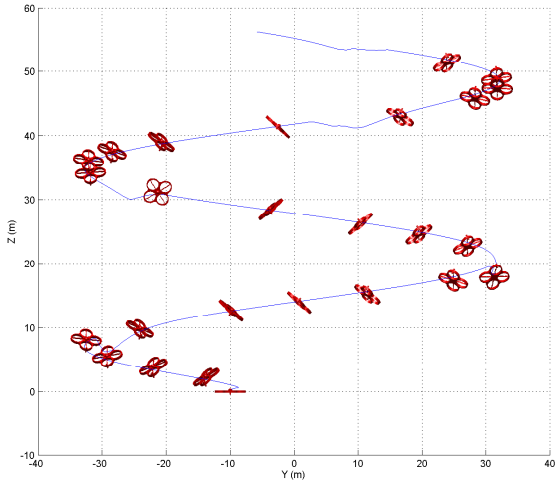

Figure 5.13: Backstepping y-z tracking under uncertainties

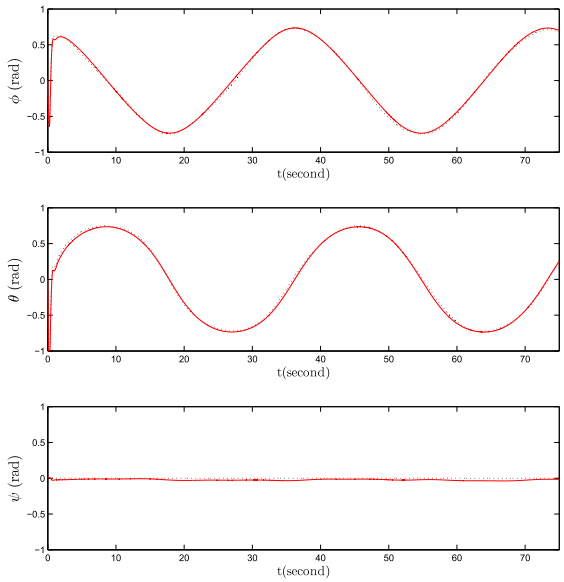

Figure 5.14: I&I Euler angles tracking under uncertainties

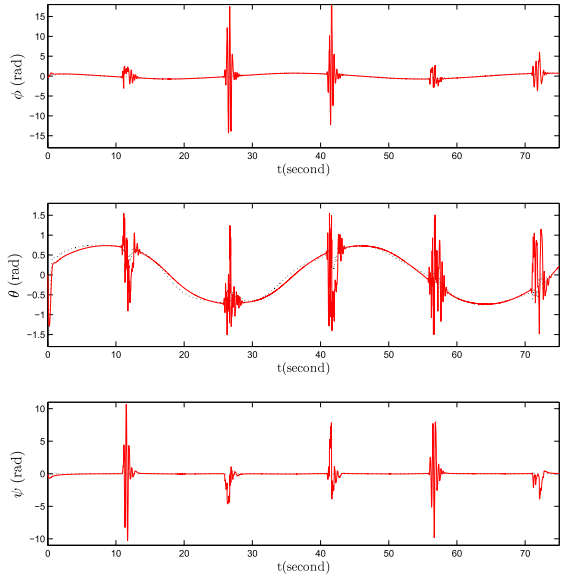

Figure 5.15: Backstepping Euler angles tracking under uncertainties

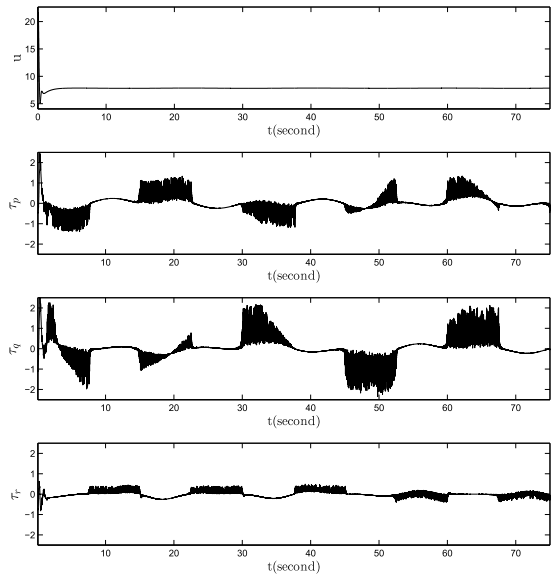

Figure 5.16: I&I control input under uncertainties

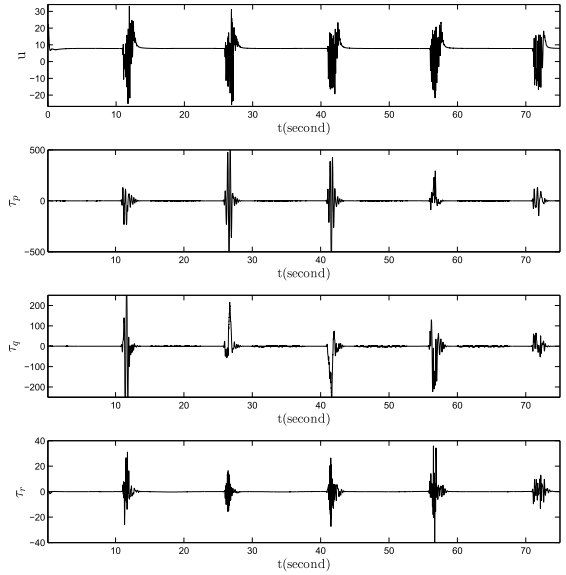

Figure 5.17: Backstepping control input under uncertainties

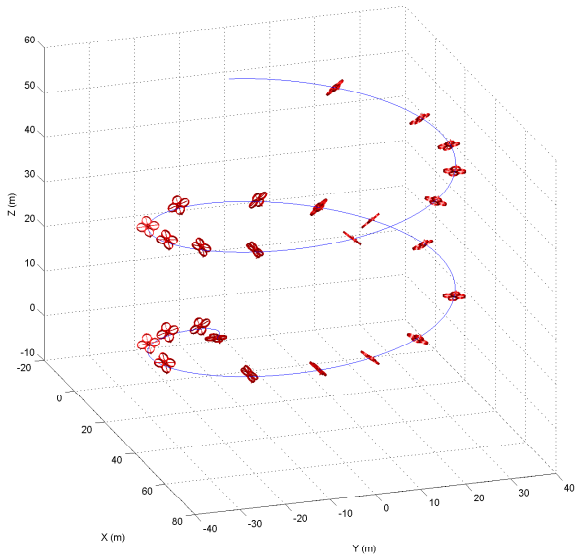

Figure 5.18: I&I 3D space trajectory tracking parameter changing after unstable point

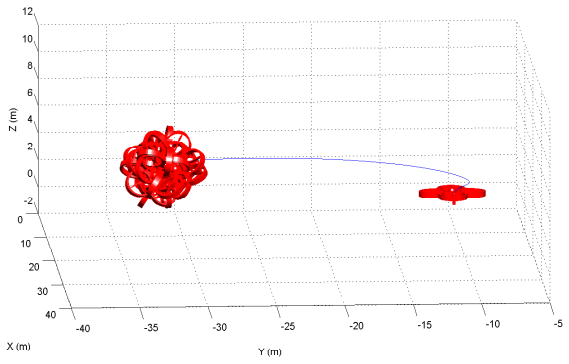

Figure 5.19: Backstepping 3D space trajectory tracking parameter changing after unstable point

5.5 Conclusions

In this chapter the trajectory tracking control design for the quadrotor is presented. A new controller based on I&I methodology is designed in the inner loop and a PD controller in the outer loop. In order to investigate the performance of I&I controller in presence of uncertainty and disturbance, backstepping controller is used as a benchmark. From the simulation results, it can be seen that the robustness of I&I control is better compared to the backstepping control. The robustness analysis of the closed-loop I&I control is presented in terms of robustness with respect to parameter uncertainties and disturbances.

5.5.1 Contribution

The main contributions in this chapter are

1. Design of I&I stabilizing controller for the underactuated quadrotor UAV.

2. Extension of the work in [1] by including the translational and rotational drag terms.

3. Stability and Robustness analysis of the closed loop system in the presence of uncertainty and exogenous disturbance.

CHAPTER 6

I&I OBSERVER DESIGN

6.1 Introduction

The I&I observer was introduced in [21]. This observer requires the invariant manifold that is rendered attractive. In this chapter, an I&I-based reduced-order observer is introduced to estimate the translational velocity of the quadrotor . For comparison, the classical Luenberger observer is presented.

Prior to the development of the I&I reduced-order observer, consider a system described by equations of the form

$$\begin{aligned} \dot{\boldsymbol{\zeta}} &= \mathbf{f}_1(\boldsymbol{\zeta}, \mathbf{y}, t) \\ \dot{\mathbf{y}} &= \mathbf{f}_2(\boldsymbol{\zeta}, \mathbf{y}, t) \end{aligned} \tag{6.1}$$

where $\boldsymbol{\zeta} \in \mathbb{R}^n$ is the unmeasurable part of the state, and $\mathbf{y} \in \mathbb{R}^m$ is the measurable part of the state. It is assumed that $\mathbf{f}_1(.)$ and $\mathbf{f}_2(.)$ are forward complete[2]. Consider the following definition

Definition 6.1 (see [21]). The dynamical system

$$\dot{\boldsymbol{\xi}} = \boldsymbol{\alpha}(\boldsymbol{\xi}, \mathbf{y}, t) \tag{6.2}$$

with $\boldsymbol{\xi} \in \mathbb{R}^p$, $p \geq n$, is called an observer for the system (6.1), if there exist mappings $\boldsymbol{\beta} : \mathbb{R}^p \times \mathbb{R}^m \times \mathbb{R} \to \mathbb{R}^p$ and $\boldsymbol{\phi} : \mathbb{R}^n \times \mathbb{R}^m \times \mathbb{R} \to \mathbb{R}^p$ that are left-invertible and such that the manifold

$$\mathcal{M} = \{(\boldsymbol{\zeta}, \mathbf{y}, \boldsymbol{\xi}, t) \in \mathbb{R}^n \times \mathbb{R}^m \times \mathbb{R}^p \times \mathbb{R} : \boldsymbol{\beta}(\boldsymbol{\xi}, \mathbf{y}, t) = \boldsymbol{\phi}(\boldsymbol{\zeta}, \mathbf{y}, t)\} \tag{6.3}$$

has the following properties.

1. All trajectories of the extended system (6.1) and (6.2)that start on the manifold $\mathcal{M}$ remain there for all future times.

2. All trajectories of the extended system (6.1) and (6.2)that start in the neighbourhood of $\mathcal{M}$ asymptotically converge to $\mathcal{M}$.

6.2 I&I Reduced-Order Observer

In this section, a general tool for constructing a reduced-order observer based on Invariance and Immersion is presented. Consider the following theorem

Theorem 6.1 ([21]) *Consider the system (6.1),(6.2) and suppose that there exist $\mathcal{C}^1$ mappings $\boldsymbol{\beta}(\boldsymbol{\xi}, \mathbf{y}, t) : \mathbb{R}^p \times \mathbb{R}^m \times \mathbb{R} \to \mathbb{R}^p$ and $\boldsymbol{\phi}(\boldsymbol{\zeta}, \mathbf{y}, t) : \mathbb{R}^n \times \mathbb{R}^m \times \mathbb{R} \to \mathbb{R}^p$, with a left-inverse $\boldsymbol{\phi}^L : \mathbb{R}^n \times \mathbb{R}^m \times \mathbb{R} \to \mathbb{R}^n$, such that the following hold.*

*(**A1**). For all* $\mathbf{y}$, $\boldsymbol{\xi}$ *and* t, $\boldsymbol{\beta}(\boldsymbol{\xi}, \mathbf{y}, t)$ *is left-invertible with respect to* $\boldsymbol{\xi}$ *and*

$$det(\frac{\partial \boldsymbol{\beta}}{\partial \boldsymbol{\xi}}) \neq 0 \tag{6.4}$$

*(**A2**). The system*

$$\begin{aligned}\dot{\mathbf{z}} = &- \frac{\partial \boldsymbol{\beta}}{\partial \mathbf{y}}(\mathbf{f}_2(\hat{\boldsymbol{\zeta}}, \mathbf{y}, t) - \mathbf{f}_2(\boldsymbol{\zeta}, \mathbf{y}, t)) + \left.\frac{\partial \boldsymbol{\phi}}{\partial \mathbf{y}}\right|_{\boldsymbol{\zeta}=\hat{\boldsymbol{\zeta}}} \mathbf{f}_2(\hat{\boldsymbol{\zeta}}, \mathbf{y}, t) - \frac{\partial \boldsymbol{\phi}}{\partial \mathbf{y}}\mathbf{f}_2(\boldsymbol{\zeta}, \mathbf{y}, t) \\ &+ \left.\frac{\partial \boldsymbol{\phi}}{\partial \boldsymbol{\zeta}}\right|_{\boldsymbol{\zeta}=\hat{\boldsymbol{\zeta}}} \mathbf{f}_1(\hat{\boldsymbol{\zeta}}, \mathbf{y}, t) - \frac{\partial \boldsymbol{\phi}}{\partial \boldsymbol{\zeta}}\mathbf{f}_1(\boldsymbol{\zeta}, \mathbf{y}, t) + \left.\frac{\partial \boldsymbol{\phi}}{\partial t}\right|_{\boldsymbol{\zeta}=\hat{\boldsymbol{\zeta}}} - \frac{\partial \boldsymbol{\phi}}{\partial t}\end{aligned} \tag{6.5}$$

with $\hat{\boldsymbol{\zeta}} = \boldsymbol{\phi}^L(\boldsymbol{\phi}(\boldsymbol{\zeta}, \mathbf{y}, t) + \mathbf{z})$, *is a (globally) asymptotically stable equilibrium at* $\mathbf{z} = 0$, *uniformly in* $\boldsymbol{\zeta}$, $\mathbf{y}$ *and* t.

Then the system (6.2) with

$$\begin{aligned}\boldsymbol{\alpha}(\boldsymbol{\xi}, \mathbf{y}, t) = &- \left(\frac{\partial \boldsymbol{\beta}}{\partial \boldsymbol{\xi}}\right)^{-1} \left(\frac{\partial \boldsymbol{\beta}}{\partial \mathbf{y}}\mathbf{f}_2(\hat{\boldsymbol{\zeta}}, \mathbf{y}, t) + \frac{\partial \boldsymbol{\beta}}{\partial t} - \left.\frac{\partial \boldsymbol{\phi}}{\partial \mathbf{y}}\right|_{\boldsymbol{\zeta}=\hat{\boldsymbol{\zeta}}} \mathbf{f}_2(\hat{\boldsymbol{\zeta}}, \mathbf{y}, t)\right. \\ &\left. - \left.\frac{\partial \boldsymbol{\phi}}{\partial \boldsymbol{\zeta}}\right|_{\boldsymbol{\zeta}=\hat{\boldsymbol{\zeta}}} \mathbf{f}_1(\hat{\boldsymbol{\zeta}}, \mathbf{y}, t) - \left.\frac{\partial \boldsymbol{\phi}}{\partial t}\right|_{\boldsymbol{\zeta}=\hat{\boldsymbol{\zeta}}}\right)\end{aligned} \tag{6.6}$$

where $\hat{\boldsymbol{\zeta}} = \boldsymbol{\phi}^L(\boldsymbol{\beta}(\boldsymbol{\xi}, \mathbf{y}, t), \mathbf{y}, t)$, *is a (global) observer for the system (6.1).*

Proof: See [21] for proof. ∎

6.3 Observer Design

In this section, the observers for the translational dynamics of the quadrotor are designed. Based on the information obtained from the input and output of the

outer loop, the unknown states of the system are estimated. The structure of the dynamics allows us to treat the translational dynamics as a linear system. If (4.10) is transformed into a state equation form

$$\begin{aligned}\dot{\mathbf{x}}_1 &= \mathbf{x}_2 \\ \dot{\mathbf{x}}_2 &= -g\mathbf{z}_e + \mathbf{J}_2(\boldsymbol{\eta}_2)\frac{u}{m}\mathbf{z}_e - k_t\mathbf{x}_2\end{aligned} \tag{6.7}$$

The term $-g\mathbf{z}_e + \mathbf{J}_1(\boldsymbol{\eta}_2)\frac{u}{m}\mathbf{z}_e$ is generated by the inner loop and is independent of $\mathbf{x}$. Let $\bar{\mathbf{u}} = -g\mathbf{z}_e + \mathbf{J}_1(\boldsymbol{\eta}_2)\frac{u}{m}\mathbf{z}_e$ then (6.7) becomes

$$\begin{aligned}\dot{\mathbf{x}}_1 &= \mathbf{x}_2 \\ \dot{\mathbf{x}}_2 &= \bar{\mathbf{u}} - k_t\mathbf{x}_2\end{aligned} \tag{6.8}$$

By using equation (6.8), two types of observers will be designed, the first one is a reduced-order I&I observer and the second one is the Luenberger observer.

The reduced-order I&I observer works as an estimator of the inertial velocities using information obtained from the inertial positions and input. The Luenberger observer estimates all the states using information from the input and output in the outer loop. The structure for both the observers can be seen in Figure (6.1)

6.3.1 I&I Observer

Consider the inertial position system described by equation 4.10, and suppose that only the position $\boldsymbol{\eta}_1$ is measurable. The objective is to design an asymptotic

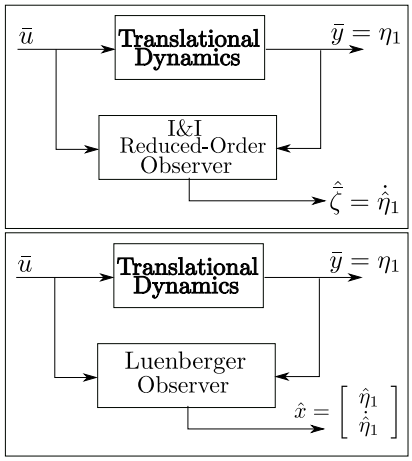

Figure 6.1: Observer Block I&I Reduced-Order Observer(Top), Luenberger Full-Order Observer(Bottom)

observer for the unmeasured states (velocity $\dot{\boldsymbol{\eta}}_1$). Note that (6.8) can be written in the form (6.1), namely

$$\begin{aligned} \dot{\mathbf{y}} &= \boldsymbol{\zeta} \\ \dot{\boldsymbol{\zeta}} &= \bar{\mathbf{u}} - k_t \boldsymbol{\zeta} \end{aligned} \tag{6.9}$$

where $\boldsymbol{\zeta} = [\zeta_1, \zeta_2, \zeta_3]^\top = \dot{\boldsymbol{\eta}}_1$ is the unmeasurable part of the system, and $\mathbf{y} = [y_1, y_2, y_3]^\top = \boldsymbol{\eta}_1$ is the measurable part. The term $\bar{\mathbf{u}} = -g\mathbf{z}_e + \mathbf{J}_1(\boldsymbol{\eta}_2)\frac{u}{m}\mathbf{z}_e$ is considered as the input, since it is produced from another system and is acting as an input to system. Before the observer is developed, it is supposed that the following assumption holds

Assumption 6.1. The translational drag coefficient is unknown but can be up-

perbounded by

$$\|k_t\|_\infty < \vartheta \tag{6.10}$$

The first step in designing the observer is to define a mapping $\boldsymbol{\phi}(\boldsymbol{\zeta}, \mathbf{y})$ that renders the manifold $\mathcal{M}$ to be attractive. Taking $\boldsymbol{\phi}(\boldsymbol{\zeta}, \mathbf{y}) = \boldsymbol{\zeta}$, the error equation $\mathbf{z} = \boldsymbol{\beta}(\boldsymbol{\xi}, \mathbf{y}) - \boldsymbol{\phi}(\boldsymbol{\zeta}, \mathbf{y})$ has the following dynamics

$$\dot{\mathbf{z}} = \frac{\partial \boldsymbol{\beta}}{\partial \boldsymbol{\xi}}\dot{\boldsymbol{\xi}} + \frac{\partial \boldsymbol{\beta}}{\partial \mathbf{y}}\dot{\mathbf{y}} - \frac{\partial \boldsymbol{\phi}}{\partial \boldsymbol{\zeta}}\dot{\boldsymbol{\zeta}} - \frac{\partial \boldsymbol{\phi}}{\partial \mathbf{y}}\dot{\mathbf{y}} \tag{6.11}$$

where $\boldsymbol{\xi} = [\xi_1, \xi_2, \xi_3]^\top$. The observer dynamics are obtained from the error dynamics in equilibrium condition with $\boldsymbol{\zeta} = \hat{\boldsymbol{\zeta}}$, where $\hat{\boldsymbol{\zeta}}$ is the estimated state, and given by the following

$$\dot{\boldsymbol{\xi}} = -\left(\frac{\partial \boldsymbol{\beta}}{\partial \boldsymbol{\xi}}\right)^{-1}\left(\frac{\partial \boldsymbol{\beta}}{\partial \mathbf{y}}\dot{\mathbf{y}}\bigg|_{\zeta=\hat{\zeta}} - \frac{\partial \boldsymbol{\phi}}{\partial \boldsymbol{\zeta}}\dot{\boldsymbol{\zeta}}\bigg|_{\zeta=\hat{\zeta}}\right) \tag{6.12}$$

Substituting equation (6.12) in (6.11), the following equation is obtained

$$\begin{aligned}
\dot{\mathbf{z}} = & -\frac{\partial \boldsymbol{\beta}}{\partial \mathbf{y}}\dot{\mathbf{y}}\bigg|_{\zeta=\hat{\zeta}} + \frac{\partial \boldsymbol{\phi}}{\partial \boldsymbol{\zeta}}\dot{\boldsymbol{\zeta}}\bigg|_{\zeta=\hat{\zeta}} + \frac{\partial \boldsymbol{\beta}}{\partial \mathbf{y}}\dot{\mathbf{y}} - \frac{\partial \boldsymbol{\phi}}{\partial \boldsymbol{\zeta}}\dot{\boldsymbol{\zeta}} \\
= & -\left[\frac{\partial \boldsymbol{\beta}}{\partial \mathbf{y}} + k_t\mathbf{I}\right](\hat{\boldsymbol{\zeta}} - \boldsymbol{\zeta}) \\
= & -\left[\frac{\partial \boldsymbol{\beta}}{\partial \mathbf{y}} + k_t\mathbf{I}\right]\mathbf{z}
\end{aligned} \tag{6.13}$$

Hence, selecting

$$\boldsymbol{\beta}(\boldsymbol{\xi}, \mathbf{y}) = \boldsymbol{\xi} + \boldsymbol{\lambda}\mathbf{y} \tag{6.14}$$

where $\boldsymbol{\lambda} = \text{diag}(\lambda_1, \lambda_2, \lambda_3)$ is a constant matrix, ensures that $(\mathbf{A1})$ is satisfied. Finally, the error dynamic equation becomes

$$\dot{\mathbf{z}} = -(\boldsymbol{\lambda} + k_t\mathbf{I})\mathbf{z} \tag{6.15}$$

if we select $\lambda_i > \vartheta, \quad i = 1, 2, 3$, then the zero equilibrium of the system (6.15) is globally asymptotically stable. Hence, $(\mathbf{A2})$ holds, and the following observer dynamic is obtained

$$\begin{aligned} \dot{\boldsymbol{\xi}} = & -\boldsymbol{\xi} - \boldsymbol{\lambda}\mathbf{y} + \bar{\mathbf{u}} - k_t\mathbf{I}(\boldsymbol{\xi} + \boldsymbol{\lambda}\mathbf{y}) \\ = & -(\mathbf{I} + k_t\mathbf{I})(\boldsymbol{\xi} + \boldsymbol{\lambda}\mathbf{y}) + \bar{\mathbf{u}} \end{aligned} \tag{6.16}$$

with the estimated states given by

$$\hat{\boldsymbol{\zeta}} = \boldsymbol{\xi} + \boldsymbol{\lambda}\mathbf{y} \tag{6.17}$$

6.3.2 Luenberger Observer

In this section, for the purpose of comparison a classical Luenberger observer is designed. Consider a linear system of the form

$$\begin{aligned} \dot{\mathbf{x}} &= \mathbf{A}\mathbf{x} + \mathbf{B}\mathbf{u} \\ \mathbf{y} &= \mathbf{C}\mathbf{x} \end{aligned} \tag{6.18}$$

where $\mathbf{x} \in \mathbb{R}^n$, $\mathbf{u} \in \mathbb{R}^m$, and $\mathbf{y} \in \mathbb{R}^p$. Rewriting equation (6.8) in the form of equation (6.18) one will obtain

$$\begin{aligned} \dot{\mathbf{x}} &= \underbrace{\begin{bmatrix} \mathbf{0} & \mathbf{I} \\ \mathbf{0} & -k_t\mathbf{I} \end{bmatrix}}_{\mathbf{A}} \mathbf{x} + \underbrace{\begin{bmatrix} \mathbf{0} \\ \mathbf{I} \end{bmatrix}}_{\mathbf{B}} \bar{\mathbf{u}} \\ \mathbf{y} &= \underbrace{\begin{bmatrix} \mathbf{I} & \mathbf{0} \end{bmatrix}}_{\mathbf{C}} \mathbf{x} \end{aligned} \tag{6.19}$$

Now consider the following observer structure

$$\dot{\hat{\mathbf{x}}} = \mathbf{A}\hat{\mathbf{x}} + \mathbf{B}\bar{\mathbf{u}} + \mathbf{L}(\mathbf{y} - \mathbf{C}\hat{\mathbf{x}}) \tag{6.20}$$

where $\mathbf{L}$ is the observer gain. Define the observer error as

$$\mathbf{e} \triangleq \mathbf{x} - \hat{\mathbf{x}} \tag{6.21}$$

and the following is obtained

$$\begin{aligned}\dot{\mathbf{e}} = \dot{\mathbf{x}} - \dot{\hat{\mathbf{x}}} &= (\mathbf{A}\mathbf{x} + \mathbf{B}\bar{\mathbf{u}}) - (\mathbf{A}\hat{\mathbf{x}} + \mathbf{B}\bar{\mathbf{u}} + \mathbf{L}\mathbf{y} - \mathbf{L}\mathbf{C}\hat{\mathbf{x}}) \\ &= (\mathbf{A} - \mathbf{L}\mathbf{C})(\mathbf{x} - \hat{\mathbf{x}}) = (\mathbf{A} - \mathbf{L}\mathbf{C})\mathbf{e} \end{aligned} \tag{6.22}$$

Then, $\hat{\mathbf{x}} \to \mathbf{x}$ as $t \to \infty$, provided the observer error dynamics is asymptotically stable. This result can be achieved if the observability condition is satisfied so that the eigenvalues of $(\mathbf{A} - \mathbf{L}\mathbf{C})$ can be placed anywhere in the left half of the complex plane by the appropriate selection of the observer gain $\mathbf{L}$.

6.4 Simulation

The simulation in this section is conducted under the assumption that some of the states are not accessible, hence the observer is introduced. The performances of I&I and Luenberger observer are investigated and compared. In both the simulations, the measurements are corrupted with Gaussian noise having zero mean.

From Figure (6.4), one can see that the estimation error for the I&I observer has zero mean, this is due to the fact that the measurements are corrupted with the noise. The variance of the estimation error for the I&I observer is much smaller compared to the Luenberger observer, as seen in Figure (6.5).

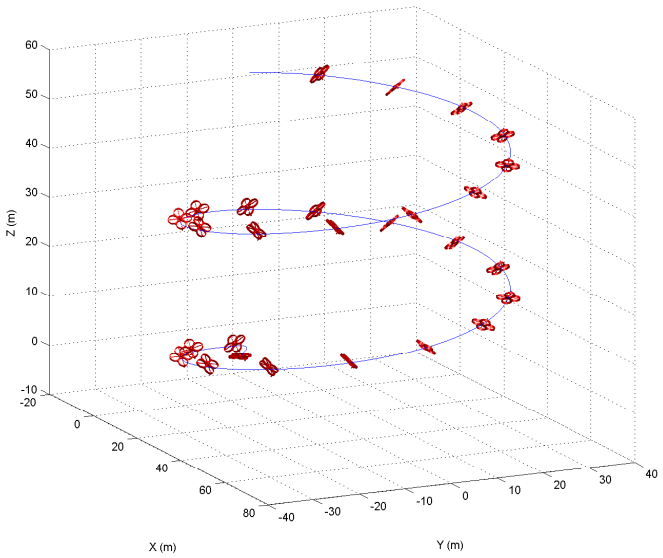

Figure 6.2: Output feedback 3D space tracking under I&I observer

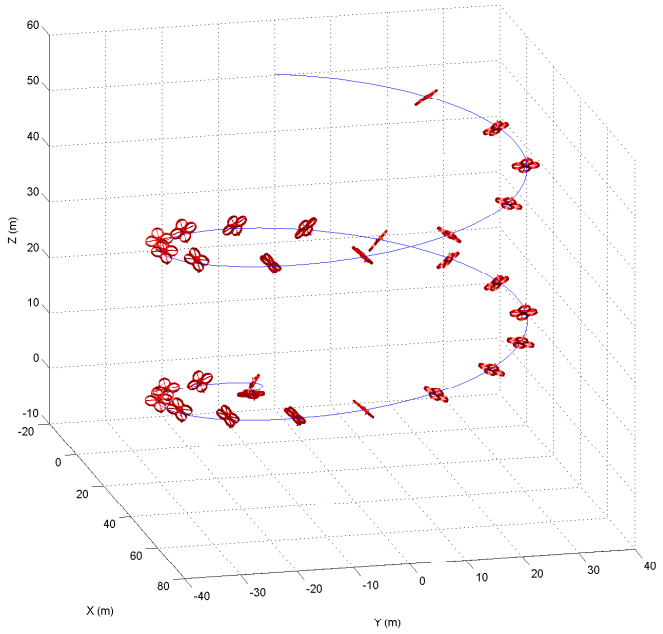

Figure 6.3: Output feedback 3D space tracking under Luenberger observer

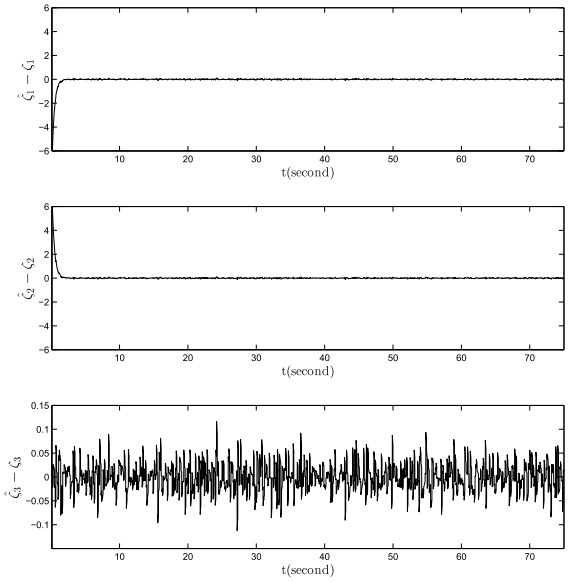

Figure 6.4: Estimation error I&I observer

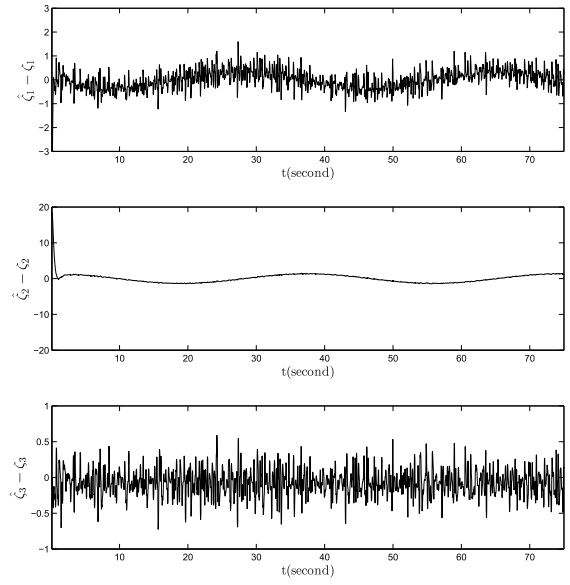

Figure 6.5: Estimation error Luenberger observer

In designing the Luenberger observer, the poles of the error dynamics are placed on the left hand side of the complex plane and far from the imaginary axis in order to provide a fast observer. This in turn amplifies the amplitude of noise in the system. This is why the variance of the estimation error of the Luenberger observer is much bigger compared to the I&I observer.

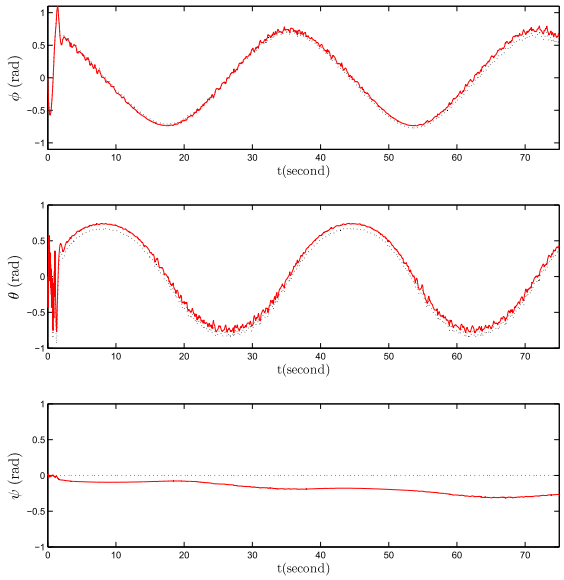

Figure 6.6: Euler angles tracking under I& observer

The results of estimation for both observers can be seen in Figure (6.6) and (6.7). The observers produce acceptable state estimation that can be used in state-feedback control design for the outer-loop. Eventhough the estimated states are used for the feedback control, the stability of the system is preserved.

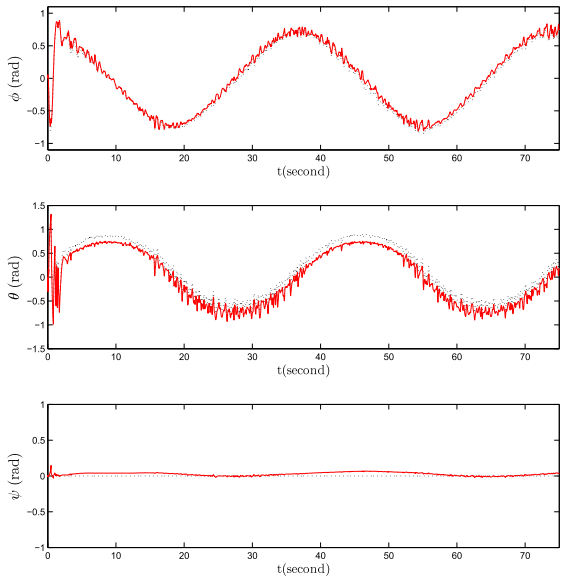

Figure 6.7: Euler angles tracking under Luenberger observer

6.5 Conclusions

This chapter has covered the design of the observers for trajectory tracking control of the quadrotor. The objective of the observers is to estimate the translational velocity utilizing information from the input and output in the outer loop.

The simulation results show that the I&I and the Luenberger observer are able to provide good estimation for the unmeasurable states. Since it is known that in linear systems the separation principle holds, the estimation results of both the observers can be used in the feedback control without affecting the stability of the system.

6.5.1 Contribution

The main contributions in this chapter are

1. Design of the I&I-based reduced-order observer for the translational dynamics the of quadrotor UAV.

2. Design of the classical Luenberger observer for benchmarking study.

CHAPTER 7

I&I ADAPTIVE CONTROL

7.1 Introduction

In this chapter, two recent adaptive control techniques used in the inner loop control of the quadrotor UAV are presented. The first is the I&I adaptive control technique which was first presented in [2]. In this technique, the certainty-equivalent control law is added by a new term that will shape the manifold such that the plant is immersed to the asymptotically stable target dynamics. The second technique is the $\mathcal{L}_1$ adaptive control developed by [31] which is used for comparison. The performances of both the techniques will be compared by the simulations in the presence of the unknown and uncertain parameters.

7.2 Adaptive Control Design

In this section, the design of two recent adaptive control techniques are proposed. The first technique is the I&I adaptive control, and the second technique is $\mathcal{L}_1$

adaptive control.

In order to design the I&I adaptive control, the rotational dynamics of the quadrotor need to be rewritten in linearly parameterized form. The details of the parametrization are presented in the next section, and the scheme of I&I adaptive control can be seen in Figure (7.1).

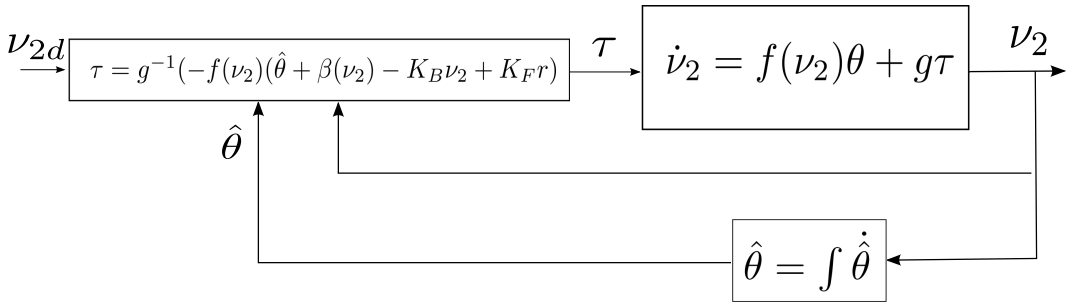

Figure 7.1: I&I Adaptive Control

For $\mathcal{L}_1$ adaptive control, the nonlinear term also needs to be rewritten into two linearly parameterized time-varying parameters. The details of linear parameterization of this nonlinear function can be found in the next section, and the scheme of this $\mathcal{L}_1$ adaptive control can be seen in Figure (7.2).

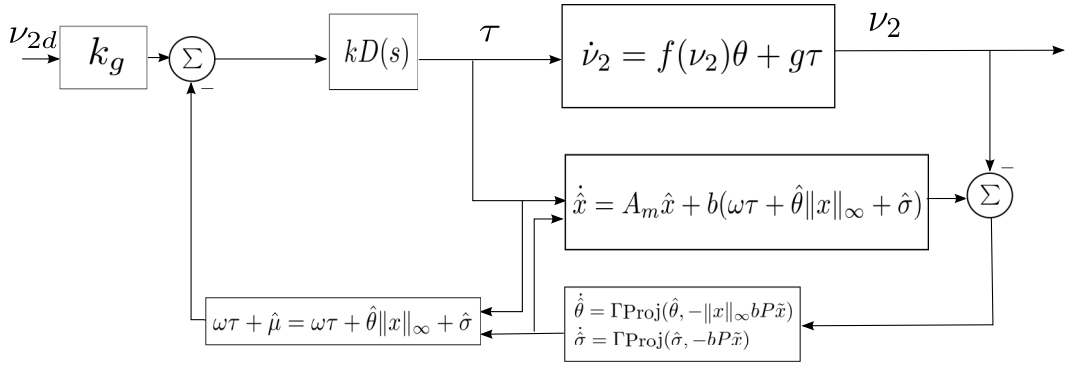

Figure 7.2: $\mathcal{L}_1$ Adaptive Control

7.2.1 I&I Adaptive Control for Linearly Parameterized Plant

Consider the system in the form of linearly parameterized plant, the dynamics can be described by

$$\dot{\mathbf{x}} = \mathbf{f}_0(\mathbf{x}) + \mathbf{f}_1(\mathbf{x})\boldsymbol{\theta} + \mathbf{g}(\mathbf{x})\mathbf{u} \tag{7.1}$$

where $\mathbf{x} \in \mathbb{R}^n$ is state, $\mathbf{u} \in \mathbb{R}^m$ is input, and $\boldsymbol{\theta} \in \mathbb{R}^q$ is an unknown parameter. The adaptive state feedback control law is given in the following form

$$\begin{aligned} \dot{\hat{\boldsymbol{\theta}}} =& \boldsymbol{\omega}(\mathbf{x}, \hat{\boldsymbol{\theta}}) \\ \mathbf{u} =& \mathbf{v}(\mathbf{x}, \hat{\boldsymbol{\theta}}) \end{aligned} \tag{7.2}$$

such that all the trajectories of closed loop system are bounded and $\lim_{t\to\infty} \mathbf{x}(t) = \mathbf{x}^*$.

In I&I adaptive control, the design of the control law is decoupled from the design of the adaptation law, which leads to more flexible control scheme [2]. If the following assumption holds

Assumption 7.1. $\exists\, \mathbf{u} = \mathbf{v}(\mathbf{x}, \boldsymbol{\theta})$, such that the system

$$\dot{\mathbf{x}} = \mathbf{f}^*(\mathbf{x}) = \mathbf{f}(\mathbf{x}) + \mathbf{g}(\mathbf{x})\mathbf{v}(\mathbf{x}, \theta) \tag{7.3}$$

has a globally asymptotically stable equilibrium at $\mathbf{x} = \mathbf{x}^*$.

Then the following theorem can be utilized in our adaptive control design.

Theorem 7.1 ([21]) *Consider the system (7.1) with an equilibrium point* $\mathbf{x}^*$ *to be stabilized, assume the following condition holds*

(A1). *There exists a mapping* $\boldsymbol{\beta} : \mathbb{R}^n \to \mathbb{R}^q$*, such that all the trajectories of the following system, with* $\mathbf{z} = \hat{\boldsymbol{\theta}} - \boldsymbol{\theta} + \boldsymbol{\beta}(x)$

$$\begin{aligned} \dot{\mathbf{z}} = & -\left[\frac{\partial \boldsymbol{\beta}}{\partial \mathbf{x}} \mathbf{f}_1(\mathbf{x})\right] \mathbf{z} \\ \dot{\mathbf{x}} = & \mathbf{f}^*(\mathbf{x}) + \mathbf{g}(\mathbf{x})(\mathbf{v}(\mathbf{x}, \theta + \mathbf{z}) - \mathbf{v}(\mathbf{x}, \boldsymbol{\theta})) \end{aligned} \tag{7.4}$$

are bounded and satisfy

$$\lim_{t \to \infty} (\mathbf{g}(\mathbf{x})(\mathbf{v}(\mathbf{x}, \boldsymbol{\theta} + \mathbf{z}) - \mathbf{v}(\mathbf{x}, \boldsymbol{\theta})) = 0 \tag{7.5}$$

then the system (7.1) is adaptively I&I stabilizable.

Proof: Proof see [21]. ∎

The rotational dynamics of the quadrotor in equation (4.14) can be rewritten into linearly parameterized system as

$$\dot{\mathbf{x}} = \mathbf{f}_0(\mathbf{x})\boldsymbol{\theta}_0 + \mathbf{f}_1(\mathbf{x})\theta_1 + \mathbf{f}_2(\mathbf{x})\theta_2 + \mathbf{f}_3(\mathbf{x})\theta_3 + \mathbf{G}\mathbf{u} \tag{7.6}$$

where

$$\mathbf{x} \triangleq \boldsymbol{\nu}_2, \qquad \mathbf{f}_0(\mathbf{x}) \triangleq \text{diag}(-qr, -pr, -pq), \qquad \boldsymbol{\theta}_0 \triangleq [I_1, I_2, I_3]^\top,$$

$$I_1 = (I_z - I_y)/I_x, \qquad I_2 = (I_x - I_z)/I_y, \qquad I_3 = (I_y - I_x)/I_z,$$

$$\mathbf{f}_1(\mathbf{x}) \triangleq [q, 0, 0]^\top, \qquad \theta_1 \triangleq I_R\Omega, \qquad \mathbf{f}_2(\mathbf{x}) \triangleq [0, p, 0]^\top, \qquad \theta_2 \triangleq -I_R\Omega,$$

$$\mathbf{f}_3(\mathbf{x}) \triangleq [p, q, r]^\top, \qquad \theta_3 \triangleq -k_r, \qquad \mathbf{G} \triangleq \text{diag}(I_x^{-1}, I_y^{-1}, I_z^{-1}), \qquad \mathbf{u} \triangleq [\tau_p, \tau_q, \tau_r]^\top$$

To satisfy Assumption 7.1, the following controller is selected

$$\mathbf{u} = \mathbf{G}^{-1}(-\mathbf{f}_0\boldsymbol{\theta}_0 - \mathbf{f}_1\theta_1 - \mathbf{f}_2\theta_2 - \mathbf{f}_3\theta_3 - \mathbf{K}_B\mathbf{x} + \mathbf{K}_F\mathbf{r}) \tag{7.7}$$

where $\mathbf{K}_F > 0$ is the feedforward gain, $\mathbf{r}$ is the bounded reference and for feedback gain $\mathbf{K}_B > 0$, the following globally exponentially stable closed loop system is obtained

$$\dot{\mathbf{x}} = -\mathbf{K}_B\mathbf{x} + \mathbf{K}_F\mathbf{r} \tag{7.8}$$

To apply I&I adaptive control on the rotational dynamics, define the following implicit manifold

$$\begin{aligned} \mathbf{z}_0 &= \hat{\boldsymbol{\theta}}_0 - \boldsymbol{\theta}_0 + \boldsymbol{\beta}_0(\mathbf{x}) \\ z_i &= \hat{\theta}_i - \theta_i + \beta_i(\mathbf{x}), \quad i = 1, 2, 3 \end{aligned} \tag{7.9}$$

and the dynamics are given by

$$\begin{aligned}
\dot{\mathbf{z}}_0 &= \dot{\hat{\boldsymbol{\theta}}}_0 + \frac{\partial \boldsymbol{\beta}_0}{\partial \mathbf{x}} \dot{\mathbf{x}} \\
&= \dot{\hat{\boldsymbol{\theta}}}_0 + \frac{\partial \boldsymbol{\beta}_0}{\partial \mathbf{x}} (\mathbf{f}_0(\mathbf{x})\boldsymbol{\theta}_0 + \mathbf{f}_1(\mathbf{x})\theta_1 + \mathbf{f}_2(\mathbf{x})\theta_2 + \mathbf{f}_3(\mathbf{x})\theta_3 + \mathbf{G}\mathbf{u}) \qquad (7.10) \\
\dot{z}_i &= \dot{\hat{\theta}}_i + \frac{\partial \beta_i}{\partial \mathbf{x}} \dot{\mathbf{x}} \\
&= \dot{\hat{\theta}}_i + \frac{\partial \beta_i}{\partial \mathbf{x}} (\mathbf{f}_0(\mathbf{x})\boldsymbol{\theta}_0 + \mathbf{f}_1(\mathbf{x})\theta_1 + \mathbf{f}_2(\mathbf{x})\theta_2 + \mathbf{f}_3(\mathbf{x})\theta_3 + \mathbf{G}\mathbf{u}) \qquad (7.11)
\end{aligned}$$

if the updating laws ($\boldsymbol{\omega}(\mathbf{x}, \hat{\boldsymbol{\theta}}) = \dot{\hat{\boldsymbol{\theta}}}$) are selected to be

$$\begin{aligned}
\boldsymbol{\omega}_0 = & -\frac{\partial \boldsymbol{\beta}_0(\mathbf{x})}{\partial \mathbf{x}} (\mathbf{f}_0(\mathbf{x})(\hat{\boldsymbol{\theta}}_0 + \boldsymbol{\beta}_0) + \mathbf{f}_1(\mathbf{x})(\hat{\theta}_1 + \beta_1 - z_1) + \mathbf{f}_2(\mathbf{x})(\hat{\theta}_2 + \beta_2 - z_2) \\
& + \mathbf{f}_3(\mathbf{x})(\hat{\theta}_3 + \beta_3 - z_3) + \mathbf{G}\mathbf{u}) \\
\omega_1 = & -\frac{\partial \beta_1(\mathbf{x})}{\partial \mathbf{x}} (\mathbf{f}_0(\mathbf{x})(\hat{\boldsymbol{\theta}}_0 + \boldsymbol{\beta}_0 - \mathbf{z}_0) + \mathbf{f}_1(\mathbf{x})(\hat{\theta}_1 + \beta_1) + \mathbf{f}_2(\mathbf{x})(\hat{\theta}_2 + \beta_2 - z_2) \\
& + \mathbf{f}_3(\mathbf{x})(\hat{\theta}_3 + \beta_3 - z_3) + \mathbf{G}\mathbf{u}) \\
\omega_2 = & -\frac{\partial \beta_2(\mathbf{x})}{\partial \mathbf{x}} (\mathbf{f}_0(\mathbf{x})(\hat{\boldsymbol{\theta}}_0 + \boldsymbol{\beta}_0 - \mathbf{z}_0) + \mathbf{f}_1(\mathbf{x})(\hat{\theta}_1 + \beta_1 - z_1) + \mathbf{f}_2(\mathbf{x})(\hat{\theta}_2 + \beta_2) \\
& + \mathbf{f}_3(\mathbf{x})(\hat{\theta}_3 + \beta_3 - z_3) + \mathbf{G}\mathbf{u}) \\
\omega_3 = & -\frac{\partial \beta_3(\mathbf{x})}{\partial \mathbf{x}} (\mathbf{f}_0(\mathbf{x})(\hat{\boldsymbol{\theta}}_0 + \boldsymbol{\beta}_0 - \mathbf{z}_0) + \mathbf{f}_1(\mathbf{x})(\hat{\theta}_1 + \beta_1 - z_1) + \mathbf{f}_2(\mathbf{x})(\hat{\theta}_2 + \beta_2 - z_2) \\
& + \mathbf{f}_3(\mathbf{x})(\hat{\theta}_3 + \beta_3) + \mathbf{G}\mathbf{u})
\end{aligned}$$

substituting these into (7.10) and (7.11), and utilizing (7.9) one will have

$$\begin{aligned}
\dot{\mathbf{z}}_0 = & -\left(\frac{\partial \boldsymbol{\beta}_0(\mathbf{x})}{\partial \mathbf{x}} \mathbf{f}_0(\mathbf{x}) \right) \mathbf{z}_0 \\
\dot{z}_i = & -\left(\frac{\partial \beta_i(\mathbf{x})}{\partial \mathbf{x}} \mathbf{f}_i(\mathbf{x}) \right) z_i \qquad (7.12)
\end{aligned}$$

If $\frac{\partial \boldsymbol{\beta}_0(\mathbf{x})}{\partial \mathbf{x}} = \gamma_0 \mathbf{I}\, \mathbf{f}_0(\mathbf{x})$, and $\frac{\partial \beta_i(\mathbf{x})}{\partial \mathbf{x}} = \gamma_i \mathbf{f}_i^\top(\mathbf{x})$, where $\gamma_0 > 0,\ \gamma_i > 0$ are selected, the following is obtained

$$\lim_{t\to\infty} \mathbf{z}(t) = 0 \qquad \Rightarrow \qquad \boldsymbol{\theta} = \hat{\boldsymbol{\theta}} + \boldsymbol{\beta}(\mathbf{x}) \tag{7.13}$$

Finally, the I&I adaptive control is given by

$$\mathbf{u} = \mathbf{G}^{-1}(-\mathbf{f}_0(\hat{\boldsymbol{\theta}}_0 + \boldsymbol{\beta}_0) - \mathbf{f}_1(\hat{\theta}_1 + \beta_1) - \mathbf{f}_2(\hat{\theta}_2 + \beta_2) - \mathbf{f}_3(\hat{\theta}_3 + \beta_3) - \mathbf{K}_B\mathbf{x} + \mathbf{K}_F\mathbf{r}) \tag{7.14}$$

7.2.2 I&I Adaptive Control Analysis

Consider the Lyapunov function candidate

$$V(\mathbf{z}) = \mathbf{z}^\top \mathbf{P} \mathbf{z} \tag{7.15}$$

the derivative of the Lyapunov function along the trajectories of the (7.12) is given by

$$\dot{V}(\mathbf{z}) = \mathbf{z}^\top (\boldsymbol{\Phi}^\top \mathbf{P} + \mathbf{P}\boldsymbol{\Phi}) \mathbf{z} \tag{7.16}$$

where

$$\mathbf{\Phi} = -\begin{bmatrix} \gamma_0 \mathbf{I}\, \mathbf{f}_0^2 & 0 & 0 & 0 \\ 0 & \gamma_1 \mathbf{f}_1^\top \mathbf{f}_1 & 0 & 0 \\ 0 & 0 & \gamma_2 \mathbf{f}_2^\top \mathbf{f}_2 & 0 \\ 0 & 0 & 0 & \gamma_3 \mathbf{f}_3^\top \mathbf{f}_3 \end{bmatrix} \tag{7.17}$$

Since $\mathbf{\Phi}$ is Hurwitz, for $\mathbf{Q}^\top = \mathbf{Q} > 0$ and unique $\mathbf{P}^\top = \mathbf{P} > 0$, the following Lyapunov equation is satisfied

$$\mathbf{\Phi}^\top \mathbf{P} + \mathbf{P}\mathbf{\Phi} = -\mathbf{Q} \tag{7.18}$$

substituting (7.16) in (7.18) one will have

$$\dot{V}(\mathbf{z}) = -\mathbf{z}^\top \mathbf{Q}\mathbf{z} \leq 0 \tag{7.19}$$

hence the system (8.10) has a globally stable equilibrium at zero, and the asymptotic stability is followed by the LaSalle's Invariance Principle.

Since $V(\mathbf{z})$ is a positive definite function and $\dot{V}(\mathbf{z}) \leq 0$, it implies $V(\mathbf{z}) \in \mathcal{L}_\infty$ which implies $\mathbf{z} \in \mathcal{L}_\infty$, and therefore the off-manifold coordinates are bounded. By integrating $\dot{V}(\mathbf{z})$ it follows that

$$V(\infty) - V(0) = -\int_0^\infty \mathbf{z}^\top \mathbf{Q}\mathbf{z} dt \tag{7.20}$$

hence $\mathbf{z} \in \mathcal{L}_2 \cap \mathcal{L}_\infty$. Since the manifold coordinate is given by $\mathbf{z} = \hat{\boldsymbol{\theta}} - \boldsymbol{\theta} + \boldsymbol{\beta}(x)$, it implies that $\hat{\boldsymbol{\theta}}, \boldsymbol{\beta} \in \mathcal{L}_2$, so all the signals in the closed loop system are bounded.

7.2.3 $\mathcal{L}_1$ Adaptive Control

To proceed with the design of the $\mathcal{L}_1$ adaptive control, linear parametrization of the nonlinear function needs to be done. One of the goals of the linear parametrization is to represent unknown parameters in the linear time-varying form, so that the dynamics of the predictor can be selected from it. The rotational dynamics presented in (4.14) can be rewritten in the form

$$\begin{aligned} \dot{\mathbf{x}} &= \mathbf{A}_m \mathbf{x} + b(\boldsymbol{\omega}\mathbf{u}_{ad} + \mathbf{f}(t, \mathbf{x}(t))), \quad \mathbf{x}(0) = \mathbf{x}_0 \\ \mathbf{y} &= \mathbf{c}^\top \mathbf{x}(t) \end{aligned} \tag{7.21}$$

where

$$\begin{aligned} \mathbf{x} &\triangleq \boldsymbol{\nu}_2, \qquad \mathbf{A}_m \in \mathbb{R}^{n\times n} \triangleq \text{ a known desired Hurwitz matrix} \\ b &= 1, \qquad \boldsymbol{\omega} \triangleq I_{\mathrm{M}}^{-1}, \qquad \mathbf{u}_{ad} \triangleq \boldsymbol{\tau} \triangleq \mathcal{L}_1 \text{ Adaptive control} \\ \mathbf{f}(t, \mathbf{x}(t)) &\triangleq \mathbf{I}_{\mathrm{M}}^{-1}(-(\boldsymbol{\nu}_2 \times \mathbf{I}_{\mathrm{M}}\boldsymbol{\nu}_2) - I_R(\boldsymbol{\nu}_2 \times \mathbf{z}_e)\Omega - k_r\boldsymbol{\nu}_2), \qquad \mathbf{c}^\top = \mathbf{I}_{3\times 3} \end{aligned} \tag{7.22}$$

To proceed with the design of $\mathcal{L}_1$ adaptive control, the Assumption 3.1 need to be satisfied. Based on these assumptions, two time-varying parameters are obtained from the nonlinear function $\mathbf{f}(t, \mathbf{x}(t))$ using $\|\mathbf{x}\|_\infty$ as a regressor. The

lemma 3.2 proves this statement and by utilizing it, (7.21) can be rewritten as

$$\begin{aligned}\dot{\mathbf{x}} &= \mathbf{A}_m\mathbf{x} + b(\boldsymbol{\omega}\mathbf{u}_{ad} + \boldsymbol{\theta}\|\mathbf{x}\|_\infty + \boldsymbol{\sigma}), \;\; \mathbf{x}(0) = \mathbf{x}_0 \\ \mathbf{y} &= \mathbf{c}^\top\mathbf{x}(t)\end{aligned} \tag{7.23}$$

From (7.23) the following state predictor is considered

$$\begin{aligned}\dot{\hat{\mathbf{x}}} &= \mathbf{A}_m\hat{\mathbf{x}} + b(\boldsymbol{\omega}\mathbf{u}_{ad} + \hat{\boldsymbol{\theta}}\|\mathbf{x}\|_\infty + \hat{\boldsymbol{\sigma}}), \;\; \hat{\mathbf{x}}(0) = \mathbf{x}_0 \\ \hat{\mathbf{y}} &= \mathbf{c}^\top\hat{\mathbf{x}}\end{aligned} \tag{7.24}$$

where $\hat{\mathbf{x}} \in \mathbb{R}^n$ is the predicted state, $\hat{\mathbf{y}} \in \mathbb{R}^n$ is the predicted output, $\hat{\boldsymbol{\theta}}$ and $\hat{\boldsymbol{\sigma}}$ are the estimated parameters. Define the error $\tilde{\mathbf{x}} = \hat{\mathbf{x}} - \mathbf{x}$, $\tilde{\boldsymbol{\theta}} = \hat{\boldsymbol{\theta}} - \boldsymbol{\theta}$, and $\tilde{\boldsymbol{\sigma}} = \hat{\boldsymbol{\sigma}} - \boldsymbol{\sigma}$, and the following error dynamic is obtained

$$\dot{\tilde{\mathbf{x}}} = \mathbf{A}_m\tilde{\mathbf{x}} + b(\tilde{\boldsymbol{\theta}}\|\mathbf{x}\|_\infty + \tilde{\boldsymbol{\sigma}}), \;\; \tilde{\mathbf{x}}(0) = 0 \tag{7.25}$$

Consider the Lyapunov function candidate

$$V(\tilde{\mathbf{x}}, \tilde{\boldsymbol{\theta}}, \tilde{\boldsymbol{\sigma}}) = \tilde{\mathbf{x}}^\top\mathbf{P}\tilde{\mathbf{x}} + \frac{1}{\Gamma}(\tilde{\boldsymbol{\theta}}^\top\tilde{\boldsymbol{\theta}} + \tilde{\boldsymbol{\sigma}}^\top\tilde{\boldsymbol{\sigma}}) \tag{7.26}$$

The derivative of the Lyapunov candidate (7.26) along the trajectory of (7.25) is

given by

$$\begin{aligned}\dot{V}(\tilde{\mathbf{x}},\tilde{\boldsymbol{\theta}},\tilde{\boldsymbol{\sigma}}) &= \dot{\tilde{\mathbf{x}}}^\top\mathbf{P}\tilde{\mathbf{x}} + \tilde{\mathbf{x}}^\top\mathbf{P}\dot{\tilde{\mathbf{x}}} + \frac{2}{\Gamma}(\tilde{\boldsymbol{\theta}}^\top\dot{\tilde{\boldsymbol{\theta}}} + \tilde{\boldsymbol{\sigma}}^\top\dot{\tilde{\boldsymbol{\sigma}}}) \\ &= -\tilde{\mathbf{x}}^\top\mathbf{Q}\tilde{\mathbf{x}} + 2\tilde{\mathbf{x}}^\top\mathbf{P}b(\tilde{\boldsymbol{\theta}}\|\mathbf{x}\|_\infty + \tilde{\boldsymbol{\sigma}}) + \frac{2}{\Gamma}(\tilde{\boldsymbol{\theta}}^\top\dot{\tilde{\boldsymbol{\theta}}} + \tilde{\boldsymbol{\sigma}}^\top\dot{\tilde{\boldsymbol{\sigma}}})\end{aligned} \tag{7.27}$$

Considering the property 3.1 of the projection operator, one can upperbound the derivative of the Lyapunov function as

$$\begin{aligned}\dot{V}(\tilde{\mathbf{x}},\tilde{\boldsymbol{\theta}},\tilde{\boldsymbol{\sigma}}) = & -\tilde{\mathbf{x}}^\top\mathbf{Q}\tilde{\mathbf{x}} + 2\tilde{\mathbf{x}}^\top\mathbf{P}b(\tilde{\boldsymbol{\theta}}\|\mathbf{x}\|_\infty + \tilde{\boldsymbol{\sigma}}) + 2(\tilde{\boldsymbol{\theta}}^\top\mathrm{Proj}(\tilde{\boldsymbol{\theta}}, -\|\mathbf{x}\|_\infty b\mathbf{P}\tilde{\mathbf{x}}) \\ & + \tilde{\boldsymbol{\sigma}}^\top\mathrm{Proj}(\tilde{\boldsymbol{\theta}}, -b\mathbf{P}\tilde{\mathbf{x}})) \\ = & -\tilde{\mathbf{x}}^\top\mathbf{Q}\tilde{\mathbf{x}} + 2\tilde{\boldsymbol{\theta}}^\top(\|\mathbf{x}\|_\infty b\mathbf{P}\tilde{\mathbf{x}} + \mathrm{Proj}(\tilde{\boldsymbol{\theta}}, -\|\mathbf{x}\|_\infty b\mathbf{P}\tilde{\mathbf{x}})) \\ & + 2\tilde{\boldsymbol{\sigma}}^\top(b\mathbf{P}\tilde{\mathbf{x}} + \mathrm{Proj}(\tilde{\boldsymbol{\sigma}}, -b\mathbf{P}\tilde{\mathbf{x}})) \\ \leq & -\tilde{\mathbf{x}}^\top\mathbf{Q}\tilde{\mathbf{x}}\end{aligned} \tag{7.28}$$

with the adaptation law given by the following

$$\begin{aligned}\dot{\tilde{\boldsymbol{\theta}}} = \dot{\hat{\boldsymbol{\theta}}} &= \Gamma\mathrm{Proj}(\tilde{\boldsymbol{\theta}}, -\|\mathbf{x}\|_\infty b\mathbf{P}\tilde{\mathbf{x}}) \\ \dot{\tilde{\boldsymbol{\sigma}}} = \dot{\hat{\boldsymbol{\sigma}}} &= \Gamma\mathrm{Proj}(\tilde{\boldsymbol{\sigma}}, -b\mathbf{P}\tilde{\mathbf{x}})\end{aligned} \tag{7.29}$$

where $\Gamma > 0$ is the adaptation law rate and $\mathbf{Q} = \mathbf{Q}^\top > 0$, with $\mathbf{P} = \mathbf{P}^\top > 0$

satisfies the Lyapunov equation

$$\mathbf{A}_m^\top \mathbf{P} + \mathbf{P}\mathbf{A}_m = -\mathbf{Q} \tag{7.30}$$

The Laplace transform of the adaptive control signal $\mathbf{u}_{ad}$ is selected to be

$$\mathbf{u}_{ad}(s) = -\frac{\mathbf{C}(s)}{\boldsymbol{\omega}}(\hat{\boldsymbol{\mu}}(s) - \mathbf{k}_g \mathbf{r}(s)) \tag{7.31}$$

where $\hat{\boldsymbol{\mu}}(s)$ and $\mathbf{r}(s)$ are the Laplace transform of $\hat{\boldsymbol{\mu}}(t) \triangleq \hat{\boldsymbol{\theta}}(t)\|\mathbf{x}\|_\infty + \hat{\boldsymbol{\sigma}}(t)$ and $\mathbf{r}(t) \triangleq$ reference signal, respectively. Feedforward gain is given by $\mathbf{k}_g \triangleq -\frac{1}{\mathbf{c}^\top \mathbf{A}_m^{-1} b}$. If the filter $\mathbf{C}(s)$ is selected to be

$$\mathbf{C}(s) \triangleq \frac{\boldsymbol{\omega k}\mathbf{D}(\boldsymbol{s})}{\mathbf{I} + \boldsymbol{\omega k}\mathbf{D}(\boldsymbol{s})} \tag{7.32}$$

with DC gain $\mathbf{C}(0) = \mathbf{I}$. The selection of $\mathbf{D}(s) = \frac{\mathbf{I}}{s}$ yields first order strictly proper transfer function

$$\mathbf{C}(s) = \frac{\boldsymbol{\omega} k}{s\mathbf{I} + \boldsymbol{\omega} k} \tag{7.33}$$

Substituting (7.32) into (7.31), the Laplace transform of the adaptive control signal becomes

$$\mathbf{u}_{ad}(s) = -k\mathbf{D}(s)(\boldsymbol{\omega}\mathbf{u}_{ad}(s) + \hat{\boldsymbol{\mu}}(s) - \mathbf{k}_g \mathbf{r}(s)) \tag{7.34}$$

Remark from [31], if the derivative of $\mathbf{f}(t, \mathbf{x})$ with respect to $\mathbf{x}$ has a uniform bound

$$\left\| \frac{\partial \mathbf{f}(t, \mathbf{x})}{\partial x} \right\| \leq \mathbf{d}_{f_x} = \mathbf{L} \tag{7.35}$$

that holds uniformly $\forall \mathbf{x} \in \mathbb{R}^n$, then the following $\mathcal{L}_1$-norm condition has to be satisfied for $\mathcal{L}_1$ adaptive control

$$\|\mathbf{G}(s)\|_{\mathcal{L}_1} \mathbf{L} < 1 \tag{7.36}$$

where

$$\mathbf{G}(s) \triangleq \mathbf{H}(s)(\mathbf{C}(s) - \mathbf{I}), \quad \mathbf{H}(s) \triangleq (s\mathbf{I} - \mathbf{A}_m)^{-1} b \tag{7.37}$$

The analysis of this nonlinear $\mathcal{L}_1$ adaptive control in detail can be seen in [31].

7.3 Simulation

Utilizing the I&I and the $\mathcal{L}_1$ adaptive control design, two simulations have been performed. The parameters of the plant in the inner loop are assumed to be unknown but bounded and are also changing randomly with Gaussian distribution. The objective of the controller is to track a bounded smooth predefined trajectory in the presence of unknown and uncertain parameters and exogenous disturbances. The trajectory is selected to be helix-shaped and the desired yaw angle is zero. By this scenario the performance of the proposed adaptive controllers are investigated.

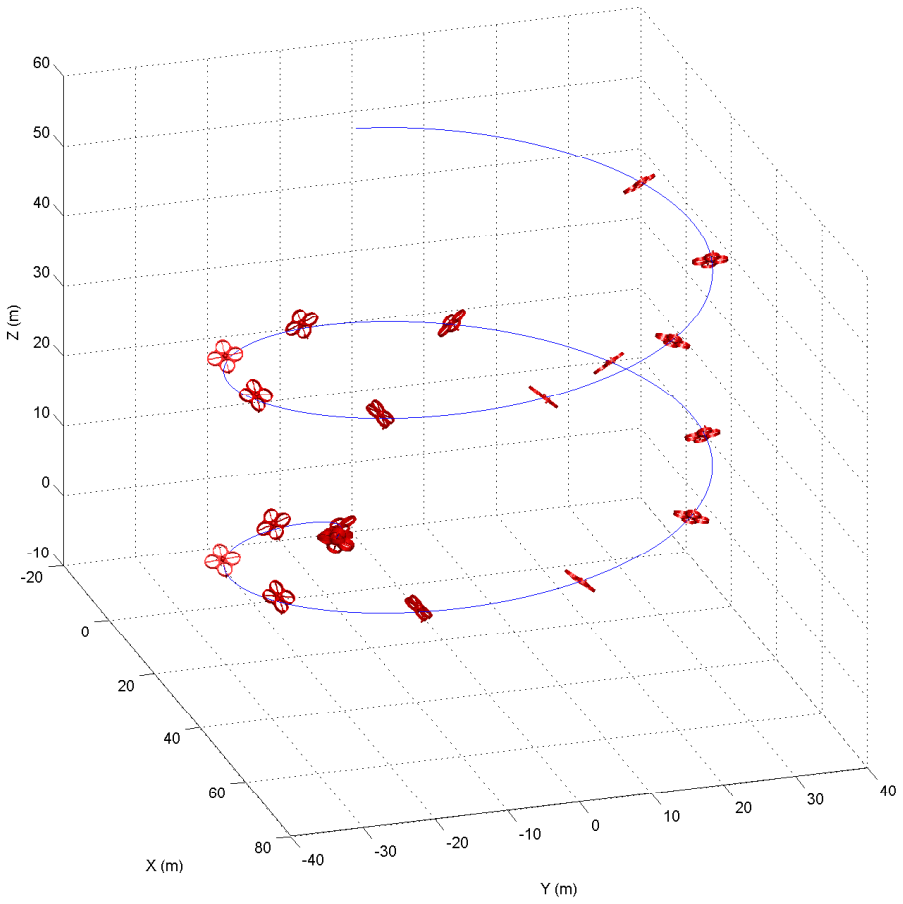

Figure 7.3: I&I 3D trajectory tracking

It can be seen from Figure (7.3)-(7.5), despite of the unknown and uncertain parameters the tracking performance of the PD controller for the translational motion, and the I&I adaptive controller for the rotational motion is acceptable. Eventhough the parameters in the outer loop are assumed to be perfectly known, the stability and tracking performance may be disturbed if the inner loop is unstable or has poor tracking performance. Hence, by this simulation, it is

shown that once the inner loop is stable and has good tracking performance, i.e $\lim_{t\to\infty} \boldsymbol{\nu}_{2d}(t) - \boldsymbol{\nu}_2(t) = 0$, the stability of the outer loop is concluded.

In order to see the control signal clearly, Figure (7.6) is zoomed. In the actual size, the control signal (τ_p, τ_q, τ_r) in the transient part reaches it highest value which is 5N.m. It is due to the non-zero initial conditions and causing the controller to use high energy to minimize the error.

In the first figure in Figure (7.7), it can be seen that the estimated parameters $(\hat{\boldsymbol{\theta}}_0 + \boldsymbol{\beta}_0(\mathbf{x}))$ that are used in the controller reach the steady state values. In the second figure in Figure (7.7), if the simulation time is increased it can be seen that it will settle in the steady state values eventually. In the theory of I&I adaptive control [21], it is stated that it is not necessary for the estimated parameters to converge to its true values.

The second simulation is conducted using $\mathcal{L}_1$ adaptive control. The environment of simulation is similar to the first simulation. From Figure (7.8)-(7.10), it can be seen that the $\mathcal{L}_1$ adaptive control provides good tracking performance in the inner loop. In the control signal (Figure(7.11)), $\mathcal{L}_1$ adaptive control produces smoother control signal compared to the I&I adaptive control. In practical point of view, smoother control signal is better, it will keep the age of the actuator longer compared to the fluctuating control signal. The fluctuating control signal also will directly damage the actuator, hence creating fault that will disturb the stability of the system.

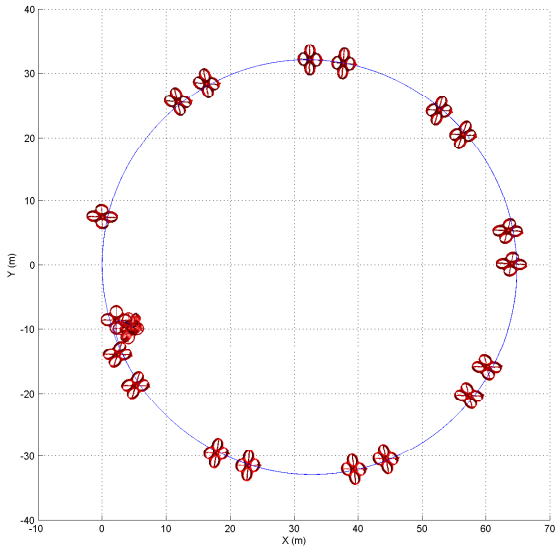

Figure 7.4: I&I x-y trajectory tracking

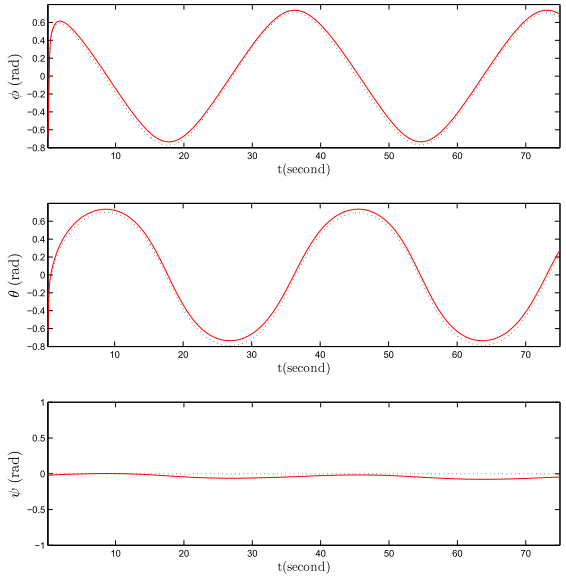

Figure 7.5: I&I Euler angles tracking

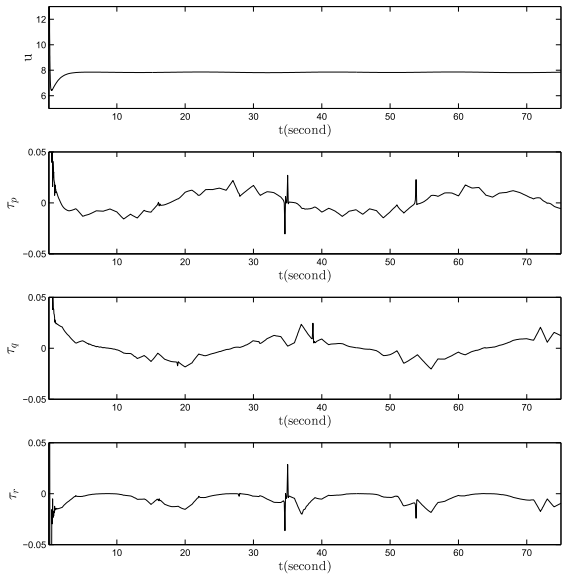

Figure 7.6: I&I control signal

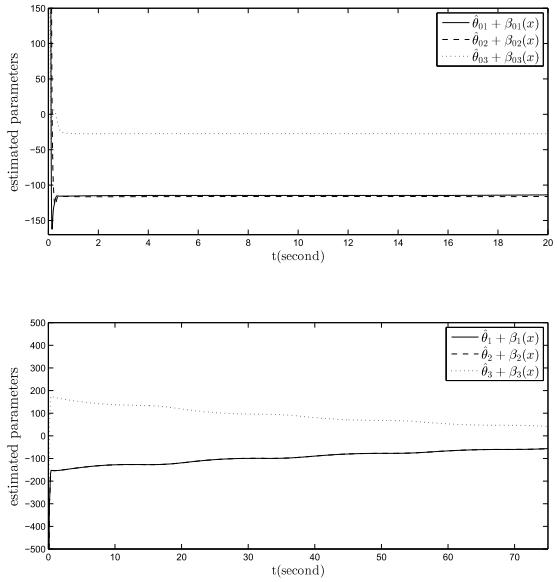

Figure 7.7: I&I ($\hat{\theta} + \beta$)

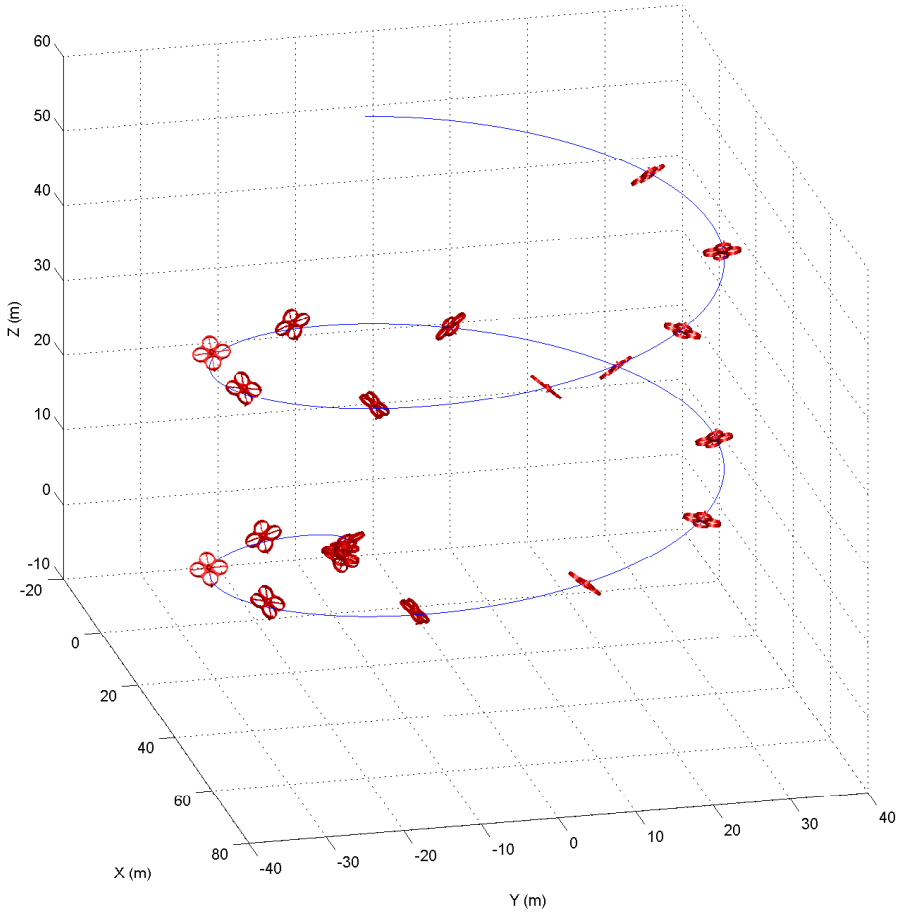

Figure 7.8: $\mathcal{L}_1$ 3D trajectory tracking

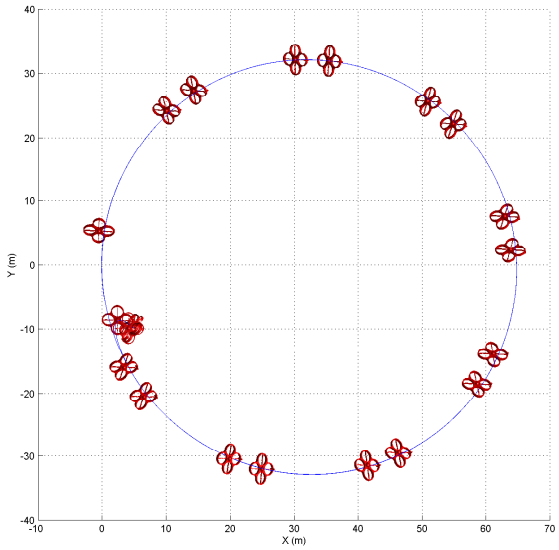

Figure 7.9: $\mathcal{L}_1$ x-y trajectory tracking

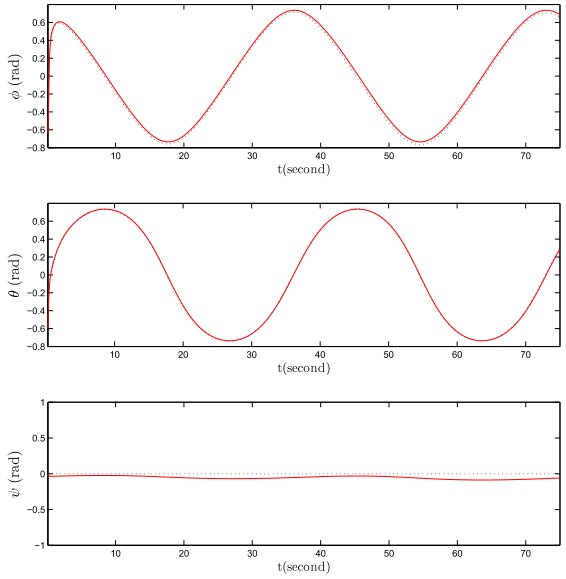

Figure 7.10: $\mathcal{L}_1$ Euler angles tracking

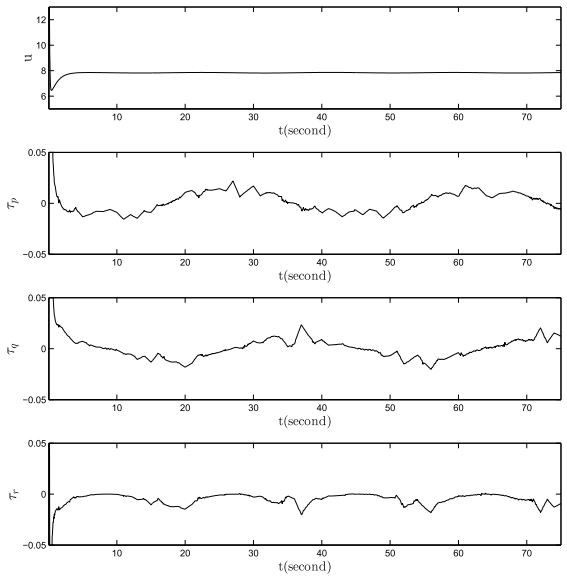

Figure 7.11: $\mathcal{L}_1$ control signal

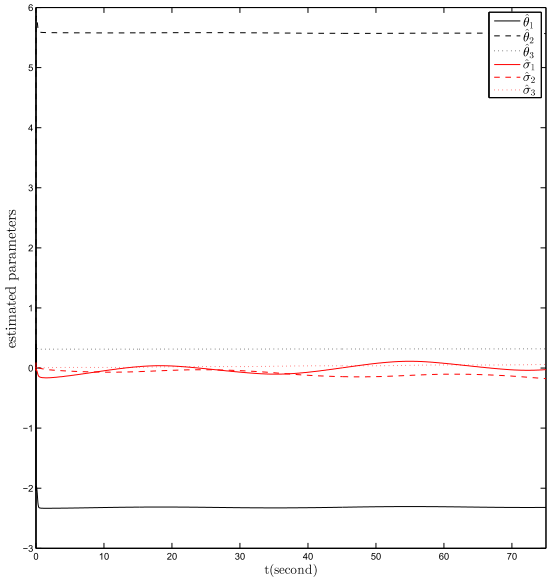

Figure 7.12: $\mathcal{L}_1$ parameters estimation

7.4 Conclusions

This chapter presents two recent techniques in adaptive control, i.e I&I adaptive control and $\mathcal{L}_1$ adaptive control, for the quadrotor UAV. The quadrotor investigated in this chapter belongs to a class of nonlinear systems and is assumed to have unknown and uncertain parameters, in which the proposed adaptive controls are required for stabilization. Based on the simulations, both the I&I and $\mathcal{L}_1$ adaptive control show acceptable performance in terms of trajectory tracking. In terms of control signal, $\mathcal{L}_1$ adaptive control has a smoother signal compared to the I&I adaptive control. In the next chapter, another benchmarking for both the adaptive controllers will be investigated in directional drilling system containing internal delay.

7.4.1 Contribution

The main contributions presented in this chapter are

1. Design of I&I adaptive control for the underactuated quadrotor UAV with unknown and uncertain parameters.

2. Analysis of I&I adaptive control.

3. Design of $\mathcal{L}_1$ adaptive control for the underactuated quadrotor UAV with unknown and uncertain parameters.

CHAPTER 8

I&I ADAPTIVE CONTROL BENCHMARKING FOR SYSTEMS WITH DELAYS: THE CASE OF DRILLING SYSTEM

8.1 Introduction

This chapter presents another benchmarking of I&I and $\mathcal{L}_1$ adaptive control which is designed for EFFSZM directional drilling control system. In this section, a short introduction of the directional drilling system and control is presented.

In oil and gas industry, the directional drilling system plays an important role in enhancing the oil and gas production. The directional drilling allows more oil and gas to be drained compared to the purely vertical drilling. Previous research shows that the directional drilling systems are able to extract oil and gas 2 to 25 times than the standard vertical drilling [49][50][51]. In directional drilling system, control is the crucial part. Specifically for trajectory tracking directional drilling system, automatic control theory needs to be utilized and investigated.

In order to design a proper control for the directional drilling system, a model that represents the dynamics of the directional drilling system needs to be formulated. In [52], a transfer function relating the centreline of the drilling hole to the actuator stimuli is derived. A quasi-polynomial is used to approximate the space-curve of the centreline of the hole, with distance m instead of t as the independent variable.

It is almost impossible to get 100% accuracy in the modelling, hence a robust controller that can handle wide uncertainties is needed. In the previous work [40][53], a recent adaptive control technique, i.e $\mathcal{L}_1$ adaptive control, is utilized. Some parameters in the model are considered to be uncertain but bounded. The objective of the controller is to stabilize the system in the presence of the parameter uncertainty and produce minimum tracking error. The results presented by the simulation show that the proposed controller can fulfill the objective.

This chapter is utilizing I&I adaptive control for a class system with unknown parameters and uncertainty in the presence of internal delay. The result of this controller will be validated by simulations and the performance will be compared to the $\mathcal{L}_1$ adaptive control.

8.2 Directional Drilling System

In directional drilling system, the transfer function relating the centreline of the drilling hole to the actuator stimuli is derived in [52]. The distance drilled is used as the independent variable instead of time, which means the differential equation

that represents the directional drilling system is presented in distance drilled (m). There are several types of model derived in [52], one of them is EFFSZM model. In EFFSZM, from the known geometry and action of actuators, the force at the drill bit are explicitly calculated. The pipe work is assumed to be infinitely stiff with zero mass and the drill bit is assumed to be finitely sharp.

Consider EFFSZM drilling system differential equation given by the following

$$\begin{aligned}\frac{dH(m)}{dm} =& \left(\frac{1+C_f}{b} - \frac{Cf}{d}\right) H(m) + \frac{1+C_f}{b}\left(V(m) - H(m-b)\right) + \frac{C_f}{d} H(m-d) \\ &+ \frac{b-a}{b\, WOB\; K_{anis}} F_{pad}(m) \\ \Psi(m) =& \frac{dH(m)}{dm} \end{aligned} \tag{8.1}$$

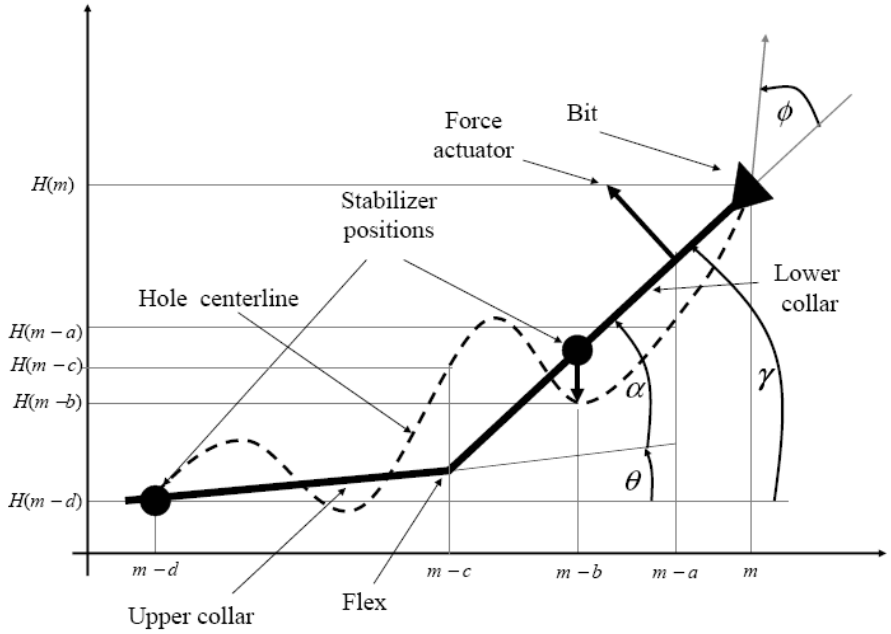

Figure 8.1: Flex-hinge Directional Drilling System [52]

where

$$C_f = \left(\frac{c-b}{K_{anis} - \frac{d-b}{d-c}} \frac{K_{flex}}{WOB} \right) \frac{d}{b(d-c)}, \qquad m \triangleq \text{the distance drilled,}$$

$H(m) \triangleq$ lateral displacement of the borehole

$a \triangleq$ distance between the force actuator and the bit

$b \triangleq$ distance between the lower stabilizer and the bit

$c \triangleq$ the relative position of the flex-joint to the bit

$d \triangleq$ the position of the upper stabilizer to the bit

$K_{flex} \triangleq$ angular spring rate of the flex joint

$K_{anis} \triangleq$ ration of rates of penetration along and across the bit

$V(m) \triangleq$ the actuator displacement at the lower stabilizer

$WOB \triangleq$ the applied drilling load

$F_{pad}(m) \triangleq$ the force actuator output

$\Psi(m) \triangleq$ the angle of borehole-propagation w.r.t the $m-$ axis

This EFFSZM drilling system is described in Figure 8.1. In the directional drilling dynamics, some parameters such as a, b, c, d, and K_{flex} are known , while WOB and K_{anis} are unknown but bounded. The values for these unknown parameters vary in the following range

$$1 < K_{anis} < 10, \qquad 5 \times 10^4 < WOB < 8.9 \times 10^4 \tag{8.2}$$

8.3 Adaptive Control Design

In this section, the design of two recent adaptive control techniques is proposed. The first technique is the I&I adaptive control and the second technique is $\mathcal{L}_1$ adaptive control for comparison. The performances of both the techniques will be compared by the simulations in the presence of unknown and uncertain parameters.

8.3.1 I&I Adaptive Control for Linearly Parameterized Plant

System (8.1) can be presented as linearly parameterized plant, which is given by

$$\frac{dH(m)}{dm} = f_0 + f_1(H)\theta_1 + f_2(H)\theta_2 + f_3(H)\theta_3 + G\theta_4 u(m) \tag{8.3}$$

where $\theta_i,\ i = 1, 2, 3, 4$ are the unknown parameters, and

$$\begin{aligned} f_0(H) &\triangleq \frac{1}{b}H(m),\ f_1(H) \triangleq H(m), \\ f_2(H) &\triangleq H(m-b),\ f_3(H) \triangleq H(m-d), \\ G &\triangleq \frac{b-a}{b\,WOB\,K_{anis}} \text{ for nominal } K_{anis} \text{ and } WOB \\ u(m) &\triangleq F_{pad}(m) \end{aligned} \tag{8.4}$$

To satisfy assumption 7.1, the following is selected

$$u(m) \triangleq v(H,\theta) = -(G\theta_4)^{-1}(f_0(H) + f_1(H)\theta_1 + f_2(H)\theta_2 + f_3(H)\theta_3 + KH(m) - K_r r) \tag{8.5}$$

where $K_r > 0$ is the feedforward gain, r is the bounded reference and for feedback gain $K > 0$, the following globally exponentially stable closed loop system is obtained

$$\frac{dH(m)}{dm} = -KH(m) + K_r r \tag{8.6}$$

In order to apply I&I adaptive control on EFFSZM system, consider the following implicit manifold

$$z_i = \hat{\theta}_i - \theta_i + \beta_i(H) \tag{8.7}$$

with the dynamics are given as

$$\begin{aligned}\frac{dz_i}{dm} =& w_i + \frac{d\beta_i(H)}{dH}\frac{dH}{dm} \\ =& w_i + \frac{d\beta_i(H)}{dH}(f_0(H) + f_1(H)\theta_1 + f_2(H)\theta_2 + f_3(H)\theta_3 + G\theta_4 u(m))\end{aligned} \tag{8.8}$$

if the updating laws are selected to be

$$
\begin{aligned}
w_1 = & -\frac{d\beta_1(H)}{dH}(f_0(H)+f_1(H)(\hat{\theta}_1+\beta_2(H))+f_2(H)(\hat{\theta}_2+\beta_2(H)-z_2) \\
& +f_3(H)(\hat{\theta}_3+\beta_3(H)-z_3)+G(\hat{\theta}_4+\beta_4-z_4)u(m)) \\
w_2 = & -\frac{d\beta_2(H)}{dH}(f_0(H)+f_1(H)(\hat{\theta}_1+\beta_1(H)-z_1)+f_2(H)(\hat{\theta}_2+\beta_2(H)) \\
& +f_3(H)(\hat{\theta}_3+\beta_3(H)-z_3)+G(\hat{\theta}_4+\beta_4-z_4)u(m)) \\
w_3 = & -\frac{d\beta_3(H)}{dH}(f_0(H)+f_1(H)(\hat{\theta}_1+\beta_1(H)-z_1)+f_2(H)(\hat{\theta}_2+\beta_2(H)-z_2) \\
& +f_3(H)(\hat{\theta}_3+\beta_3(H))+G(\hat{\theta}_4+\beta_4-z_4)u(m)) \\
w_4 = & -\frac{d\beta_4(H)}{dH}(f_0(H)+f_1(H)(\hat{\theta}_1+\beta_1(H)-z_1)+f_2(H)(\hat{\theta}_2+\beta_2(H)-z_2) \\
& +f_3(H)(\hat{\theta}_3+\beta_3(H)-z_3)+G(\hat{\theta}_4+\beta_4)u(m)) \qquad (8.9)
\end{aligned}
$$

one will have

$$
\begin{aligned}
\frac{dz_j}{dm} &= -\left(\frac{d\beta_j(H)}{dH}f_j(H)\right)z_j \quad \text{(for j= 1, 2, 3)} \\
\frac{dz_4}{dm} &= -\left(\frac{d\beta_4(H)}{dH}Gu(m)\right)z_4 \qquad (8.10)
\end{aligned}
$$

If $\frac{d\beta_j(H)}{dH}=\gamma_j f_j(H)$, and $\frac{d\beta_4(H)}{dH}=\gamma_4 Gu(m)$ where $\gamma_i>0$ are selected, the following is achieved

$$
\lim_{m\to\infty} z_i(m)=0 \quad \Rightarrow \quad \theta_i=\hat{\theta}_i+\beta_i(H) \qquad (8.11)
$$

Finally, the I&I adaptive control is given by

$$v(H, \hat{\theta}_i + \beta_i) = -\left(G(\hat{\theta}_4 + \beta_4)\right)^{-1}(f_0(H) + f_1(H)(\hat{\theta}_1 + \beta_1(H)) + f_2(H)(\hat{\theta}_2 + \beta_2(H)) + f_3(H)(\hat{\theta}_3 + \beta_3(H)) + KH(m) - K_r r) \tag{8.12}$$

The selection of $\beta_4(H)$ has to be done considering the probability of the singularity in the control law. If the following is selected

$$\beta_4(H) = c + Gu(m)H(m) \tag{8.13}$$

for $c \in \mathcal{R}$ and $\beta_4 \neq -\hat{\theta}_4$, the singularity problem will not exist.

8.3.2 I&I Adaptive Control Stability Analysis

Consider the Lyapunov function candidate

$$V(z) = z^\top P z \tag{8.14}$$

where $P^\top = P > 0$, the derivative of the Lyapunov function along the trajectories of the (8.10) is given by

$$\dot{V}(z) = z^\top(\Phi^\top P + P\Phi)z \tag{8.15}$$

where

$$\Phi = -\begin{bmatrix} \gamma_1 f_1^2 & 0 & 0 & 0 \\ 0 & \gamma_2 f_2^2 & 0 & 0 \\ 0 & 0 & \gamma_3 f_3^2 & 0 \\ 0 & 0 & 0 & \gamma_4 (Gu)^2 \end{bmatrix} \tag{8.16}$$

Since Φ is Hurwitz, the following Lyapunov equation is satisfied

$$\Phi^\top P + P\Phi = -Q \tag{8.17}$$

where $Q^\top = Q > 0$, then one will have

$$\dot{V}(z) = -z^\top Q z \leq 0 \tag{8.18}$$

hence the system (8.10) has a globally stable equilibrium at zero and the asymptotic stability is followed by the LaSalle's Invariance Principle.

Since $V(z)$ is a positive definite function and $\dot{V}(z) \leq 0$, it implies $V(z) \in \mathcal{L}_\infty$ which implies $z \in \mathcal{L}_\infty$, and therefore the off-manifold coordinates are bounded. By integrating $\dot{V}(z)$ it follows that

$$V(\infty) - V(0) = -\int_0^\infty z^\top Q z dt \tag{8.19}$$

hence $z \in \mathcal{L}_2 \cap \mathcal{L}_\infty$. Since the manifold coordinate is given by $z = \hat{\theta} - \theta + \beta(x)$, it implies that $\hat{\theta}, \beta \in \mathcal{L}_2$, so all the signals in the closed loop system are bounded.

8.3.3 $\mathcal{L}_1$ Adaptive Control

The EFFSZM system dynamics presented in (8.1) can be rewritten in the form

$$\begin{aligned}
\dot{x}(m) &= A_m x(m) + b_0(\omega u(m) + \theta_0^\top(m)x(m) + \theta_1^\top(m)x(m-\tau_1) \\
&\quad + \theta_2^\top(m)x(m-\tau_2) + \sigma(m)) \\
x(m) &= 0 \ \ \forall\, m \in [-\tau_2, 0] \\
y(m) &= c_0^\top x(m)
\end{aligned} \tag{8.20}$$

where $A_m \in \mathbb{R}$ is Hurwitz, $\theta_0, \theta_1, \theta_2 \in \mathbb{R}$ are unknown, ω is unknown with known sign, and b_0, c_0 are known. The delay $\tau_1, \tau_2 \in \mathbb{R}^+$, $(\tau_1 < \tau_2)$ are known, $\sigma(m)$ is the input disturbance.

Assumption 8.1.

1. The parameters $\theta_0, \theta_1, \theta_2$ belong to given compact convex sets $\Theta_0, \Theta_1, \Theta_2$ respectively, and continuously differentiable with uniformly bounded derivatives.

$$\begin{aligned}
&\theta_0(m) \in \Theta_0, \qquad \theta_1(m) \in \Theta_1, \quad \theta_2(m) \in \Theta_2, \ \ \forall\, m \geq 0 \\
&\theta_{\max\,0} \triangleq \max_{\theta\in\Theta_0}\|\theta\|_1, \quad \theta_{\max\,1} \triangleq \max_{\theta\in\Theta_1}\|\theta\|_1, \quad \theta_{\max\,2} \triangleq \max_{\theta\in\Theta_2}\|\theta\|_1, \\
&\|\dot{\theta}_0(m)\| \leq d_{\theta_0}, \ \ \|\dot{\theta}_1(m)\| \leq d_{\theta_1}, \quad \|\dot{\theta}_2(m)\| \leq d_{\theta_2}, \ \ \|\dot{\sigma}(m)\| \leq d_\sigma,
\end{aligned} \tag{8.21}$$

   The disturbance is upper-bounded by $|\sigma(m)| \leq \Delta, \ \ \forall\, m \geq 0$, where $\Delta > 0$ is a known conservative bound. The unknown parameter ω is lower and

upper bounded by

$$\omega_l \leq \omega \leq \omega_u, \;\; 0 < \omega_l < \omega_u \tag{8.22}$$

Based on equation 8.20, the predictor for $\mathcal{L}_1$ adaptive control is given by the following equation

$$\begin{aligned}
\dot{\hat{x}}(m) &= A_m \hat{x}(m) + b_0(\hat{\omega}u(m) + \hat{\theta}_0^\top(m)x(m) + \hat{\theta}_1^\top(m)x(m-\tau_1) \\
&\quad + \hat{\theta}_2^\top(m)x(m-\tau_2) + \hat{\sigma}(m)) \\
\hat{x}(m) &= 0 \;\; \forall \; m \in [-\tau_2, 0] \\
\hat{y}(m) &= c_0^\top \hat{x}(m)
\end{aligned} \tag{8.23}$$

where $\hat{x}(m) \in \mathbb{R}$ is the predicted state, $\hat{y}(m) \in \mathbb{R}$ is the predicted output, $\hat{\theta}, \hat{\omega}, \hat{\sigma}$ are the estimated parameters. The adaptive laws for these estimated parameters with the projection are given by the following

$$\begin{aligned}
\dot{\hat{\theta}}_0(m) &= \Gamma \mathrm{Pr}(\hat{\theta}_0(m), -\tilde{x}^\top(m)Pb_0x(m)), \;\; \hat{\theta}_0(0) = \hat{\theta}_{00} \\
\dot{\hat{\theta}}_1(m) &= \Gamma \mathrm{Pr}(\hat{\theta}_1(m), -\tilde{x}^\top(m)Pb_0x(m-\tau_1)), \;\; \hat{\theta}_1(0) = \hat{\theta}_{10} \\
\dot{\hat{\theta}}_2(m) &= \Gamma \mathrm{Pr}(\hat{\theta}_2(m), -\tilde{x}^\top(m)Pb_0x(m-\tau_2)), \;\; \hat{\theta}_2(0) = \hat{\theta}_{20} \\
\dot{\hat{\sigma}}(m) &= \Gamma \mathrm{Pr}(\hat{\sigma}(m), -\tilde{x}^\top(m)Pb_0), \;\; \hat{\sigma}_0(0) = \hat{\sigma}_0 \\
\dot{\hat{\omega}}(m) &= \Gamma \mathrm{Pr}(\hat{\omega}(m), -\tilde{x}^\top(m)Pb_0u(m)), \;\; \hat{\omega}_0(0) = \hat{\omega}_0
\end{aligned} \tag{8.24}$$

where $\Gamma > 0$ is the adaptation law rate, $\tilde{x}(m) = \hat{x}(m) - x(m)$, and for some $Q = Q^\top > 0$, with $P = P^\top > 0$ satisfies the Lyapunov equation

$$A_m^\top P + P A_m = -Q \tag{8.25}$$

The control signal is defined by

$$u(s) = -kD(s)(\hat{\eta} - k_g r(s)) \tag{8.26}$$

where $\hat{\eta} \triangleq \hat{\omega} u(m) + \hat{\theta}_0^\top(m) x(m) + \hat{\theta}_1^\top(m) x(m - \tau_1) + \hat{\theta}_2^\top(m) x(m - \tau_2) + \hat{\sigma}(m)$, and $r(m)$ are the inverse Laplace transform of $\hat{\eta}(s)$ and $r(s)$. Feedforward gain $k_g \triangleq -\frac{1}{c_0^\top A m^{-1} b_0}$, and $k > 0$. Strictly proper transfer function $D(s)$ leads to a strictly proper stable

$$C(s) \triangleq \frac{\omega k D(s)}{1 + \omega k D(s)} \tag{8.27}$$

with DC gain $C(0) = 1$. The selection of $D(s) = \frac{1}{s}$ yields first order strictly proper transfer function

$$C(s) = \frac{\omega k}{s + \omega k} \tag{8.28}$$

The following norm condition has to be satisfied for $\mathcal{L}_1$ adaptive control

$$\|G(s)\|_{\mathcal{L}_1} (\theta_{\max 0} + \theta_{\max 1} + \theta_{\max 2}) < 1 \tag{8.29}$$

where

$$H(s) \triangleq (s\mathbb{I} - A_m)^{-1} b_0, \quad G(s) \triangleq H(s)(C(s) - 1) \tag{8.30}$$

The analysis of this $\mathcal{L}_1$ adaptive control can be seen in [40].

8.4 Simulation

In order to test the proposed adaptive controls under parameter uncertainty, simulations were carried out in two major parts. The first part is for the I&I adaptive control and the second for $\mathcal{L}_1$ adaptive control. In each part, the simulations are conducted for several cases of uncertain parameters. The uncertain parameters K_{anis} and WOB are bounded and belong to the following range

$$1 \leq K_{anis} \leq 10, \qquad 5 \times 10^4 \leq WOB \leq 8.9 \times 10^4 \tag{8.31}$$

with the nominal values chosen to be $K_{anis} = 10$ and $WOB = 8.9 \times 10^4$, while

$$\begin{aligned} &a = 0.305\text{m}, \quad b = 0.953\text{m}, \quad c = 1.407\text{m}, \\ &d = 2\text{m}, \quad K_{flex} = 8.577 \times 10^5 \text{N . m/rad} \end{aligned} \tag{8.32}$$

are known parameters with exact values. The control input $F_{pad}(m)$ is considered to be bounded by

$$|F_{pad}(m)| \leq 10^7 \text{N} \tag{8.33}$$

The first case of simulation for I&I adaptive control is conducted with reference $H_{ref}(m) = 0.1\sin(0.05m) + (m/200)$ and the constant uncertain parameters are given by

$$K_{anis} = 1, \quad WOB = 5 \times 10^4 \tag{8.34}$$

which are different from the nominal values. As seen in Figure (8.2), the proposed I&I adaptive control is able to stabilize the system and follow the predefined reference as expected.

The second case is conducted with reference $H_{ref}(m) = 0.1\sin(0.05m) + (m/200)$ and random time-varying bounded uncertain parameter K_{anis} and WOB with gaussian distribution. The performance of the controller is presented in Figure (8.3). It can be seen that the I&I adaptive control is able to produce acceptable stabilization performance and maintaining small tracking error.

The last case of I&I adaptive control simulation uses a non-smooth reference for the angle of borehole-propagation with respect to the m-axis $\Psi_{ref}(rad)$ and random time-varying bounded uncertain parameter K_{anis} and WOB with gaussian distribution. As seen in Figure (8.4), the proposed controller is once again

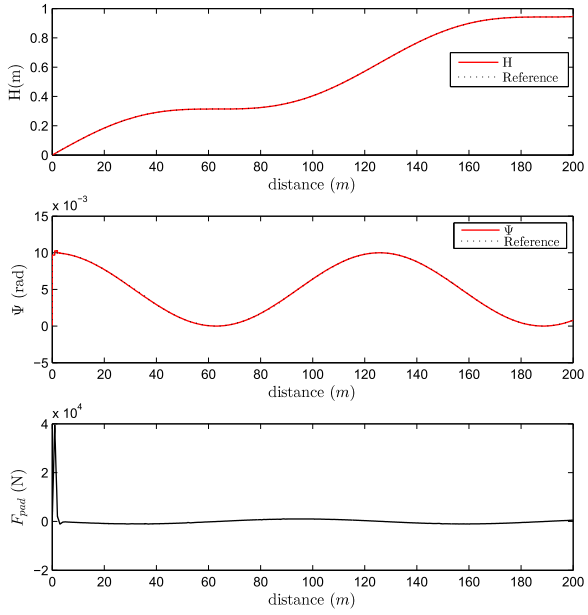

Figure 8.2: I&I Adaptive Control ($K_{anis} = 1$ and $WOB = 5 \times 10^4$)

maintaining its stability and performance in the presence of unknown and uncertain parameters.

For $\mathcal{L}_1$ adaptive control, similar cases of simulation are conducted. The selected tuning parameters for this controller satisfying the following norm condition

$$\|G(s)\|_{\mathcal{L}_1}(\theta_{\max 0} + \theta_{\max 1} + \theta_{\max 2}) = 9.0181 \times 10^{-17} < 1 \tag{8.35}$$

The results of the proposed $\mathcal{L}_1$ adaptive control can be seen in Figure (8.6-8.8). The performances of this controller are acceptable, but if the results are compared with the previous method, the I&I adaptive control produces better performances in general.

In terms of magnitude, the control signal produced by I&I adaptive is smaller

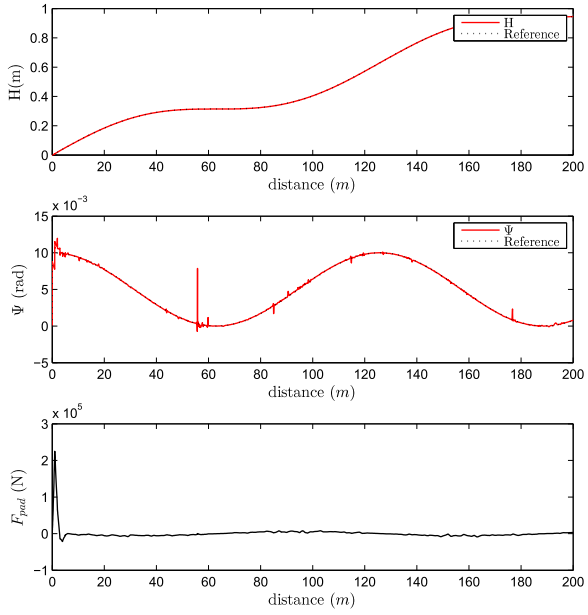

Figure 8.3: I&I Adaptive Control (K_{anis} and WOB are changing)

and smoother than the $\mathcal{L}_1$ adaptive, hence I&I adaptive control consumes less energy than $\mathcal{L}_1$ adaptive control.

In terms of controller tuning and implementation in the simulation, for EFF-SZM drilling system in particular, the I&I adaptive is better because it is easier. For $\mathcal{L}_1$ adaptive, several trials need to be done although all the selection of the tuning parameters satisfy the $\mathcal{L}_1$-norm condition. Overall, both the controllers produce acceptable tracking performance and robust w.r.t parameter uncertainty.

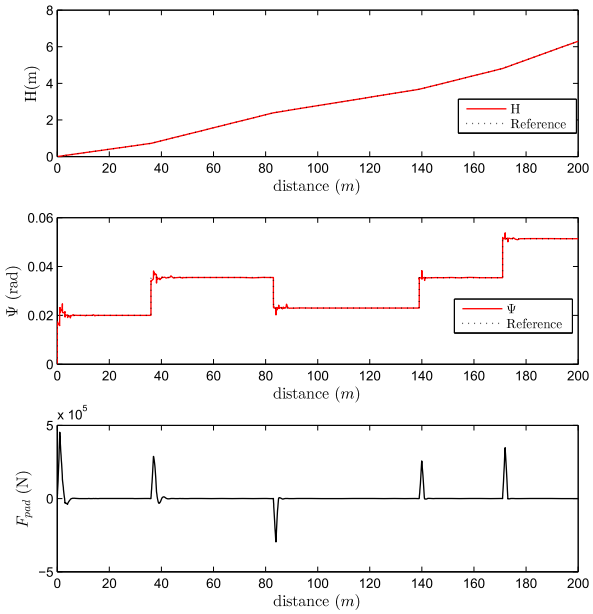

Figure 8.4: I&I Adaptive Control (K_{anis} and WOB are changing)

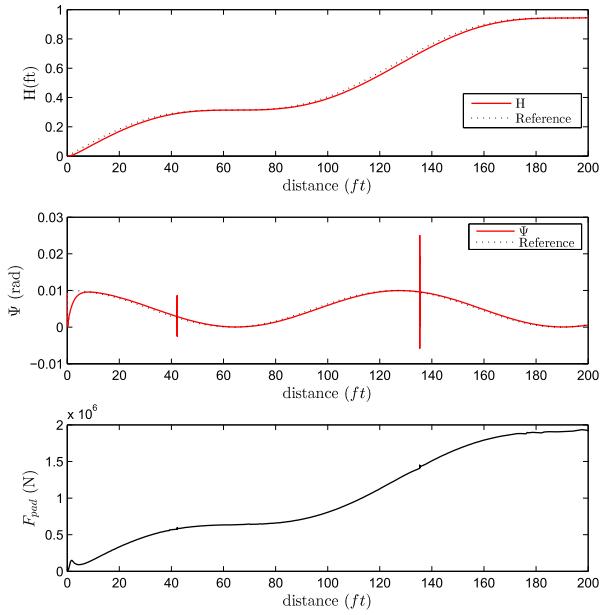

Figure 8.5: $\mathcal{L}_1$ Adaptive Control ($K_{anis} = 10$ and $WOB = 8.9 \times 10^4$)

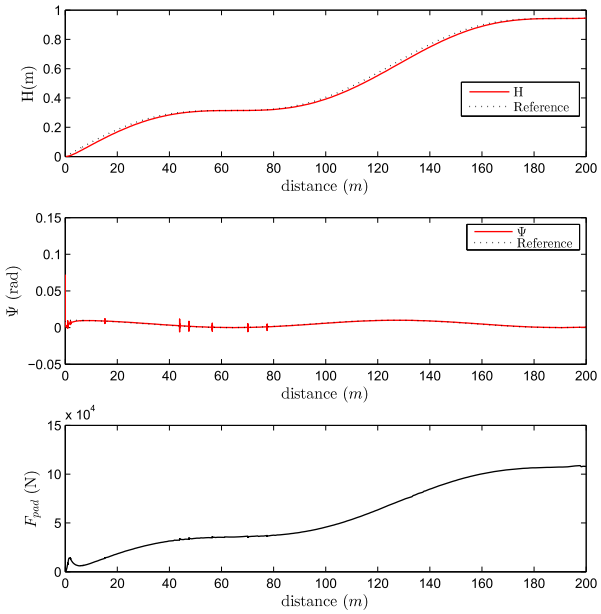

Figure 8.6: $\mathcal{L}_1$ Adaptive Control ($K_{anis} = 1$ and $WOB = 5 \times 10^4$)

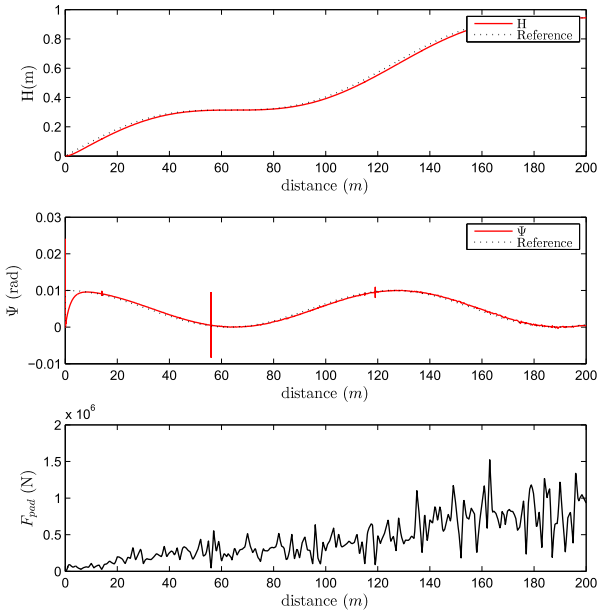

Figure 8.7: $\mathcal{L}_1$ Adaptive Control (K_{anis} and WOB are changing)

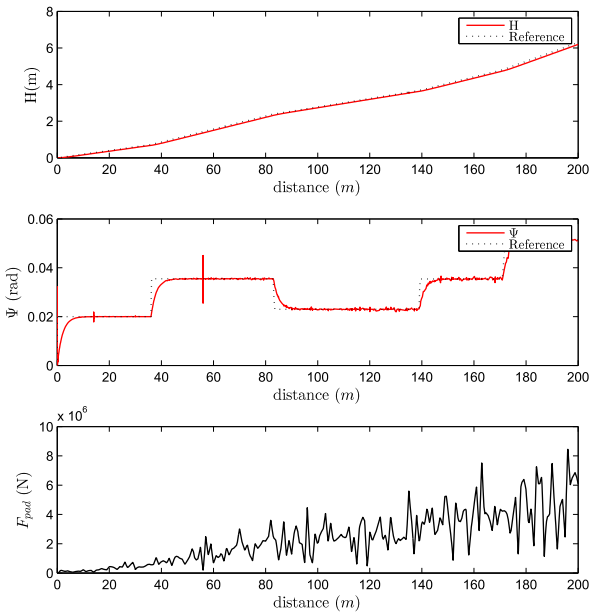

Figure 8.8: $\mathcal{L}_1$ Adaptive Control (K_{anis} and WOB are changing)

8.5 Conclusions

This chapters presents two recent techniques in adaptive control, i.e I&I adaptive control and $\mathcal{L}_1$ adaptive control, for EFFSZM directional drilling system. The EFFSZM directional drilling system belongs to a class of uncertain system with internal delay, in which the proposed adaptive controls are required for stabilization. Based on simulations, the I&I adaptive control shows better performance compared to $\mathcal{L}_1$ adaptive control in terms of tracking error and energy consumption of the control signal.

8.5.1 Contribution

The main contributions presented in this chapter are

1. Design of I&I adaptive control for EFFSZM directional drilling system containing internal delay and uncertain parameters.

2. Re-production of $\mathcal{L}_1$ adaptive control for EFFSZM directional drilling system containing internal delay and uncertain parameters for the benchmarking study.

CHAPTER 9

CONCLUSIONS

9.1 Summary of Contributions

In this thesis, the following problems have been investigated

Chapter 5

1. Design of I&I stabilizing controller for the underactuated quadrotor UAV.
2. Extension of the work in [1] by including the translational and rotational drag terms.
3. Stability and Robustness analysis of the closed loop system in the presence of uncertain parameters and exogenous disturbances.

Chapter 6

1. Design of I&I-based reduced-order observer for the translational dynamics of the quadrotor UAV.

2. Design of the classical Luenberger observer for benchmarking.

Chapter 7

1. Design of I&I adaptive control for the underactuated quadrotor UAV with unknown and uncertain parameters.
2. Analysis of I&I adaptive control.
3. Design of $\mathcal{L}_1$ adaptive control for the underactuated quadrotor UAV with unknown and uncertain parameters.

Chapter 8

1. Design of I&I adaptive control for EFFSZM directional drilling system contains an internal delay and uncertain parameters.
2. Re-production of $\mathcal{L}_1$ adaptive control for EFFSZM directional drilling system contains an internal delay and uncertain parameter for the benchmarking study.

9.2 Concluding Remarks

The work in this thesis can be summarized as the following

1. The design of I&I stabilizing controller proposed in this thesis can be immediately applied to many mechanical systems. The mathematical development of the controller is found to be easier than the backstepping technique since one does not need to find and solve the Lyapunov function candidate.

2. The I&I-based reduced order observer is found to be applicable in the estimation of unknown translational velocity. In terms of estimation error, the performance of this observer is better compared to the classical Luenberger observer.

3. The design of I&I adaptive controller is a straightforward application for the UAV system. For the unknown and uncertain parameters, the proposed adaptive control works perfectly. The requirement to have a faster controller in the inner loop is satisfied.

4. The I&I adaptive control is also applicable on a system with an internal delay. The derivation of the controller is straightforward from the I&I adaptive control for linearly parametrized plant development.

9.3 Future Work

1. Nonlinear target dynamics for the I&I stabilization may be considered for acrobatic trajectory tracking control for the quadrotor.

2. The proposed designs may be applied to the real system.

REFERENCES

[1] Z. Zuo, "Trajectory tracking control design with command-filtered compensation for a quadrotor," *Control Theory & Applications, IET*, vol. 4, no. 11, pp. 2343–2355, 2010.

[2] A. Astolfi and R. Ortega, "Immersion and invariance: a new tool for stabilization and adaptive control of nonlinear systems," *Automatic Control, IEEE Transactions on*, vol. 48, no. 4, pp. 590–606, 2003.

[3] V. Mistler, A. Benallegue, and N. M'sirdi, "Exact linearization and noninteracting control of a 4 rotors helicopter via dynamic feedback," in *Robot and Human Interactive Communication, 2001. Proceedings. 10th IEEE International Workshop on.* IEEE, 2001, pp. 586–593.

[4] H. Bai, H. Y. Wang, and S. H. Shao, "Position tracking and attitude stable control for an unmanned quadrotor vehicle," *Advanced Materials Research*, vol. 645, pp. 492–496, 2013.

[5] A. Tayebi and S. McGilvray, "Attitude stabilization of a four-rotor aerial robot," in *Decision and Control, 2004. CDC. 43rd IEEE Conference on*,

vol. 2. IEEE, 2004, pp. 1216–1221.

[6] E. Altug, J. Ostrowski, and R. Mahony, "Control of a quadrotor helicopter using visual feedback," in *Robotics and Automation, 2002. Proceedings. ICRA'02. IEEE International Conference on*, vol. 1. IEEE, 2002, pp. 72–77.

[7] R. Xu and U. Ozguner, "Sliding mode control of a quadrotor helicopter," in *Decision and Control, 2006 45th IEEE Conference on*. IEEE, 2006, pp. 4957–4962.

[8] H. Bouadi, M. Bouchoucha, and M. Tadjine, "Sliding mode control based on backstepping approach for an uav type-quadrotor," *International Journal of Applied Mathematics and Computer Sciences*, vol. 4, no. 1, pp. 12–17, 2007.

[9] C. Liu, S. J. Tang, S. Y. Yang, and J. Guo, "Fuzzy sliding-mode control for quad-rotor trajectory tracking," *Applied Mechanics and Materials*, vol. 278, pp. 1593–1600, 2013.

[10] H. Voos, "Nonlinear control of a quadrotor micro-uav using feedback-linearization," in *Mechatronics, 2009. ICM 2009. IEEE International Conference on*. IEEE, 2009, pp. 1–6.

[11] A. Benallegue, A. Mokhtari, and L. Fridman, "High-order sliding-mode observer for a quadrotor uav," *International Journal of Robust and Nonlinear Control*, vol. 18, no. 4-5, pp. 427–440, 2008.

[12] T. Madani and A. Benallegue, "Sliding mode observer and backstepping control for a quadrotor unmanned aerial vehicles," in *American Control Conference, 2007. ACC'07.* IEEE, 2007, pp. 5887–5892.

[13] M. Guisser, H. Medromi, H. Ifassiounen, J. Saadi, and N. Radhy, "A coupled nonlinear discrete-time controller and observer designs for under-actuated autonomous vehicles with application to a quadrotor aerial robot," in *IEEE Industrial Electronics, IECON 2006-32nd Annual Conference on.* IEEE, 2006, pp. 1–6.

[14] M. Boutayeb, E. Richard, H. Rafaralahy, H. Souley Ali, and G. Zaloylo, "A simple time-varying observer for speed estimation of uav," in *World Congress*, vol. 17, no. 1, 2008, pp. 1760–1765.

[15] T. Dierks and S. Jagannathan, "Output feedback control of a quadrotor uav using neural networks," *Neural Networks, IEEE Transactions on*, vol. 21, no. 1, pp. 50–66, 2010.

[16] A. Astolfi, D. Karagiannis, and R. Ortega, *Nonlinear and adaptive control with applications.* Springer Verlag, 2007.

[17] M. Huang, B. Xian, C. Diao, K. Yang, and Y. Feng, "Adaptive tracking control of underactuated quadrotor unmanned aerial vehicles via backstepping," in *American Control Conference (ACC), 2010.* IEEE, 2010, pp. 2076–2081.

[18] P. Stingu and F. Lewis, "Adaptive dynamic programming applied to a 6dof quadrotor," *Computational Modeling and Simulation of Intellect: Current State and Future Perspectives. IGI Global*, 2010.

[19] C. Coza, C. Nicol, C. Macnab, and A. Ramirez-Serrano, "Adaptive fuzzy control for a quadrotor helicopter robust to wind buffeting," *Journal of Intelligent and Fuzzy Systems*, vol. 22, no. 5, pp. 267–283, 2011.

[20] M. Imran Rashid and S. Akhtar, "Adaptive control of a quadrotor with unknown model parameters," in *Applied Sciences and Technology (IBCAST), 2012 9th International Bhurban Conference on.* IEEE, 2012, pp. 8–14.

[21] A. Astolfi, D. Karagiannis, and R. Ortega, *Nonlinear and adaptive control with applications.* Springer, 2008.

[22] J. Acosta, R. Ortega, A. Astolfi, and I. Sarras, "A constructive solution for stabilization via immersion and invariance: The cart and pendulum system," *Automatica*, vol. 44, no. 9, pp. 2352–2357, 2008.

[23] T. Wimbock, C. Ott, and G. Hirzinger, "Immersion and invariance control for an antagonistic joint with nonlinear mechanical stiffness," in *Decision and Control (CDC), 2010 49th IEEE Conference on.* IEEE, 2010, pp. 1128–1135.

[24] E. Hristea, H. Siguerdidjane *et al.*, "Stabilization of a magnetic suspension by immersion and invariance and experimental robustness study," in *Proceedings of 18th IFAC World Congress*, 2011, pp. 7210–7215.

[25] N. Manjarekar, R. Banavar, and R. Ortega, "Stabilization of a synchronous generator with a controllable series capacitor via immersion and invariance," *International Journal of Robust and Nonlinear Control*, 2011.

[26] A. Das, K. Subbarao, and F. Lewis, "Dynamic inversion with zero-dynamics stabilisation for quadrotor control," *Control Theory & Applications, IET*, vol. 3, no. 3, pp. 303–314, 2009.

[27] K. Fujimoto, M. Yokoyama, and Y. Tanabe, "I&i-based adaptive control of a four-rotor mini helicopter," in *IECON 2010-36th Annual Conference on IEEE Industrial Electronics Society*. IEEE, 2010, pp. 144–149.

[28] E. Stingu and F. L. Lewis, "An approximate dynamic programming based controller for an underactuated 6dof quadrotor," in *Adaptive Dynamic Programming And Reinforcement Learning (ADPRL), 2011 IEEE Symposium on*. IEEE, 2011, pp. 271–278.

[29] C. Cao and N. Hovakimyan, "Design and analysis of a novel $\mathcal{L}_1$ adaptive controller, part i: Control signal and asymptotic stability," in *American Control Conference, 2006*. IEEE, 2006, pp. 3397–3402.

[30] C. Cao and N. Hovakimyan, "Design and analysis of a novel $\mathcal{L}_1$ adaptive controller, part ii: Guaranteed transient performance," in *American Control Conference, 2006*. IEEE, 2006, pp. 3403–3408.

[31] N. Hovakimyan and C. Cao, *$\mathcal{L}_1$ adaptive control theory: guaranteed robustness with fast adaptation*. Siam, 2010, vol. 21.

[32] C. Cao and N. Hovakimyan, "Stability margins of $\mathcal{L}_1$ adaptive control architecture," *IEEE Transactions on Automatic Control*, vol. 55, no. 2, p. 480, 2010.

[33] N. Hovakimyan, C. Cao, E. Kharisov, E. Xargay, and I. M. Gregory, "$\mathcal{L}_1$ adaptive control for safety-critical systems," *IEEE Control Systems Magazine*, vol. 31, no. 5, pp. 54–104, 2011.

[34] J. Wang, V. V. Patel, C. Cao, N. Hovakimyan, and E. Lavretsky, "Novel $\mathcal{L}_1$ adaptive control methodology for aerial refueling with guaranteed transient performance," *Journal of guidance, control, and dynamics*, vol. 31, no. 1, pp. 182–193, 2008.

[35] I. M. Gregory, C. Cao, E. Xargay, N. Hovakimyan, and X. Zou, "$\mathcal{L}_1$ adaptive control design for nasa airstar flight test vehicle," in *AIAA Guidance, Navigation, and Control Conference*, AIAA-5738, 2009.

[36] B. Michini and J. How, "$\mathcal{L}_1$ adaptive control for indoor autonomous vehicles: design process and flight testing," in *Proceedings of the AIAA Guidance, Navigation and Control Conference, Chicago, IL*, 2009.

[37] J. Wang, V. Patel, C. Woolsey, N. Hovakimyan, and D. Schmale, "$\mathcal{L}_1$ adaptive control of a uav for aerobiological sampling," in *American Control Conference, 2007. ACC'07.* IEEE, 2007, pp. 4660–4665.

[38] D. Maalouf, V. Creuze, and A. Chemori, "A novel application of multivariable $\mathcal{L}_1$ adaptive control: From design to real-time implementation on an under-

water vehicle," in *Intelligent Robots and Systems (IROS), 2012 IEEE/RSJ International Conference on.* IEEE, 2012, pp. 76–81.

[39] D. Wang, L. Qiang, F. Liu, and K. Wang, "Quadrotor longitudinal controller based on $\mathcal{L}_1$ adaptive control method," *Journal of Projectiles, Rockets, Missiles and Guidance*, vol. 6, p. 012, 2011.

[40] H. Sun, Z. Li, N. Hovakimyan, T. Basar, and G. Downton, "$\mathcal{L}_1$ adaptive control for directional drilling systems," in *Proceedings of the 2012 IFAC Workshop on Automatic Control in Offshore Oil and Gas Production.* IFAC, 2012, pp. 72–77.

[41] S. Wiggins, *Introduction to applied nonlinear dynamical systems and chaos.* Springer Verlag, 2003, vol. 2.

[42] C. I. Byrnes, F. D. Priscoli, and A. Isidori, *Output regulation of uncertain nonlinear systems.* Birkhauser, 1997.

[43] C. Cao and N. Hovakimyan, "$\mathcal{L}_1$ adaptive controller for a class of systems with unknown nonlinearities: Part i," in *American Control Conference, 2008.* IEEE, 2008, pp. 4093–4098.

[44] J.-B. Pomet and L. Praly, "Adaptive nonlinear regulation: Estimation from the lyapunov equation," *Automatic Control, IEEE Transactions on*, vol. 37, no. 6, pp. 729–740, 1992.

[45] H. Goldstein, C. Poole, J. Safko, and C. Mechanics, "Pearson," *New Delhi*, vol. 28, no. 4, 2002.

[46] J. Wen, "Control of nonholonomic systems," *The Control Handbook*, pp. 1359–1368, 1996.

[47] A. Freddi, A. Lanzon, and S. Longhi, "A feedback linearization approach to fault tolerance in quadrotor vehicles," in *Proceedings of The 2011 IFAC World Congress, Milan, Italy*, 2011.

[48] H. Khalil and J. Grizzle, *Nonlinear systems*. Prentice hall New Jersey, 1996, vol. 3.

[49] E. M. Molvar, "Drilling smarter: Using directional drilling to reduce oil and gas impacts in the intermountain west," *Prepared by Biodiversity Conservation Alliance, Report issued Feb*, vol. 18, p. 34, 2003.

[50] L. Aalund and K. Rappold, "Horizontal drilling taps more oil in the middle east," *Oil & gas journal*, vol. 91, no. 25, pp. 47–51, 1993.

[51] W. G. Deskins, W. J. McDonald, and T. B. Reid, "Survey shows successes, failures of horizontal wells," *Oil and Gas Journal*, vol. 93, no. 25, 1995.

[52] G. Downton, "Directional drilling system response and stability," in *Control Applications, 2007. CCA 2007. IEEE International Conference on*. IEEE, 2007, pp. 1543–1550.

[53] H. Sun, Z. Li, N. Hovakimyan, T. Basar, and G. Downton, "$\mathcal{L}_1$ adaptive controller for a rotary steerable system," in *Intelligent Control (ISIC), 2011 IEEE International Symposium on*. IEEE, 2011, pp. 1020–1025.

Vitae

- Name: Arief Barkah Koesdwiady
- Nationality: Indonesia
- Date of Birth: November 3^{rd}, 1985
- Email: *abeka@alumni.itb.ac.id, ariefbarkah@gmail.com*
- Permanent Address: Jakarta, Indonesia